HELLENIC REPUBLIC
National and Kapodistrian University of Athens
—— EST. 1837 ——

Interdisciplinary M.Sc. course in Nanomedicine

Academic Year 2020-2021

ം ☙

M.Sc. Thesis Subject:

"Breath analysis of Volatile Organic Compounds
for early-stage disease detection
using nanomaterials"

ം ☙

M.Sc. Candidate: Kaloumenou Maria

Supervisor Professor: Tsoukalas Dimitrios

Committee co-members: Efstathios Efstathopoulos, Nefeli Lagopati

September 1, 2021
Athens

TABLE OF CONTENTS

ABBREVIATIONS

ADH	Alcohol dehydrogenase
AECOPD	Acute Exacerbations Chronic Obstructive Pulmonary Disease
ALDH	Aldehyde Dehydrogenase
BBT	Breast Benign Tumor
BPD	Benign Pulmonary Disease
BPN	Benign Pulmonary Nodules
BPR	Biobased Polyester
CAR	Carboxen
CNTs	Carbon Nanotubes
COPD	Chronic Obstructive Pulmonary Disease
CT	Computed Tomography
CYP450	Cytochrome p450
DCIS	Ductal carcinoma *in situ*
DVB	Divinylbenzene
e-Nose	Electronic Nose
FeNO	Fractional exhaled Nitric Oxide
GC	Gas Chromatography
GC-MS	Gas Chromatography – Mass Spectrometry
GO	Graphene Oxide
HCA	Hierarchical Cluster Analysis
HSA	Health Science Authority
HSP	Hansen Solubility Parameter
HS-SPME	Headspace-Solid-phase Microextraction
ICS	Inhaled corticosteroids
IDEs	Interdigitated electrodes
LC	Lung Cancer
LCC	Large-cell carcinoma
LOD	Limit of Detection
LSPR	Localized Surface Plasmon Resonance
MCNPs	Monolayer/Molecularly Capped Nanoparticles
MIP	Molecularly imprinting polymer
MOS	Metal Oxide Semiconductors
MRI	Magnetic Resonance Imaging
NFs	Nanofibers
NPs	Nanoparticles
NRs	Nanorods
NSCLC	Non-small cell Lung Carcinoma

NSs	Nanoshells
NTD	Needle Trap Device
NWs	Nanowires
PC	Poly (carbonate)
PCL	Poly (caprolactone)
PDMS	Polydimethylsiloxane
PEDOT:PSS	Poly (3,4-ethylenedioxythiophene) : Poly (styrene sulfonic acid)
PEG	Poly (ethylene glycol)
PLA	Poly (lactic acid)
PMMA	Poly (methyl methacrylate)
PNMD	Pulmonary non-malignant disease
ppb	Parts per billion
ppm	Parts per million
PUFAs	Polyunsaturated Fatty Acids
QCM	Quartz Crystal Microbalance
QDs	Quantum dots
RGO	Reduced Graphene Oxide
ROS	Reactive Oxygen Species
RT	Room Temperature
SAW	Surface Acoustic Wave
SCLC	Small Cell Lung Carcinoma
SERS	Surface Enhanced Raman Scattering
SPME	Solid-phase Microextraction
TD	Thermal Desorption
TMDs	Transition Metal Dichalcogenides
VOCs	Volatile Organic Compounds

Abstract

Undoubtedly, early-stage disease diagnosis is of particular importance, increasing the chances for effective treatment, in comparison to advanced-disease stages. Lack of patient compliance for the existing diagnostic methods, however, limits prompt diagnosis, rendering the development of non-invasive diagnostic tools mandatory. One of the most promising non-invasive diagnostic methods that has attracted the research interest during the last years is breath analysis. Volatile Organic Compounds (VOCs) contained in the exhaled breath are considered as important potential biomarkers of various types of diseases. The diagnostic ability of VOC-patterns detection using analytical techniques and, especially, sensors, has been demonstrated. The progressive development of novel nanomaterials, suitable for sensing element creation, enhances the development of effective diagnostic sensors, comprising a major topic of current research. The current thesis aims, firstly, to present an overview of the various types of nanomaterials and sensors investigated for diagnostic sensors development. Further on, taking into consideration the importance of sensible sensing-material selection, the parameters affecting the interactions of VOCs with polymers – a common component of sensing elements – are summarized. Last but not least, a series of polymers that could potentially detect repeatedly identified VOCs as potential biomarkers of asthma, COPD, lung and breast cancer, using a polymer coated-MNSs based chemiresistor are proposed.

Chapter 1: Introduction

Disease diagnosis is conventionally conducted using expensive, time-consuming, invasive techniques, applied by appropriately trained health care professionals. For instance, gastroscopy, laryngoscopy and coronary angiography are used for gastric cancer, lung cancer and myocardial infraction diagnosis, respectively[1]. Other commonly used methods like CT[2] or mammography, used for breast cancer[3], may be also harmful, due to radiation exposure. As a result, patient compliance and utilization of such diagnostic methods, are remarkably reduced for a significant part of the population. However, disease, and especially cancer, early-stage diagnosis, by effective high-risk population screening, renders treatment easier.[4] For this reason, ameliorated diagnostic methods are imperative.

Metabolomics, one of the '-omics' disciplines, that have progressively become a promising diagnostic tool in medical research, offers a comprehensive analysis of the metabolites contained in biological samples, by the combination of analytical techniques with bioinformatics.[5] The term Volatolomics is referred to the chemical processes that correlates with VOCs emitted by body fluids[6], such as peripheral blood, urine and sweat, as well as feces, nasal mucous, gaseous skin excretions and exhaled breath[6, 7,8]. The decreased sample complexity due to non-volatile compounds absence, the highly developed appropriate analytical techniques and the ability of direct or continuous breath analysis using gas sensors render exhaled breath an exceptional source of VOCs as biomarkers.[8,9] Thus, the analysis of the exhaled breath, which is closely related to critical biochemical alternations of the organism, holds a great promise for non-invasive disease diagnosis[1,10].

Inorganic gases (*e.g.,* CO_2, CO and NO), VOCs (*e.g.,* acetone, isoprene, ethane, pentane) and non-volatile compounds/exhaled breath condensates (*e.g.,* peroxynitrite, cytokines and isoprostanes) constitute the human breath. VOCs comprise metabolic products that pass from the bloodstream to the alveolar air *via* the alveolar pulmonary membrane, to be exhaled through the respiratory tract.[1,11,12] A unique pattern of VOCs characterizes a specific disease[6], thus, analysis of exhaled VOCs could potentially lead to disease diagnosis[12]. Apart from early diagnosis, screening of high-risk populations and assessment of therapy efficiency will potentially be permitted via breath analysis, due to being a non-invasive, inexpensive[6] and rapid method, characterized by increased patient compliance.[13]

A great number of different diseases have been investigated for potential diagnosis via breath analysis. It has been demonstrated that lung diseases (*e.g.,* LC, Chronic Obstructive Pulmonary disease (COPD), asthma and cystic fibrosis) are correlated with different relative composition and concentrations of VOCs, which lead to characteristic VOC patterns.[14] Apart from lung diseases, systemic diseases, such as neurodegenerative diseases[15] metabolic disorders, infectious diseases[16,17] and cancer are, also, reported to correlate with the formation of specific VOC patterns, thus holding promise for breath diagnosis.[18]

The application of breath analysis on disease diagnosis may be achieved via two general methods; analytical techniques and gas sensors.[17,19,20,21] The approach used differs between the two methods, which possess different advantages. During the last years, research interest has focused on gas sensor applications in breath analysis, as they are considered particularly promising diagnostic tools, applicable in clinical practice[19,20,21].

In general, gas sensors comprise inexpensive and simple[16,19,20] easy-to-use devices, that are small in size and, thus, portable[16,20]. Along with the characteristics referred, short response time and direct acquisition of the results, as well as short sensor recovery time[16], render gas sensors attractive for point-of-care and personalized screening, diagnosis and disease follow up[20]. Especially nanomaterial-based sensors exhibit unique chemical, physical and optical characteristics and fast kinetics, attributed to the incorporation of nanomaterials[20].

Various nanomaterials have been used for the development of different types of gas sensors[7]. Sensor components are selected wisely, depending on the chemical and physical properties of analytes[6]. The first aim of this thesis is to provide an overview of the categories of nanomaterials and gas sensors investigated for disease diagnosis. Thereafter, this thesis aims to compile the VOCs repeatedly identified and characterized as discriminative for the respiratory diseases asthma and COPD and the malignant diseases lung and breast cancer. Finally, the thesis focuses on the appropriate polymer selection for the sensing film of a polymer-coated MNPs-based chemiresistor, for the detection of the VOCs selected after the literature research. The selected diseases are of great interest, as asthma and COPD are characterized by similar symptoms,[19] with COPD being usually underdiagnosed[22,23], while the selected malignant diseases comprise two of the five more frequent and mortal cancers[4].

Chapter 2: Background Knowledge

2.1. Breath analysis

2.1.1. VOCs of Exhaled Breath

Since 400 BC, Hippocrates (460-370 BC) had observed that certain medical imbalances were characterized by specific odors[1],[24]– liver problems/fishy, kidney problems/urine-like, diabetes/sweet and lung abscess/rotten smell – while diseases were categorized based on distinct odors in Chinese medicine in ancient times[24]. In 1971, 250 VOCs of frozen breath were detected – but not identified[1] – by Linus Pauling, using gas chromatography, initiating the modern breath testing[1],[24],[25]. Since then, more than 2,000 VOCs have been detected in the exhaled breath[16] that appertain to hydrocarbons, alcohols, aldehydes, ketones, esters[16],[26], ethers, carboxylic acids, heterocyclic hydrocarbons[16], aromatic compounds, nitriles[16],[26], sulphides and terpenoids[16] and may be endogenous or exogenous.

Endogenously created VOCs comprise high-vapor-pressure (body and RT) (fragments of[27]) byproducts of normal or pathophysiological metabolic pathways[7],[27],[28], as well as of microbiome metabolism[27]. They are produced either in airways region or in other parts of human body[28], representing the metabolism of the whole organism. In the first case, the VOC are released into the exhaled breath in a direct way.[28] In the second case, produced VOCs enter and circulate in the bloodstream, and, during gas exchange in the alveoli or the airways, excretion to the exhaled breath occurs[15],[28]. Depending on blood solubility, VOCs are exchanged in different sites of the respiratory tract. Poorly blood soluble, nonpolar VOCs, with blood-air partition coefficient ($\lambda_{b:a}$) < 10, are exchanged in the alveoli, in contrast to blood soluble VOCs with $\lambda_{b:a}$ > 100, exchanged in lung airways. VOCs of intermediate solubility (10 < $\lambda_{b:a}$ < 100) undergo pulmonary gas exchange in both sites.[15],[16]

Exogenously originated VOCs are correlated with the environment and the habits of the person.[27] VOCs related with cleaning fluids, personal care products, plastic-related VOCs[27], blazes or air pollution due to industrial/transport gas emissions[16] enter human organism through extended inhalation and are excreted via exhaled breath. Smoking habits[15], food and food supplements, drinks or medication also consist important VOC sources[15],[27]. Other important confounding factors affecting the profile of exhaled VOCs are age, gender, ethnicity, living place and lifestyle[15],[29]. Consequently, immediate and recent environmental exposure should be taken into consideration during breath analysis.[27]

N_2, O_2, CO_2, water vapor and Ar – the dominant constituents of the atmospheric air – consist the most usually detected inorganic (except water) gases in the human exhaled breath, without having undergone modifications.[16,28,30] Also, H_2, CO and NO consist normal inorganic gases.[30] NH_3, acetaldehyde, the alcohols methanol, propanol[16] and ethanol, acetone, isoprene[16,26] and the saturated alkanes methane, ethane and propane[26] are the most usual VOCs detected in the exhaled breath, with ammonia and acetone found to be the most abundant (~0.8 ppm[16] and ~0.3-1 ppm[26], respectively). The sulfides H_2S and carbonyl sulfide are also reported as normal components of the breath of humans.[30]

2.1.2. Origins of different VOC classes – Metabolic Disorders

Oxidative stress, reactions catalyzed by cytochrome p450 (CYP450) and liver enzymes and lipid peroxidation are the main biochemical processes correlated with endogenous VOCs.[15,31] Their main features are presented on Table 1 . The correlation of oxidative stress and airway inflammation with exhaled VOCs is summarized in Figure 1. Different VOC classes are potentially correlated with different biochemical reactions and different exogenous sources.

Hydrocarbons (aliphatic) are primarily products of oxidative stress, which leads to lipid peroxidation of PUFAs of the cellular and subcellular membranes.[6,31] Generally, hydrocarbons are rapidly excreted in exhaled breath, due to low blood solubility.[9,17,31] Some hydrocarbons, such as pentane – a product of lipid peroxidation of ω6 fatty acids – are readily metabolized by CYP450 in hepatocytes.[17] Concerning unsaturated hydrocarbons, isoprene (2-methyl-1,3-butadiene), one of the most abundant VOCs of exhaled breath, is potentially by-product of mevalonic pathway, a key-step of cholesterol synthesis in cytosol[9,17,32,33,34]. Cyclic hydrocarbons, on the other hand, are exogenous compounds deriving mainly from plastics and fuel combustion[35].

Alcohols contained in food and alcohol beverages[9] are transported to blood, through gastrointestinal tract, while they also derive from the hydrocarbons metabolism of (CYP450)[9]. Alcohols are mainly metabolized by the enzyme ADH and the CYP450 in liver and only a small fraction is excreted in breath, as well as urine, sweat, feces, breast milk and saliva.[6]

Table 1: Definition of main biochemical pathways and examples of correlated VOC classes and diseases.

Process	Definition	Related VOC categories	Examples of diseases
Oxidative stress	Result of disproportional relation between ROS and ROS intermediates inactivation and/or induced damage repair[32,36]. ROS oxidize surrounding compounds or lead to radical formation[36]. ROS overproduction or decreased antioxidant system activation[36], provoke peroxidative damage of proteins, PUFAs and DNA of the cells.[11,36]	Alkanes, methylated alkanes, aldehydes[28]	Cancer, carcinogenesis [11,35], COPD[28,36], asthma[28], IDF, atherosclerosis [36], inflammation[36,35].
PUFAs peroxidation	Increased reactivity of the hydrogens of the methylene $-CH_2-$ groups, caused by the multiple double bonds present alongside, permits free radical chain reactions, extensive auto-oxidation and, finally, fatty acid peroxidation.[36]	Methylated alkanes[9], alkanes, e.g.,, ethane[6,14,36] (ω3 PUFAs[9,17]) and pentane[6,14,36] (ω6 PUFAs[9,17]), alcohols, e.g., propanol and butanol[14,36], secondary carbonyl oxidation products i.e. hexanal (ω6 PUFAs oxidative cleavage[35]), octanal and nonanal.[14,32]	Cancer, atherosclerosis, inflammatory diseases, aging[31].
Inflammation	Chronic diseases characteristic, closely connected with ROS production and oxidative stress. Inflammatory mediators and activated inflammatory cells stimulate ROS production. ROS activate pro-inflammatory signaling, activating specific pathways, *i.e.,* NF-κB pathway.	Inflammation-specific VOCs belong to products of pathways linked with ROS overproduction, *e.g.,* lipid peroxidation.[36]	Asthma[14], COPD [21]
CYP450 Enzymes – over-activation	Large array of various oxidase enzymes, able to catalyze the oxidation of organic compounds, normally activated as detoxification mechanism. [9]	Hydroxylation of alkanes towards alcohols. Alcohol oxidation towards aldehydes (CYP2E1, liver). Hydroxy-peroxide reduction towards aldehydes/ketones[9]	Carcinogenesis[9]
Liver enzymes – over-activation	*Oxidoreductases*: enzymes mainly in liver, transform alcohols to aldehydes/ketones, reducing the nicotinamide adenine dinucleotide (NAD$^+$ to NADH). *ADH*: oxidation of primary, secondary and cyclic secondary alcohols and hemiacetals, to aldehyde formation. *ALDH*: aldehydes transformed into carboxylic acids.[9]	Carboxylic acids, aldehydes, ketones[9]	Cancer[9]

ADH: Alcohol dehydrogenase, **ALDH:** Aldehyde Dehydrogenase, **COPD**: Chronic obstructive pulmonary disease, **CYP450:** Cytochrome p450, **IPF:** idiopathic pulmonary fibrosis, **NF-κB:** nuclear factor kappa B

Aldehydes comprise normal products of common biotransformation pathways[9], such as metabolism of alcohols (CYP450, ADH) and reduction of the lipidic hydroxyperoxide intermediate of PUFAs peroxidation.[6,9,35]. Exogenous origin of aldehydes is also possible, as they consist food additives, ingredients of personal care products[34] and tobacco smoke (*e.g.,* saturated; formaldehyde, acetaldehyde, propionaldehyde, butyraldehyde and

unsaturated; acrolein and crotonaldehyde) and by-products of detoxification processes of tobacco by CYP450[9].
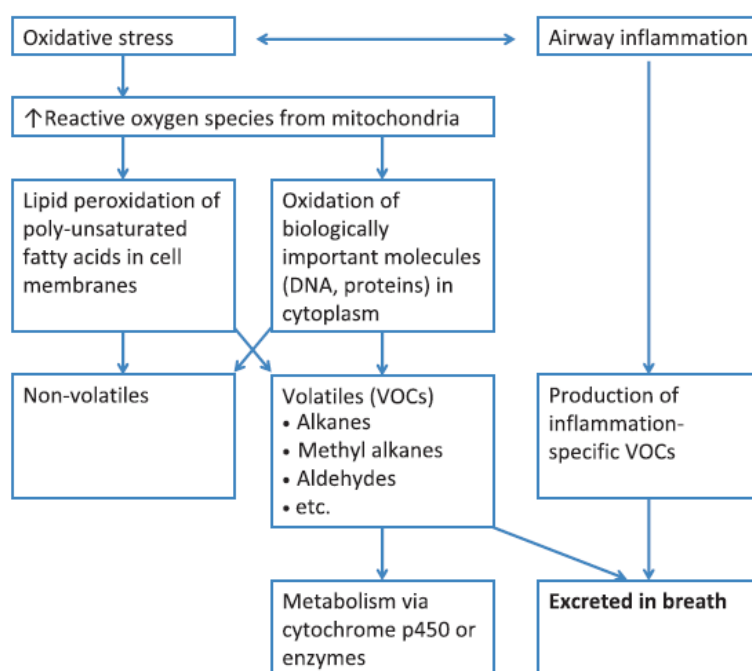
Figure 1: Diagram summarizing the correlation of VOCs found in the exhaled breath with oxidative stress and inflammatory conditions. *Reprinted with permission from Ref.[28]. Copyright © 2012 John Wiley & Sons Ltd*

Ketones, produced by liver in significant quantities, are correlated with increased lipid oxidation, especially as secondary product of PUFAs peroxidation (CYP450)[9,17]. Amino acids metabolism is, also, closely linked with ketone production[6,9]. In several pathophysiological conditions, *e.g.,* advanced cancer and cachexia, protein metabolism is increased, increasing the ketone levels.[31] Acetone, one of the most abundant VOCs, derives from the decarboxylation of excess Acetyl-CoA and acetoacetate, in liver[9,17]. It is noteworthy that, among ketones, acetone is produced in smaller amounts, however exhalation is intense due to its high vapor pressure[9]. Diet is an important confounding factor affecting ketone production, closely linked with fat and protein metabolism[6].

Aromatic compounds are commonly contained in exhaled breath. However, no known creation metabolic pathway exists, thus, endogenous production is accounted as improbable.[34] Aromatic compounds are exogenous, mainly as environmental pollutants deriving from anthropogenic actions, while they are also tobacco smoke[9,31,34] and alcohol[9,31] components. Health risk is increased by the presence of aromatic compounds in

human body[9,34] as they provoke peroxidative damage to proteins, DNA and PUFAs, after inserting cytosol and reaching cell organelles, leading to age-related diseases[9,31].

Among organic *nitrogen compounds,* nitriles are exogenously originated VOCs found in tobacco smoke and polluted air. Due to their increased reactivity, they can provoke peroxidation damage in the fatty tissues in which they are stored.[6] Acetonitrile, one of the most common exhaled nitriles, is a main constituent of cigarette smoke[17]. Inflammatory conditions have been correlated with nitrogen containing compounds presence[36].

Last but not least, the class of *sulfur compounds*, *e.g.,* dimethyl sulfide, dimethyl disulfide and methanethiol, are detected in exhaled breath[33]. Dimethyl sulfide and dimethyl disulfide are produced by the auto-oxidation of methanethiol (CH_3SH), which is produced by the metabolism of sulfur-containing amino acids[32], mainly L-methionine metabolism[33]. Sulfur-containing compounds, also, comprise inflammation biomarkers.[36]

2.1.3.   VOCs and Disease Diagnosis

VOCs of exhaled breath are regarded as normal[16]. However, concentration differences for some exhaled VOCs could potentially be associated with an abnormal condition of the body[16], as the metabolic processes producing the VOCs are altered in a distinctive way by different diseases[1,12]. Disease-related concentration alternations conventionally concern a group of VOCs rather than a single compound[28]. Apart from this, the concentration of a single compound may alternate due to more than one pathophysiological processes, thus being non-specific[14]. Consequently, diagnosis of complex, heterogeneous diseases is scarcely achieved by the recognition of one characteristic stand-alone VOC.[7,14] A mixture of exhaled VOCs, called VOC pattern or "breathprint", consists the signature of a specific disease, being correlated with the underlying pathophysiology, and should, thus, be recognized, for disease diagnosis to be achieved.[7,14,28]

Notably, the composition and concentration of exhaled VOCs – factors fundamentally correlated with the VOC pattern formed and used for diagnosis – depends not only on their systemic production, but also on their physicochemical properties, the respective blood concentration and the different alveolar processes of clearance[15]. Higher concentration of a VOC in the mixed venous blood increases alveolar concentration. However, increased ratio between alveolar ventilation and cardiac output, *e.g.,* during stress, decreases

alveolar concentration. Alveolar concentration is also influenced by blood solubility of VOCs, expressed by $\lambda_{b:a}$. Higher solubility decreases alveolar concentration. Considering the storage of various VOCs in the fat tissue, the "fat:blood" partition coefficient should, also, be taken into consideration. Blood concentration of some classes of VOCs is fundamentally connected with the total fat tissue and the total blood volume of an individual.[7]

Additionally, exhaled VOCs are fundamentally connected with the compartment of the respiratory tract studied.[27] The exhaled breath is composed of two main parts; the dead space and the alveolar air. The air of the upper respiratory tract, where blood-breath gas exchange does not occur, comprises the dead-space air ($\sim$150 mL). On the other hand, the air of lower airways, were exchange of VOCs is conducted, comprises the alveolar air. The composition of dead-space air is similar with the ambient air previously inhaled and, consequently, the amounts of VOCs of alveolar air are about two to three times greater than those of dead-space air.[36] Further differentiation of exhaled VOCs in correlation with the airway department is possible. Systemic VOCs undergo passive diffusion in alveolar-capillary interface and are added to the VOCs diffused via the bronchial region (solubility-dependent differentiation, *see 2.1.1*). These two groups of VOCs, along with the VOCs of host/microbiome metabolism, are, finally, added in the VOCs of mouth and nose.

Apparently, appropriate sampling procedure should be applied, depending on the clinical research aim, for the desired part of breath and, thus, VOCs to be collected[27]. The three possible ways of sampling the exhaled breath are upper airway (dead-space air only)[36], mixed air (whole breath) or lower airway/end-exhaled collection, containing only the end of a forced breath (alveolar air). Low-airway sample is, actually, the subject under study.[10,36]

Several diseases types are investigated for potential diagnosis via breath analysis.[7] Respiratory diseases, including Asthma, COPD, Obstructive Sleep Apnea Syndrome, Pulmonary Arterial Hypertension and Cystic Fibrosis,[37] have been extensively studied. Malignant diseases are, also, under extensive investigation for the identification of potential breath biomarkers. LC, Gastric, Head and Neck, Breast (BC), Colon and Prostate cancer comprise the most representative examples. Breathomics is an enticing diagnostic tool for various neurodegenerative diseases, as well. The correlation of Alzheimer's and Parkinson's diseases and Multiple Sclerosis with different VOC patterns are reported.[15]

Metabolic disorders, such as Diabetes and Hyperglycemia, are, also, included.[16,17] Lastly, the significance of metabolic alternations caused by specific species or strains of bacteria has been demonstrated for infectious disease diagnosis.[18,36] In this case, the combination of bacteria-derived VOCs,[36] and VOCs produced by the host due to immune response to bacterial antigens, as well as VOCs formed due to the host response to bacterial products/metabolites (and vice versa) is detected. Differentiation of the origin of those VOCs is not clinically important.[38] Infectious diseases, like Upper Respiratory Tract Infection, *Mycobacterium Tuberculosis* infection, *Pseudomonas* infection, *Helicobacter pylori* infection have been investigated[16,17]. Recently, research interest focused on the diagnosis of SARS-CoV-2 viral infection via breath analysis, as well, with remarkable results,[39,40,41] with a diagnostic test, "*BreFence Go COVID-19 Breath Test System*", developed by Breathonix[42] being already provisionally approved by the HSA.[43,44]

2.2. Analytical Techniques and breath analysis

Gas Chromatography (GC), used for the separation of compounds contained in a complex gas mixture, is combined with Mass Spectrometry (MS) for the identification of each distinct compound of the mixture[45]. GC-MS comprises the gold-standard method for the analysis of the pattern of VOCs of the exhaled breath.[1,28, 45] Both quantitative analysis – characterized by high sensitivity (ppb to ppt)[1] – and qualitative analysis – providing information concerning the potential metabolic disease pathways[45] – are achieved.[20,28]

For the detection of very low concentrations of VOCs, to be achieved, the pre-concentration of the breath sample is imperative. Pre-concentration techniques commonly combined with GC-MS include thermal desorption[17,45] (using sampling bags/sorbent tubes[45], mainly Tenax tubes[17]), headspace solid-phase microextraction (HS-SPME)[12,17] (using silica fibers, coated with polymeric nanofilm, mainly CAR/PDMS[17]) and Needle Trap Device[17,46] (sorbent polymer – CAR, PDMS and/or DVB – packed in a needle[17]). Apart from GC-MS, also selected ion flow tube-mass spectrometry (SIFT-MS) and ion mobility spectrometry (IMS), proton transfer reaction-mass spectrometry (PTR-MS) [21,28], proton reaction transfer time-of-flight mass spectrometry (PRT-TOF-MS)[1] and GC coupled with mass spectrometry (GC-MS), ion mobility spectrometry (CC-IMS) or flame ionization detector (GC-FID)[17] comprise analytical techniques commonly used for breath analysis.

However, spectrometry and spectroscopic methods exhibit important limitations.[15] Bulky equipment of high cost is used, by appropriately trained personnel, while the analysis is time-consuming[15,47] providing no real-time results[45]. Also, pre-concentration methods, required before the analysis, could potentially lead to sample loss/contamination.[20,47] Thus, despite the advantages of those analytical techniques, their use in clinical practice for point-of-care[19] or screening[45] is prevented.

2.3. Gas sensors and breath analysis

During recent years, methods other than analytical techniques, specifically sensors and e-Noses containing nanomaterials, have exhibited the prospect of becoming strong diagnostic tools *via* breath analysis and are rising up to the existing clinical challenges[19,20,21].

2.3.1. Sensors – Basic Principles and Characteristics

In general, the term *sensor* refers to a device able to receive a signal or stimulus, of physical or chemical nature, and respond, producing an electrical signal. *Chemical sensors* comprise devises that respond to various chemical stimuli and are used in order to identify and quantify specific chemical substances of liquid or gaseous phase (gas sensors). They are extensively used in industry, for process quality control and minimization of health risks due to dangerous gases exposure[48], while their use is investigated in the fields of environmental and health care[49]. The working principle of a chemical sensor is depicted in Figure 2.[50]
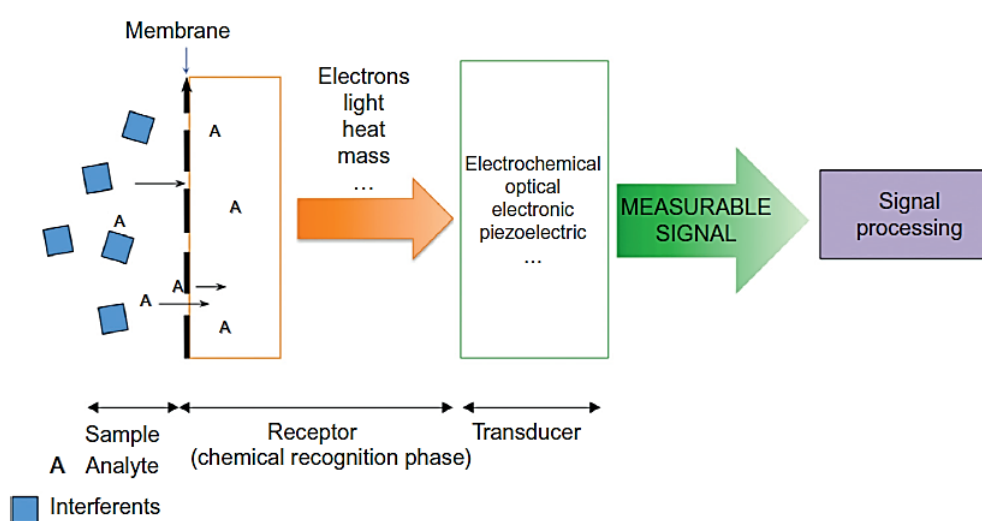

Figure 2. Depiction of the basic working principle of a chemical sensor. *Reprinted with permission from Ref. [50] Copyright © 2014 Elsevier Inc.*

The *recognition element* of the sensor is responsible for the chemical recognition of the desired compound (analyte) and is able to transform the chemical information (*e.g.,* pH, concentration) into a measurable form of energy.[50] The molecular interaction of the sensor with the targeted analyte during exposure leads to commonly reversible physical or chemical alternations.[30] A thin film is commonly used to enhance recognition element function, by interacting with the analyte molecules, participating in a chemical equilibrium along with the analyte or selectively catalyze a reaction. The second important chemical sensor component is the *transduction element,* or else *transducer,* which converts the chemical information into a measurable analytical signal, based on electrochemical, optical

Table 2. Definitions of performance parameters used for sensor evaluation.[26]

Parameter	Definition
Sensitivity	Alternation of sensor output response per unit of analyte concentration over the entire range of signals. Greater performance of the sensor is indicated by higher sensitivity.
Selectivity	Ability to differentiate the targeted analytes in a complex mixture of various gases. Exposure of the sensor in a sample containing the desired analytes in the presence of potential confounding compounds permits the measurement of selectivity (using the calibration curves of response vs concentration, the ratio of response signal of the analyte to those of interfering compounds is measured).
Limit of Detection	The lowest concentration of gas analyte that the sensor can reliably detect.
Dynamic Range	The range of operation, from the limit of detection to the upper limit of detection.
Response time	The time that the sensor needs for a stable response (90% of final response) to be achieved.
Recovery Time	The time that a sensor needs to reach the initial state (10% of the baseline) after the analyte is removed from the sensing chamber.
Signal-to-noise ratio	The ratio of the intensity of a sensor signal (desired) to the intensity of the background noise (undesired).
Stability	The ability of producing the same output response over time, for a given experimental condition.
Reproducibility	The ability of the sensor to produce equal output response for different experimental conditions.

piezoelectric or electronic properties.[50] The electrical output signal of the sensor can be channeled, amplified, and modified by electronic devices[48]. Gas sensors respond to the presence of an analyte commonly by changing the electrical signal measured (current, capacitance, resistance/impedance, voltage or electrical potential). The evaluation of gas sensor performance is achieved by quantifying a series of specific parameters (Table 2).[26]

2.3.2. Use of nanomaterial-based sensors in breath analysis

2.3.2.1. Advantages of nanomaterial-based sensors

During last decades, research interest has notably focused on the development of chemical sensors incorporating nanomaterials.[6,50,51,52] Despite exhibiting inability of qualitative

analysis in complex samples and poor quantitative performance, as well as humidity sensitivity and relatively short life, nanomaterial-based gas sensors possess major advantages that render them exceptionally promising[16]. The small dimensions (typically 1-100 nm) increase the surface-to-volume ratio and the interaction sites of nanomaterials[6,15]. The creation of novel interfaces[53,54] leads to high sensor sensitivity and small response/recovery times[6,15]. Higher specificity for a desired analyte is also achieved, by sensibly selecting physical and chemical properties of the nanomaterials[6,15]. Those properties are attributed to the size, shape and composition of nanomaterials[54] and can, thus, be easily modified[6,15]. The similar dimensions between nanomaterials and biomolecules renders the former attractive for application in medical diagnostic devices[54]. Combination of nanomaterials with different properties – easily accomplished by large-scale manufacturing methods[15] – permits synergistic sensing ability of the device[6,15], also characterized by simple, portable and energy-efficient operation[6].

2.3.2.2. Sensing Approaches

Exhaled VOCs analysis using sensors – especially nanomaterial-based – can be achieved by two different approaches. In the first case, a targeted approach is applied, using a selective mechanism.[7,27] The target is recognized by a *selective chemical sensor*, designed to measure this single compound in a complex mixture, based on lock-key mechanism[7]. Such selective sensors have been developed for NO, NH_3, acetone, H_2O_2[6,15], H_2S and CH_3SH[15].

Disease diagnosis via breath analysis can be achieved detecting a unique VOC pattern, rather than a single exhaled compound, as already mentioned. *Semi-selective/cross-reactive sensors* are artificially intelligent nanoarrays[15] mimicking natural sensing systems[54,55], also called "electronic noses" (e-Noses), "artificial olfactory systems" (for gas analytes) or "electronic tongues" (for liquid analytes). Distinct sensors constituting the array respond to all/large part of the components of a complex mixture[54], at the same time, in a competitive way[55]. Due to their diversity, each individual sensor of the array responds differently (yet not chemically selectively) to a given mixture. Statistical pattern-recognition algorithms and classification techniques are used for the establishment of analyte-specific response patterns, combining the responses of the sensor array elements.[54] As a result, an algorithm able to distinguish different mixtures of VOCs is constructed[55]. It is noteworthy

that even the analytical techniques, *e.g.,* GC-MS, are progressively used for the analysis of total patterns of VOCs, instead of targeting a stand-alone biomarker[28]
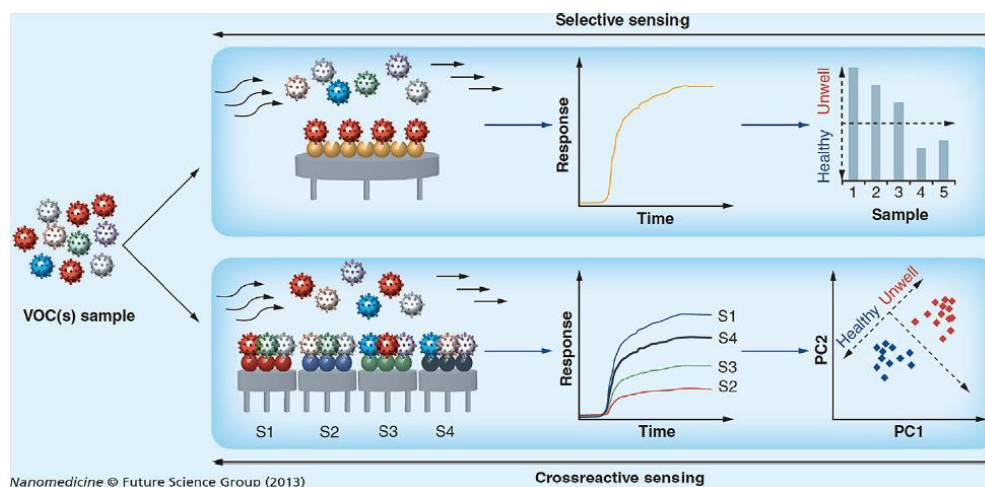
Figure 3. Schematic representation of working principle of nanomaterial-based selective sensors and cross-reactive sensor arrays. *Reprinted with permission from Ref. [20] Copyright © 2020 Elsevier Inc.*

Multivariate data analysis, a fundamental tool in breath analysis, improves the human perception of experimental data[29]. Response data obtained after sensor array exposure to a complex chemical mixture are processed by multivariate data analysis[56] in order to assess the discriminating ability of the sensor array[29,57], as well as for the elimination of potential confounding variables (i.e. environmental temperature and humidity).[56] Multivariate data analysis is also useful for breath analysis using analytical techniques, permitting the identification of the most discriminant VOCs between the different groups studied[18]. Numerous multivariate analysis methods are used in e-Nose systems, including Canonical Discriminate Analysis (CDA), Partial Least Squares regression (PLS regression), Discriminant Function Analysis (DFA) and Principal Component Analysis (PCA).[56] PCA comprises the most commonly used method in e-Nose systems[56], while DFA is also frequently used.

PCA is an unsupervised learning technique in which the multidimensional data space is reduced to its main components.[29] Linear combinations of original data (i.e. sensor values) capturing the maximum variance between all data points are acquired[29,58], leading to a reduced set of variables[59], called principal components (PCs). The differentiation of the PCs maintaining most of the original data information from the PCs with the minimum effects, which are excluded, is achieved by appropriate algorithm[59]. PCs define new orthogonal axes, for the multidimensional data to be represented in two or three dimensions only[29,58]

(data of lower dimension[59]). Thus, a visualized statistical analysis is obtained, permitting discrimination of otherwise entangled data[59]. PC1 is characterized by the greatest response variance, while the magnitudes of variance are diminished from PC2 to PC3 and so on[29,58].
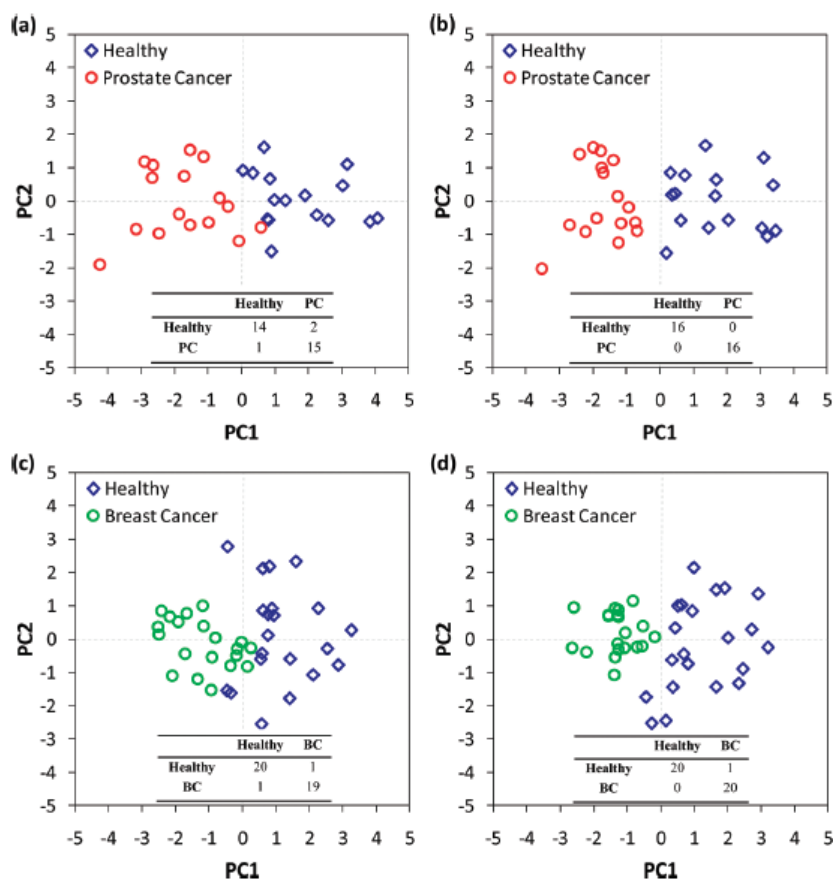
Figure 4. Representative two-dimensional PCA plots for breath analysis results, for prostate cancer diagnosis (a) without and (b) with relative humidity compensation, and for breast cancer diagnosis (c) without and (d) with relative humidity compensation. *Reprinted with permission from Ref. [58] Copyright © 2012, American Chemical Society.*

DFA is a linear supervised pattern recognition method, also used for multidimensional experimental data reduction[60]. DFA aims to separate previously known groups to the best possible extent[61]. The determination of the classes to be discriminated is conducted prior to the analysis[60]. Input variables are linearly combined, to achieve the maximum variance between classes and the minimum variance in each class[60,61]. DFA output is a set of canonical variables (CVs) which comprise the dimensions that fulfil the previous two requirements. The first CV is the most powerful discriminating dimension[60].

In order to evaluate sensor array suitability for disease diagnosis, assessing the ability to correlate VOCs with the appropriate disease, machine learning techniques[60], such as

Support Vector Machines (SVM), k-nearest neighbor (k-NN) and neural network analysis[56], are also needed. Machine learning techniques are a field of artificial intelligence aiming at permitting machines to automatically imitate a specific behavior, designing and developing algorithms based on empirical data, representative of the relation between the observed attributes[62]. The automatic learning of complex patterns and the intelligent decision making, based on current data, comprises one of the principal research fields in machine learning[62] and is especially useful in the development of e-Noses for disease diagnosis.

ANN is a commonly used machine learning technique, inspired by human nervous system. The most discriminant sensing features are firstly determined and comprise the input data of the ANN. The input data are connected with the output (i.e. the classification of samples to specific disease) by the ANN, using a set of appropriate functions. The classification from the available inputs is ameliorated by optimizing specific parameters, such as the number of neurons (calculation centers), which are in charge of the calculations of the system.[60]

2.3.2.3. *Required properties of sensors for application in breath analysis*

A number of requirements have to be fulfilled for the use of a nanomaterial-based sensor in breath analysis for disease diagnosis. Reproducibility[6] and high sensitivity, for small concentration alternations to be detected[15], are two fundamental parameters. Low limit of detection (LOD)[15,26] (ppb[54]), wide range of response[54] and increased selectivity are of great importance, in order to detect the exhaled VOCs in the presence of water vapor found in the humidified clinical samples[15]. Stable baseline in VOC absence[6], short response and recovery times are imperative[15,26], while full recovery of the sensor after analyte removal from the sample chamber is essential as well. Alternatively, disposable sensors can be used, providing simple and low-cost production are possible, permitting massive manufacturing.[15] Last but not least, operation at RT is important[54].

2.4. Polymeric Films and Gas Absorption

Gas sensors commonly possess a thin polymeric film as a sensing element, interacting with the gaseous analytes, provoking an alternation of a measurable property. As analyzed later, polymeric films are commonly combined with nanomaterials. The second part of the thesis analyzes the factors affecting response and selectivity of a polymeric film-based sensor. Consequently, it is necessary to describe the background of the processes that take place.

Gas absorption into the sensing polymer is the key process changing a measurable film property (mass, resistance). On Table 3, four usually confused terms, with similar terminology are presented[63,64]. Gas absorption is deemed as gas dissolution in absorbent[64], while adsorption and absorption usually occur simultaneously[63]. Measurable property alternation, due to gas absorption, both thermodynamically and kinetically controlled[65]. Gas absorption is governed by the diffusion laws (Fick's First and Second Low, kinetic factor[66]), while gas solubility (thermodynamic factor[66]) in the polymer is also required[67].

Table 3. Definitions of adsorption (physical/chemical), absorption and sorption.

Phenomenon	Definition
Physical Adsorption	Surface phenomenon. Gas molecules: on the surface of the material, via dispersion forces.[63]
Chemisorption	Surface phenomenon. Gas molecules: on the surface of a material, via chemical bonding.[63]
Absorption	Bulk phenomenon[64]. Gas entrance inside the absorbent, changes the solid structure, without chemical bond formation. Swelling of absorbent swelling is commonly caused.[63]
Sorption	Physical sorption and absorption, without chemical bonding formation.[63]

2.4.1. Diffusivity

The diffusion coefficient D, or else *diffusivity* (in m^2/s) expresses the amount of matter (m) passing through a unit area per second, due to a unit gradient of concentration. D is, time and temperature and gas concentration dependent[66], while it is also significantly dependent on the polymeric material[68]. In the case that D is only temperature dependent diffusion is called *Fickian diffusion*. Simple gases undergo Fickian diffusion in polymers, while D is independent on the concentration of the penetrant and penetrant-polymer interactions are weak. In contrast, in the case of organic vapors, gas-polymer interactions are stronger and D is concentration dependent.[66] Generally, gas diffusion is thermally activated. The energy required for the dissolved molecule to jump into another hole of molecular size of the polymeric matrix (activation energy of diffusion) comprises the predominant parameter of diffusion. In the case of organic vapor, activation energy is gas concentration dependent.[66] It is, generally, greater for larger molecules, while diffusivity is smaller.[66,68] Thus, diffusivity is closely correlated with the molecular size of the analyte.

Diffusivity comprises an important parameter determining the sensor-response rate. Gas diffusion acceleration in the polymer leads to faster change of the measurable property and, thus, faster response. Recovery time is, also, expected to be reduced, as desorption is

the reverse process of absorption.[69] Consequently, factors affecting gas diffusivity in the polymeric matrix are expected to determine sensor response/recovery time.

2.4.2. Solubility

Gas absorption in the polymeric matrix is also dependent on gas solubility in the polymer, or else the affinity of the gas for certain polymers, which is a thermodynamic factor[66]. In general, the nature and the magnitude of polymer-penetrant interactions in reference to penetrant-penetrant and polymer-polymer interactions determine the penetrant solubility in a polymer. Shape and size distribution of open spaces between the polymeric chains, in which the penetrant molecules dwell, also comprises an important factor.[70] Organic-vapor solubility in polymers follows primarily the general rule of solubility "like dissolves like", i.e. it is driven intermolecular forces formed between the two compounds. These may include dispersion/non-polar, permanent dipole-permanent dipole/polar and hydrogen bonding interactions.[67,71] From a similar point of view, chemical structure similarity of polymer and gas could be taken into account, as similar chemical structures favor solubility.[66]

2.4.2.1.   Hansen solubility parameter (HSP)

Various theories and methods have been proposed to predict gas solubility and sorption in polymers[71,72,73,74,75,76,77,78,79], with some concerning, specifically, polymeric sensing films of gas sensors[80,81]. Remarkably, *solubility parameter, δ*, firstly introduced by Hildebrand and evolved by Hansen, comprises a widely used method in industry and academia, and has been applied for the prediction of gas solubility in polymers. The simplicity of this approach has rendered δ a key parameter for various similar applications, including solvent selection in industry, surface characterization and prediction of polymer compatibility, permeation rates, solubility, rubber swelling extent[67,71] and drug-excipient miscibility[82].

The total energy of attractive forces holding the molecules of a liquid together (*cohesive energy*) equals the vaporization energy, E[66,67,71,74]. δ is defined by (eq.1), where the *cohesive energy density* (*ced*), refers to the cohesive energy per unit volume (V: molar volume):[67,71,74]

$$\delta = \sqrt{ced} = \sqrt{E/V} \,, \mathrm{MPa}^2 \quad (1)$$

Taking into consideration the dispersion, E_d, polar, E_p, and hydrogen bonding, E_h, cohesive energies, due to the respective intermolecular forces, Hansen defined δ as:

$$\delta^2 = {\delta_d}^2 + {\delta_p}^2 + {\delta_h}^2 \quad (2)$$

where δ_d, δ_p and δ_h are the solubility parameters derived from E_d, E_p and E_h.[67,74] The interactions between small molecules of one substance as expressed by δ, can be used to predict their interactions with the molecules of another (or the monomers of a polymer) and, thus, their miscibility.[83] Miscibility between a polymer and a solvent, for example, is favored if their δ are equal or similar.[66] Respectively, since solubility is demanded for gas absorption in polymers to occur, similar HSPs are expected to enhance gas absorption. Thus, absorption equilibrium probably correlates with HSP values.[67] The difference between HSPs is given by the equation (3), where (P) and (G) indicate the polymer and gas, respectively. The smaller the $\Delta\delta$, the greater the gas solubility in the polymer is.[66]

$$\Delta\delta = \sqrt{\left(\delta_{d(P)} - \delta_{d(G)}\right)^2 + \left(\delta_{p(P)} - \delta_{p\,(G)}\right)^2 + \left(\delta_{h(P)} - \delta_{h(G)}\right)^2} \quad (3)$$

2.4.2.2.   Calculation of HSP – Van Krevelen Method

Solubility parameters of molecules and polymers can be calculated by group contribution methods. In group contribution methods, the desired property of a molecule is estimated by the values that the groups, from which the molecule is composed of, possess for this property, using additive rules. Despite providing an approximation of the property, group contribution methods are characterized by simplicity and have been used for the estimation of a variety of different properties, leading to satisfying results.[67] Various methods have been developed for the estimation of Hansen solubility parameters, including those by Hoy, van Krevelen and Hoftyzer and Hansen and Beerbower, among others.[67] Despite leading to somehow different results, those methods have effectively been applied.[67,84,85] Specifically, van Krevelen method has been extensively used[84,85] and comprises an easily applicable method.

Van Krevelen method is based on the molar attraction constant, defined as

$$F = \sqrt{ced} \cdot V \quad (4)$$
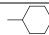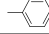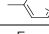
The additive rules on which this method is based are the following:

$$\delta_d = \frac{\sum F_{di}}{V} \quad (5) \qquad \delta_p = \frac{\sqrt{\sum F_{pi}^2}}{V} \quad (6) \qquad \delta_h = \sqrt{\frac{\sum E_{hi}}{V}} \quad (7)$$

where F_d and F_p are the dispersion and polarity components of molar attraction constant, respectively, and E_h is the hydrogen bonding energy. The group contributions F_{di}, F_{pi} and E_{hi} for various structural groups are presented on Table 4. In the case that two identical polar

groups are located in symmetrical positions, δ_p is multiplied by a symmetry factor. For molecules with several planes of symmetry, $\delta_h = 0$.[66]

Table 4: Solubility parameter component group contributions – Hoftyzer–Van Krevelen method.[66]

Structural Group	F_{di} $(MJ/m^3)^{1/2} \cdot mol^{-1}$	F_{pi} $(MJ/m^3)^{1/2} \cdot mol^{-1}$	E_{hi} J/mol
−CH₃	420	0	0
−CH₂-	270	0	0
>CH−	80	0	0
>C<	-70	0	0
=CH₂	400	0	0
=CH−	200	0	0
=C<	70	0	0
−⬡	1620	0	0
−⬡	1430	110	0
−⬡ (o, m, p)	1270	110	0
−F	(220)	–	–
−Cl	450	550	400
−Br	(550)	–	–
−CN	430	1100	2500
−OH	210	500	20,000
−O−	100	400	3000
−COH	470	800	4500
−CO−	290	770	2000
−COOH	530	420	10,000
−COO−	390	490	7000
HCOO−	530	–	–
−NH₂	280	–	8400
−NH−	160	210	3100
>N−	20	800	5000
−NO₂	500	1070	1500
−S−	440	–	–
=PO₄	740	1890	13,000
Ring	190	–	–
One plane of symmetry	–	0.50x	–
Two planes of symmetry	–	0.25x	–
More planes of symmetry	–	0x	0x

Chapter 3: Methods

The current thesis is based on a profound literature research, conducted during the period 25/02-30/05/2021, using the databases Scopus, PubMed and SpringerLink. The aim of the thesis is, firstly, to provide an overview of the types of nanomaterial based-gas sensors used for breath analysis, and, thereafter, to propose a method for polymeric sensing film-selection, for a polymer-coated metallic nanoparticle-based sensor, for asthma, COPD, LC and BC-related discriminant VOC detection. Thus, the three fields on which the literature research focused on include:

1) Exploited properties of nanomaterials and working principle of sensors potentially used in breath analysis for disease diagnosis – current applications.

2) VOCs identified patients' breath and characterized as discriminant for the diseases selected, in more than one studies, using analytical techniques, and

3) Factors affecting gas absorption in polymer and, thus, the selectivity and response of sensors using polymeric sensing films.

In the databases referred, the combinations of key words [nanomaterials AND sensors AND breath], [nanomaterials AND sensors AND "breath analysis"], ["nanomaterial-based sensors" AND vocs], ["nanomaterial-based sensors" AND "breath analysis"], ["sensor array" AND voc AND breath], ["electrochemical sensor" AND vocs] and ["electrochemical sensor" AND "breath analysis"] were used for the first subject, [asthma AND voc], [breathomics AND asthma], ["volatile organic compounds" AND asthma AND diagnosis], ["breath analysis" AND asthma], [copd AND voc], [breathprint AND copd], ["exhaled breath" AND voc AND copd], [lung cancer" AND voc], [copd AND "lung cancer" AND "breath analysis"], [asthma AND "lung cancer" AND "breath analysis"], ["breast cancer" AND voc] and ["breath analysis" AND "breast cancer"] for the second, and ["gas sensing materials" AND polymers], ["gas sorption in polymers"] ["gas solubility in polymers"] and [polymer AND "gas adsorption"] for the last field.

The articles selected were written in English and published after January 1, 2004. Duplicate articles and conference papers were excluded.

As far as the research for the categories of nanomaterials and sensors is concerned, research articles, review articles and book chapters were included. The studies selected focus on the detection of VOCs in both synthetic and real-world samples, using non-commercial sensors based on conventional materials and/or nanomaterials. In the case of synthetic samples, the targeted VOCs were either selected as biomarkers by the researchers, or characterized generally in the literature as known disease biomarkers.

For the compilation of the VOCs that are reported to differentiate asthma, COPD, LC or BC patients from healthy subjects research and review articles were selected. Only human studies were used, in which breath samples were analyzed, using analytical techniques, and the identity of VOCs was determined, while experiments based on cell lines were excluded. Retrieved studies concerning the use of commercial electronic noses for disease diagnosis were separately selected.

The determination of the factors and the properties of the polymer that affect sensor response and selectivity towards VOCs was based on research articles, as well as book chapters. The selected studies focused on sensors possessing polymeric sensing films, on which diffusion and solution of the analytes occur. It should be noted that some of the book chapters used were published before 2004. The reference lists of the articles were reviewed as well, for additional relevant studies to be included.

Chapter 4: Results

4.1. Nanomaterial-based sensors in breath analysis

4.1.1. Categories and Properties of Nanomaterials Used

Different nanomaterials have been used in several gas sensors for VOC detection, as transduction elements[6]. Metallic NPs, carbon nanotubes, silicon nanowires[6] two-dimensional materials, metal oxide semiconductors in the form of nanowires, nanorods or nanoribbons[26] and hybrid materials are representative investigated nanomaterials.[52]

4.1.1.1 Metallic nanoparticles (MNPs)

Noble metals (Au, Ag, Pt, Pd) possess exceptional chemical, physical and electronic properties.[86] They exhibit increased conductivity[26], mechanical robustness[86], oxidation resistance and, thus, chemical stability.[26,86] In the form of NPs, additional novel properties – attributed to the increased surface area and the domination of quantum-mechanical rules[87] – are exhibited, with optical (LSPR phenomenon)[47] and electrical[87] being the most interesting for gas sensing. The mechanical, optical and electrical properties of MNPs are composition, size, periodicity and interparticle distance dependent[87]. Notably, chemical environment-dependence of those properties renders MNPs promising for gas-sensing[47,86].

MNPs, extensively investigated in gas sensors for breath analysis applications, are usually combined with other nanomaterials (*e.g.,* CNTs, graphene, MOS), to form more effective sensing materials, by increasing sensitivity and selectivity of the sensing element[26,47]. AuNPs, for example, can be used for thiol vapors and H_2S sensitive detection, due to increased chemical affinity[86,88]. Concerning gas-sensor sensitivity, it is, in general, enhanced by the presence of NPs, including metallic, on the surface of other sensing nanomaterials, due to defects formation, on which gases are preferably adsorbed. Smaller NPs lead to greater surface area, increasing the defects and, thus, sensor sensitivity.[89] MNPs can, also, be functionalized with a variety of organic ligands, forming thin films with tunable chemical selectivity (molecularly-capped NPs, MCNPs), characterized by controllable interparticle distance and, thus, reproducible production.[54] Apart from organic ligands, also polymers can be used as coating materials of MNPs, for chemical cross-selectivity to be achieved[57].

4.1.1.2. Metal oxide semiconductors (MOS)

MOS are commonly used in different types of sensors as sensing materials, oxidizing or reducing gas detection. Transition MOS (*e.g.,* NiO, Cr_2O_3) are more efficient for gas sensing

applications than the non-transition MOS (ZnO, SnO_2), due to more than one preferred oxidation states.[7] Increased affinity of MOS for negatively charged oxygen species (e.g., O_2^-, O^-), in contrast to compound semiconductors (e.g., GaAs)[90], provokes the creation of surface-trapped charge density; electron depletion layers are formed in n-type and hole accumulation layers in p-type semiconductors[7,90]. Gas interaction with the adsorbed oxygen species alternates the surface charge density, alternating resistance.[7] Specifically, oxidation of reducing gases by the adsorbed oxygen species leads to electron transfer towards the semiconductor surface. The adsorption of oxidizing gases, on the other hand, provokes removal of additional electrons from semiconductor surface.[90]

Both n-type MOS, including SnO_2, ZnO, WO_3, TiO_2, MoO_3, In_2O_3 and Fe_2O_3, and p-type MOS, such as Co_3O_4, CuO, NiO, Cr_2O_3 and Mn_3O_4, have been used in gas sensors for disease diagnosis[90]. MOS sensitivity is affected by numerous parameters, such as morphology, porosity, particle size, film thickness and doping of MOS, decoration with noble metals, as well as operation temperature.[24] Consequently, various MOS of different structures have been investigated for gas sensors as diagnostic tools, for a variety of diseases. MOS are commonly combined with noble MNPs and 2D-materials. WO_3, for example, has been used as villi-like nanostructures[91], Pt-NP decorated nanotubes[92] and hemitubes combined with graphene[93] for NO[91,92], toluene[92], acetone or H_2S[93] detection, as asthma, LC, diabetes and halitosis biomarkers, respectively. Pt-NP decorated SnO_2 nanotubes/hierarchical fibers[94], SnO_2-NPs/noble metal NPs decorated-SnO_2 nanosheets[95] CuO decorated-SnO_2 NWs[96] have been studied as well, for acetone, toluene[94] nonanal[95] and H_2S[96] detection.

Interestingly, in some cases MOS arrays, such as Pt/Si/Pd or Ti-doped SnO_2 NPs[97], pristine and PtNP-decorated WO_3 hemitubes[98] and WO_3, SnO_2 or In_2O_3-based thin films/Au-thin films/villi-structures[99] have also been used for cross-sensitive applications, for diseases such as LC, diabetes, halitosis, kidney disorders and asthma. Notably, among the semiconducting nanomaterials CNTs, graphene-based nanomaterials and MOS, the latter have exhibited the highest response towards acetone, thus holding great promise for diabetes diagnosis[90]. Despite their enticing applications, however, MOS possess important limitations, including high temperature operation[26] (150-500ºC) and confinement to single gas detection, due to lack of selectivity towards polar-nonpolar compounds.[7]

4.1.1.3. Carbon nanotubes (CNTs)

CNTs are investigated as gas sensing materials for their interesting electrical, mechanical, optical and thermal properties[26,100], as well as for their compatibility with other nanomaterials for enhanced performance[7]. CNTs are divided into single wall CNTs (SWCNTs), with a diameter range 1-5 nm[86], and multi wall CNTs (MWCNTs), with a diameter range 5-100 nm[7] and an interlayer spacing of 3.4 Å[86]. Concerning their electrical properties, which are most commonly exploited, SWCNTs act as metallic conductors or semiconductors (depending on the chiral angle between hexagons and tube axis), while MWCNTs behave as metallic conductors, with current density up to 10^9 A/cm^2.[7]

CNTs-analyte interaction may include Van der Waals or donor-acceptor interactions. Gas adsorption-provoked charge-transfer, though, is the main mechanism of CNTs-based gas sensing. SWCNTs, specifically, can function as p-type semiconductors.[7,26,86] Oxidizing gas-adsorption, such as NO_2, decreases sensing-layer resistance, due to electron withdrawing by the gas. In contrast, reducing analyte-adsorption, such as NH_3, increases resistance.[26] Apparently, in this case SWCNTs comprise both the sensing element and the transducer[86].
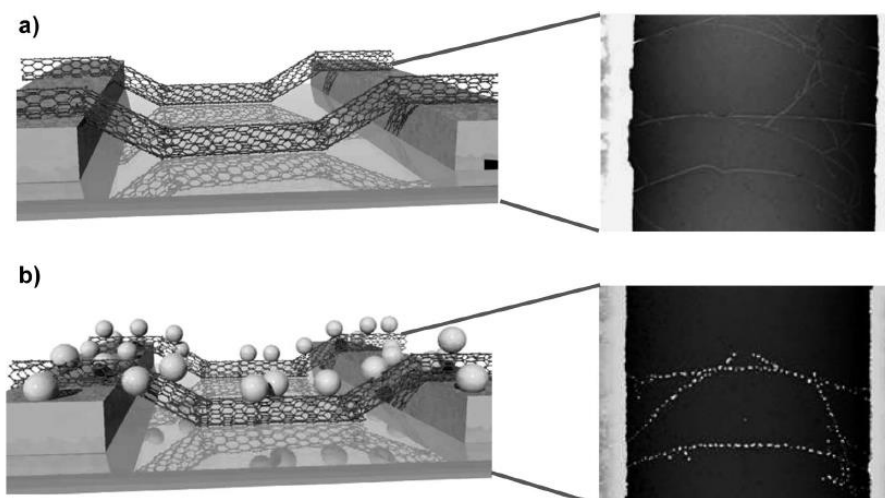
Figure 5. Schematic representation and SEM images of (a) carboxylated SWCNTs aligned between Au electrodes and (b) Au-decorated carboxylated SWCNTs, as a sensing film of gas sensor (FET), for enhanced H_2S sensing. *Reprinted with permission from Ref. [88] Copyright © 2011 Wiley-VCH Verlag GmbH&Co. KGaA, Weinheim.*

Both categories of CNTs, however, are characterized by lack of chemical selectivity, high H_2O affinity, low sensitivity for nonpolar compounds[54] and slow recovery[7]. For this reason, functionalization is imperative. Decoration with MNPs for enhanced selectivity (*e.g.,* AuNPs

for H$_2$S detection[88]) is referred in the literature.[54] More importantly, CNTs are commonly functionalized with analyte specific entities, covalently (esterification, amidation of carboxyl groups added to CNTs) or non-covalently (supramolecularly, via Van der Waals and π-π interactions).[86] Modification of CNTs with non-polymeric organic layers[54] (*e.g.,* polycyclic aromatic hydrocarbons[101]) or polymers[86] (*e.g.,* PCL, PLA, PC, PMMA and BPR[102]) have been used for the development of effective cross-reactive gas sensors as diagnostic tools via breath analysis. Additionally, CNTs-polymer based sensors targeting single volatile biomarkers, most commonly ammonia, have been developed[86,103,104].

4.1.1.4. Nanowires (NWs)

NWs have, also, been investigated for gas sensing systems, with SiNWs being by far the most common. MOS-NWs have also been investigated as semiconducting sensing elements for VOCs detection, as previously referred. SiNWs possess interesting optical and electrical properties and compatibility with the technologies currently used in microelectronics[54], acting as n-type or p-type semiconductors, with maximum operation temperature that of 150 °C. Conductivity is altered depending on the nature of the gaseous analyte (oxidizing/reducing) and the type of SiNWs (n- or p-type), while the adsorption of charged oxygen species (O$_2^-$ at 150 °C) determines the NWs conductance properties, respectively to MOS.[105] VOC polarity is of great importance, as well, as physical adsorption of polar molecules, via Van der Waals or electrostatic interactions, affects the surface potential[7,105].
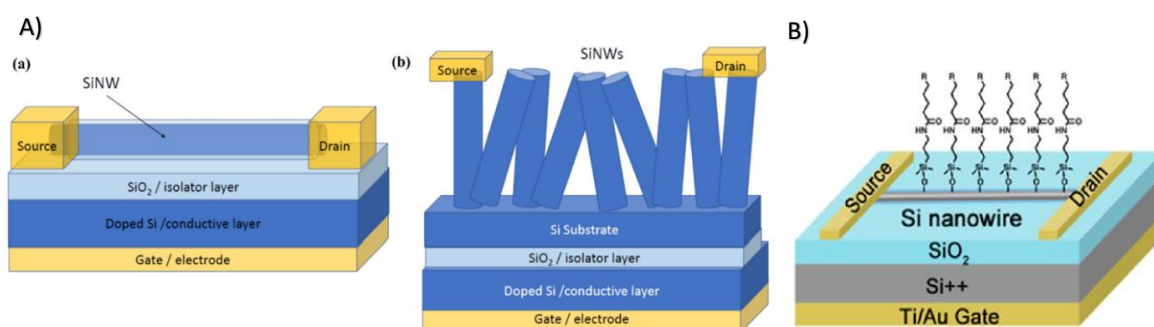
Figure 6. Schematic representation of A) SiNW-based gas sensor (FET) with horizontally (a) or vertically (b) formed NWs. *Reprinted from Ref. [105],* and B) molecularly modified SiNWs-based gas sensor (FET). *Reprinted with permission from Ref. [108] Copyright © 2014, American Chemical Society.*

Modification of SiNWs properties is feasible[7]. SiNWs doping determines sensor sensitivity, affecting the number of charge carriers of the NWs, similarly to MOS[105]. Chemical functionalization with appropriate molecular ligands (*e.g.,* alkane-backbone silane[106],

trichloro phenethyl silane or heptanoyl chloride[60]), on the other hand, enhances sensor selectivity, as non-polar vapor detection by pristine SiNWs is inefficient, in contrast to polar VOCs[7]. Molecular modification serves, also, the fabrication cross-reactive sensor arrays, for the detection of VOC patterns as potential biomarkers[54,60,107,108].

4.1.1.5. Two-dimensional (2D) materials

2D-materials, such as graphene, MoS_2, $MoSe_2$, WSe_2 and $NbSe_2$ have been investigated for gas sensor development. Their main advantage is the low-powered sensor operation at RT, while they are characterized by unique electrical properties[26] and large surface-to-volume ratio[26,109]. The latter renders 2D materials excellent candidates for gas sensing applications[109]. Gas analyte adsorption at the multiple active sites of the edges and surface defects of the layer alternates the electronic properties of the material. Similarly to CNTs, charge-transfer interactions comprise the basis of gas sensing mechanism.[26] Gas adsorption alternates the resistivity of the sensor, depending on the type of gas (reducing/oxidizing) and semiconducting 2D-material (p-/n-type)[109]. Among 2D-materials, MOS, previously analyzed, transition metal dichalcogenides and graphene are extensively used in gas sensing systems, targeting disease diagnosis via breath analysis[7,90,109].
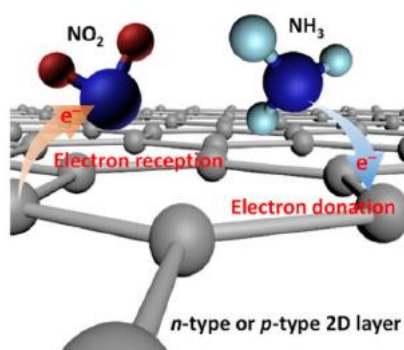
Figure 7. Schematic representation of surface charge transfer interactions between NO_2 and NH_3 molecules and a semiconducting (p- or n-type) 2D material. *Reprinted with permission from Ref. [109] Copyright © The Korean Institute of Metals and Materials 2018.*

Transition metal dichalcogenides (TMDs) (MX_2, M: transition metal, X: S, Se or Te), such as MoS_2, $MoSe_2$, WSe_2 and $NbSe_2$,[26] WS_2, SnS_2 and $SnSe_2$[110], possess great structural and optical features[111] and tunable semiconducting properties[110], that render them prospective materials for e-Nose development. TMDs are able to create flexible structures and operate at low temperatures, however, the increased response/recovery times and the inability to

fully recover after analyte exposure are important limitations[110]. To cope with these issues, catalytic MNPs, which also improve sensor selectivity, may be combined[110,111].

Graphene is characterized by exceptional electrical, thermal and mechanical properties, with the low resistivity (10^{-6} Ω) at RT and the large surface-area (2630 m^2/g, higher than CNTs', 1000 m^2/g[90]) being the most promising for gas sensing. Graphene can also behave as a p-type semiconductor, while chemical functionalization is easily achieved.[7,110] Graphene derivatives have also been used for gas sensing applications. Graphene oxide (GO) is characterized by a lower cost of production, however, its application in electronic devices is hindered by reduced conductivity. Reduced graphene oxide (RGO), on the other hand, exhibits tunable conductivity, along with greater gas responses than graphene, due to the presence of oxygen functional groups that enhance gas adsorption.[109,110]

Graphene has been studied for selective, rather than cross-reactive, gas sensor development, targeting mainly NO_2, NH_3 and H_2S, [109] as potential biomarkers for diabetes, asthma, renal diseases, halitosis and LC[90]. The detection of other biomarkers, such as formaldehyde[112], toluene and 1,2-dichlorobenzene[113] by graphene-based sensors or acetone by a RGO-based sensor[114] are also reported. However, it is noteworthy that the use of RGO-based gas sensors for biomarker-selective detection needs further investigation, since the underlying gas-functional groups interactions are evasive.[90]

2D materials are usually combined with various nanomaterials, for enhanced sensing[7]. The poor sensing performance of pristine 2D materials is primarily attributed to the weak interactions of the adsorbed molecules and sensing layer[26]. Graphene and RGO combined with MOSs[93,112] and MNPs[95] may serve the development of gas sensing diagnostic tools.

4.1.1.6. Hybrid Materials

Apparently, combinations of nanomaterials to form *hybrid materials* are extensively investigated for gas sensing applications in disease diagnosis. The combination of different (nano)materials improves sensing selectivity and sensitivity[7,26,54] due to their synergic action, rendering hybrids particularly promising.[53] Combinations of CNTs with MNPs, 2D materials with MOS or MNPs, as well as MNPs[57,115], MOS NPs or CNTs with polymers are only some of the combinations reported[7]. Particularly polymers ((semi-)conducting/non-conducting[56]) are commonly used for chemical selectivity to be achieved. Conducting

polymers (*e.g.,* polyaniline, polypyrrole, polythiophene), with conjugated double bonds in their backbone, combine the electronic, magnetic and optical properties of metals or semiconductors with the mechanical properties of common polymers. Conductivity alternation is provoked by electrically-active analyte adsorption, due to redox interactions with either the backbone or the incorporated particles, in the case of composites.[86] Non-conducting polymers are used as sensing films, incorporating conductive NPs such as MNPs[57], CNTs[86] or carbon black particles[116], for semi-selective analyte absorption, which leads to mass or conductivity changes of the polymeric nanocomposites. Molecular imprinting polymers (MIPs) are a new class of sensing films, in which artificial analyte-specific cavities have been created, for specific molecular recognition.[117,118]

4.1.2. Types of Nanomaterial-based Sensors in Breath Analysis

Different types of nanomaterial-based sensors have exhibited promising diagnostic ability via breath analysis[7]. In the following part, those chemical gas sensors are categorized and presented depending on the transduction method applied.

4.1.2.2. Optical Sensors

Optical gas sensors detect analytes by measurable changes of absorption, luminescence, scattering, reflectivity, refractive index or optical path length[56], provoked by the interaction of the radiation with the desired gas or a selective layer[48]. In the first two cases, light intensity or wavelength are measured.[56]

Optical Fiber based

Working Principle

Optical fibers, possessing a chemical reagent (*e.g.,* chemical dye) or a sorbent phase (*e.g.,* polymeric film) as a reactive layer, are commonly used as transduction elements in optical gas sensors[6,48], specifically for VOC detection[6]. Upon vapor exposure, optical or structural changes of the reactive layer alter the effective index and, thus, the light transmission properties of the fiber.[6]

Sensing materials and diseases/analytes

Nanomaterials, single polymers or combinations have been used for optical fiber modification, as sensing films for VOC detection. Hydrocarbon and aromatic compound detection, as potential biomarkers of various diseases, (Table 5), for instance, has been achieved, using a poly[methyl(3,3,3-trifluoropropyl)siloxane]-coated optical fiber, with low

LOD, attractive for disease diagnosis.[119] As a hybrid material, a thin film of poly (allylamine hydrochloride) and SiNPs, infused with tetrakis (4-sulfophenyl) porphine, has been used as an optical-fiber coating, for the selective detection of methanol, in presence of water and other alcoholic vapors.[120] Also, PMMA-based fibers functionalized with nanocrystalline bismuth oxide clad have effectively detected NH_3, ethanol, methanol and acetone, exhibiting increased selectivity for methanol.[121]

The use of graphene, usually combined with MNPs[122,123] has, also, been investigated. PtNPs-GO[122] and AgNPs-GO[123] functionalized optical fibers have been efficiently developed for NH_3 selective detection. Remarkably, PtNPs-functionalization increased the sensitivity in comparison to pristine GO, while the concentration of AgNPs was inversely correlated with the sensing sensitivity, thus designating the benefits, as well as the vulnerability of the synergistic effects of hybrid materials.

Despite the fast response and recovery of such optical sensors, as well as their extensive investigation, in laboratory level, in the field of breath analysis for VOCs detection, they are scarcely studied for real sample experiments[6].

Colorimetric
Working principle

Colorimetric sensors, usually classified as a sub-group of optical sensors[87], are based on environmentally dependent color changes[15]. Chemo-responsive indicators, able to chemically react and change color in a distinct way upon exposure to different gas analytes[6] are used, permitting analyte identification[6,15]. Thus, the response upon analyte exposure is based, not on the physical properties, but the chemical reactivity of the indicators[15].

Sensing materials and diseases/analytes

There are five possible categories to which an indicator may belong to; pH responsive, (Brønsted acidity/basicity); metal-ion-containing dyes (Lewis basicity – electron pair donation); redox-responsive metal salts; nucleophilic indicators (responsive to electrophilic analytes); dyes with large permanent dipoles (e.g., solvatochromic dyes)[6]. Such optical sensors have been extensively investigated for cross-reactive applications in the field of breath analysis, mainly for LC diagnosis (Table 5)[124,125,126,127]. The main challenges of such sensors, however, include low sensitivity, high limits of detection and response times.

Furthermore, their irreversible operation, that renders the development of disposable single-use tests obligatory, is of great importance.[7,128]
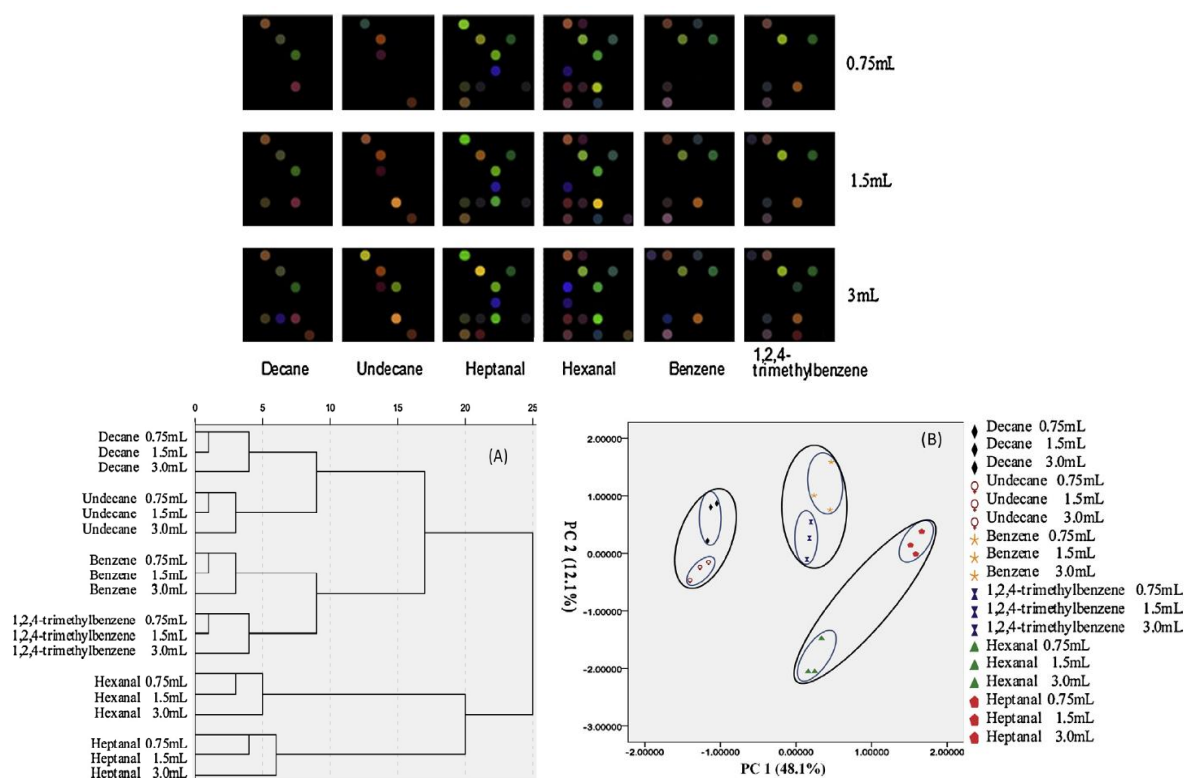
Figure 8. Detailed color difference maps of six VOCs at three volumes (0.75 mL, 1.5 mL and 3 mL saturated vapor, respectively) saturated analyte vapor at 20°C, acquired by a metalloporphyrin-AuNRs and dyes based optical chemical sensor. Detailed HCA (A) and scatter diagram of PCA (B) for the six VOCs of three volume concentrations at 6.5 min. *Reprinted with permission from Ref. [129] Copyright © 2014 Elsevier B.V.*

Nanomaterials have been used for enhanced sensing properties. For the detection of VOCs as LC biomarkers, for instance, the use of AuNRs modified metalloporphyrins, protected from photodegradation, lead to good repeatability and increased long-term sensor stability and shelf-life.[129] Apart from MNPs, other nanomaterials can be used for the enhanced colorimetric sensors performance. Lead Acetate (PbAc$_2$) NPs anchored to polyacrylonitrile nanofibers, for example, were investigated, for H$_2$S colorimetric detection, as a halitosis biomarker, with a LOD of 400 ppb, far lower than the 5 ppm of PbAc$_2$ paper tests.[130]

LSPR-based

Working principle

Non-conventional chromophores, such as MNPs (*e.g.,* Au, Ag, Cu), have also been investigated in optical sensors, due to their interesting optical properties. Localized surface

plasmon resonance (LSPR)-based gas sensors[47,56] are based on the dependence of the NP refractive index on the surrounding dielectric environment of the NP[47] (*i.e.,* coating, surrounding medium, supportive substrate[87]). Refractive index alternation changes the wavelength of the incident light. The main advantage of MNPs are the extinction coefficients of several orders of magnitude higher than those of conventional dyes, in the visible region, allowing higher sensitivity and lower LOD for the desired analyte.[87]

Sensing materials and diseases/analytes

Optical detection of VOCs using various compositions and shapes of MNPs has been reported. AuNPs, AgNPs and AuNSs have been used for chlorobenzene, *m*-xylene, pentanol, toluene and octane[131]. Hybrid materials containing MNPs have been used as well. Polymer-coated Au nano-islands, for instance, have effectively detected a-pinene.[132]

SERS-based

Working Principle

Another, more widespread, application of the LSPR phenomenon of MNPs in optical sensors is SERS[47], *i.e.,* the enhancement of Raman signals enhancement due to the LSPR phenomenon. SERS is a vibrational spectroscopy technique[133] that permits single-molecule detection levels, and has been investigated, among others, for VOCs detection, as potential biomarkers[134].

Sensing materials and diseases/analytes

Functionalization of different MNPs with appropriate molecules has been reported for selective VOC-detection. Aldehyde detection as LC biomarkers, by SERS-based sensors seems prospective.[134,135] Dendritic Ag nanocrystals, coated with the aldehyde-selective probe molecule *p*-aminothiophenol achieved low LOD (low ppb), in presence of confounding LC biomarkers (hydrocarbons, alcohols, ketones, esters, nitrogen and aromatic compounds).[135] NO detection, as a biomarker of asthma[47], as well as hypertension, arteriosclerosis, diabetes and rheumatoid arthritis, has also been achieved. *o*-Phenylenediamine-modified AuNPs have permitted selective chemical reaction between functionality moieties and NO, that leads to nanoprobe SERS variations, achieving a LOD of $1.7 \cdot 10^{-7}$ M, in presence of H_2S and CO.[133]

As it can be observed, SERS-based sensors have been developed for the selective detection of a specific VOC or classes of VOCs, rather than cross-reactive detection. Notably, optical

sensors, in general, are not preferred for e-Nose development, mainly due to their size and the complexity of the signal conditioning systems needed.[56]

4.1.2.3. Piezoelectric Sensors

Generally, piezoelectric materials produce voltage due to mechanical stress applied, and vice versa[87]. Piezoelectric sensors are sensitive to mechanical stress[15] and are used as mass-sensitive sensors[47]. Acoustic wave devices are used in piezoelectric sensors, also called mass, gravimetric or microbalance sensors. An oscillator circuit is used for acoustic waves generation, allowing the piezoelectric crystal used to resonate.[48] The most important categories of piezoelectric gas sensors are the QCM and SAW[56].

Quartz Crystal Microbalance (QCM)

Working Principle

QCM sensors possess quartz crystal resonators functionalized with different appropriate sensing elements (*e.g.,* metalloporphyrins[136,137], sensitive polymers, MOS or nanomaterials).[6,56,128] The acoustic wave propagates through the bulk of the crystal perpendicularly to the surface, as well as on the surface with motion parallel to it.[87] When a gas is absorbed on the sensitive surface of a crystal, the mass changes, alternating the resonance frequency.[128] Typically, mass increase, decreases the oscillation frequency of the resonator[48], which comprises the measured physical quantity[128].

Sensing materials and diseases/analytes

QCM sensors are extensively used for both selective and cross-reactive VOC detection, and are potentially applicable in breath analysis. MOS have been used as sensing films for selective detection (*e.g.,* ZnO NWs[138] and vertically-aligned ZnO NRs[139] for NH_3 detection). Notably, VOC detection with MOS-QCM sensors is feasible at RT, despite the use of MOS, as detection is directly connected to mass alternation, thus semiconductor charge carriers are not needed[139]. Polymeric materials have been extensively used as well. Selective detection using polymeric nanofibers (*e.g.,* PAA/PVA[140] and PEI/PVA[141] nanofibers for NH_3 and formaldehyde detection, respectively) and MIP-composites (SiNPs-containing MIP for hexanal detection, as LC biomarker, in presence of trimethyl amine, NH_3, ethanol, acetone, acetic acid and diethyl ether[118]) has been demonstrated.

For cross-reactive applications, hybrid[142] (Table 5) and polymeric sensing materials could potentially be applied in breath analysis. Thiophene derivatives used for acetic acid,

toluene, acetone, *p*-xylene, ethanol, 1-octanol, acetonitrile and water discrimination based on polarity[143], macrocyclic calixarene derivatives for ketones, alcohols, aromatic, chlorinated compounds detection[144] and MIP used for hexanal, nonanal and benzaldehyde detection[117] are some representative examples. Metalloporphyrin-based cross-reactive sensors, though, investigated in real-world samples, seem as the most promising among QCM sensors, as observed on Table 5. Such sensors have been examined for asthma, COPD, halitosis[6], LC and Tuberculosis diagnosis[7] with particularly increased accuracy percentages.

Surface Acoustic Wave
Working Principle

In *SAW* gas sensors, the acoustic wave propagates only in parallel to the surface of the piezoelectric crystal, penetrating about one acoustic wavelength in depth into the crystal. Motion at the surface is both parallel and perpendicular to it.[87] Crystal surface is modified with a chemically selective layer[48,56]. Exposure to the analyte affects the propagation waves[48], as the mass (acoustic field of the SAW) and/or the electrical conductivity (electric field of the SAW, associated with the acoustic field) of the chemical interface are changed[15]. Propagation frequency alternation of the SAW is caused and can, then, be measured[6,56].

Sensing materials and diseases/analytes

Non-functionalized[145,146] or polymer-functionalized[147] SAW sensors have been combined with GC columns, as detectors, for point-of-care diagnostic systems development. Breast cancer[145], Tuberculosis[146] and LC[147] patients, for instance, have been effectively diagnosed, with accuracy 79%, 84% and 80%, respectively. Mere SAW sensors are, also, used for the detection of both polar and non-polar VOCs, after modification with appropriate sensing films.[6]

As in QCM sensors, MOS and polymers have been extensively used. MOS-based sensing films, including ZnO, SiO_2, TiO_2, Co_3O_4, WO_3 and combinations[7,148] have most commonly been used for selective VOCs detection (*e.g.,* ZnO/SiO_2 bi-layer nanofilms[149] or SiO_2/TiO_2 films[150] for NH_3, ZnO/WO_3[151] for ethanol detection). More interestingly, cross-reactive detection by MOS-based SAW sensors has been reported. Using a layer of amino-terminated iron oxide NPs, butanol, isopropanol, toluene and xylene, were detected with low LOD (1, 12, 3 and 0.5 ppm, respectively)[152]. Polymeric film-based SAW sensors are more widespread for cross-sensitivity. Sensor arrays with polymeric coatings of different

composition (*e.g.,* eight different polymeric coatings for chloroform, octane and xylene discrimination[153]) or thickness (*e.g.,* polyisobutylene films of thickness 10, 50 and 100 nm for chloroform, chlorobenzene, o-dichlorobenzene, heptane, toluene, hexane and octane discrimination[154]) have been reported. Such MOS and polymer-based SAW sensors hold a great promise for potential breath analysis applications.

Additionally, CNTs[7,148] and hybrid materials[53,89] have, also, served as sensing films. SWCNTs and MWCNTs dispersed in ethanol or toluene, for example, have been separately tested for ethanol, toluene and ethyl acetate sensing at RT, with a LOD of 1 ppm.[155] The main advantage of CNTs is the enhanced SAW sensor-sensitivity, due to the ability to sense variations not only in mass, but also in conductivity.[148] MWCNTs combined with other materials (*e.g.,* polyepichlorohydrin and polyurethane with different MWCNTs percentages in a 4 sensors-array, for toluene and octane detection[156] and CeO_2 for acetone and ethanol detection[157]) have permitted selectivity enhancement. Calixarene-modified AuNRs/AgNCs[53] and pristine or AuNPs-functionalized zeolitic-imidazole-framework nanocrystals[158] used for the detection of LC and diabetes biomarkers, respectively, in low ppm levels, comprise examples of attractive hybrid materials, as well (Table 5).

In comparison to QCM sensors, SAW are generally characterized by higher sensitivity, while, as it can be observed, surface modification abilities are wider. On the other hand, it can be noticed that, in both cases, apart from the sensing film composition that determines sensor selectivity, the high surface area of the nanostructures comprises the fundamental factor enhancing sensitivity, due to the creation of more adsorption sites (defects).[89,139,141,152] In general, piezoelectric gas sensors, investigated primarily in synthetic samples, are characterized by increased sensitivity, small response time and low-powered operation. However, the low signal-to-noise ratio and the complex electronic circuits required may render this type of sensors less enticing for efficient e-Noses.[56]

4.1.2.4. *Electrochemical sensors*

Working Principle

Electrochemical sensors are divided into potentiometric (voltage measurement), amperometric (electric current measurement) or conductometric (conductivity or resistivity measurement) and demand a close circuit for the measurement[48]. Analyte

detection occurs on appropriate electrodes, on which a chemical reaction, oxidation or reduction, takes place. Electrochemical sensors typically consist of a *sensing* (*working*) *electrode* and a *counter electrode*, separated by a thin layer of electrolyte.[87] The sensing electrode, on which the reaction occurs, is characterized by high surface-to-volume ratio, for signal enhancement, and is composed of catalytic materials, *e.g.,* platinum, palladium or carbon-coated metals,[48] specific for the desired analyte[87]. Analyte-electrode reaction generates a sufficient electrical signal[87], measured with respect to the counter electrode.[48]

Sensing materials and diseases/analytes

Electrochemical sensors have mainly been used for selective detection of gas biomarkers. For this purpose, conventional, polymeric and hybrid materials have been studied. Prussian Blue electrocatalyst-modified carbon electrodes on wearable, paper-based sensor, has been developed, for example, for H_2O_2 detection, as a lung-disease biomarker[159]. As an example of polymeric sensing films, cylindrical-nanoporous semiconducting polymers have permitted NH_3 detection in ppb levels, via a redox reaction[160]. Hybrid materials, especially containing 2D nanosheets, are also reported in the literature for oxygen-compounds. AuNPs decorated-MoS_2 nanoflakes for instance, have been used for oxygen-based VOCs detection, such as the diabetes biomarker acetone[111], while solid proton-conducting electrolyte based on sulfonic acid co-functionalized cellulose nanofibers and GO nanosheets has been developed for ethanol detection via oxidation, with LOD 25 ppm[161].

Cross-reactive electrochemical sensors have been reported as well, for *in vivo/in vitro* studies, aiming at diabetes, lung[162] and gastric cancer[163] diagnosis (Table 5). Polymers[162] and nanomaterials, including MNPs, CNTs, SiNWs, graphene derivatives and combinations, have been used. Remarkably, ultrahigh sensitivity for two gastric cancer biomarkers (Table 5) has been achieved using a Au-AgNPs-MWCNTs glass carbon electrode, attributed to the high surface area of both MWCNTs (Au-AgNPs adsorption enhancement) and Au-AgNPs (electron-transfer acceleration). The synergistic catalytic activity of the bimetallic NPs, on the other hand, enhances sensor-selectivity.[163] Notably, electrochemical sensors are constrained detecting the electrically inert simple aromatic compounds and hydrocarbons, as the target analyte should be electrochemically active.[87] However, recently, the detection of cyclohexane, along with formaldehyde, has been reported using a SiNW-rGO sensing film, due to cyclohexane-oxidation catalysis by rGO.[164]
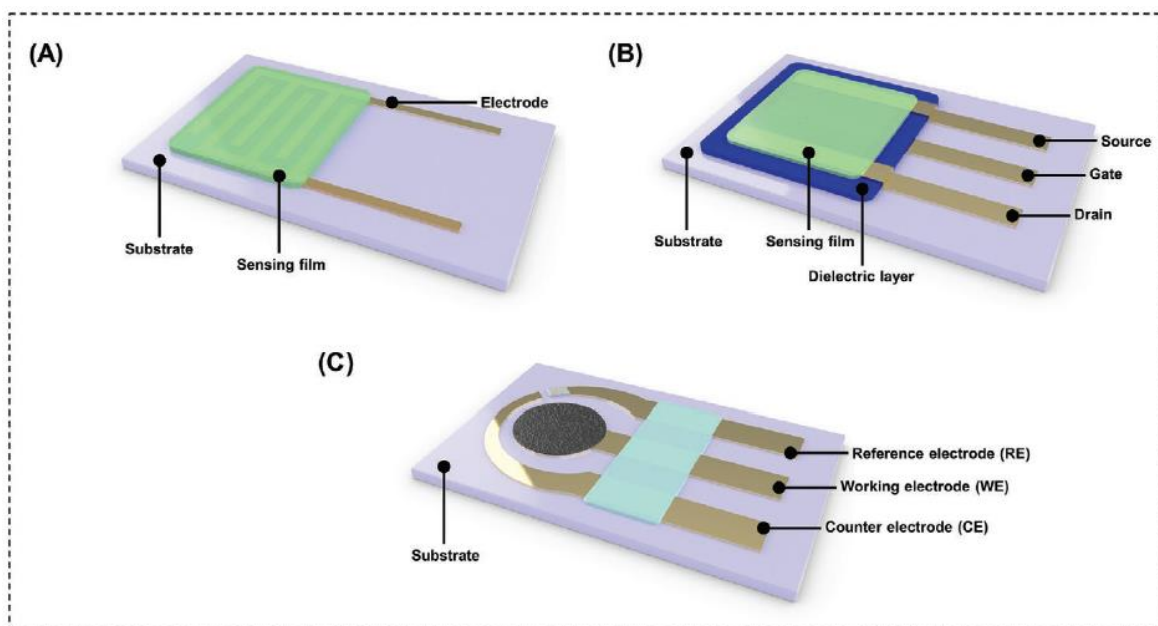
Figure 9. Schematic representation of a (A) chemiresistor (B) transistor and (C) electrochemical sensor. *Reprinted with permission from Ref. [26] Copyright © 2021 Wiley-VCH GmbH.*

4.1.2.5. Field-effect Transistors (FET)

Working Principle

Field-effect Transistors are voltage-controlled[6] devices consisting of two electrodes – the source and the drain electrode – a semiconducting channel, an insulating gate and a conducting gate electrode[26]. The current flows between the source terminal and the drain terminal through the semiconducting channel, by applying a source-drain potential. Voltage applied between the source terminal and the gate terminal controls the current flowing between the source and the drain, as well as the conductivity of the conduction channel. For a constant source-gate voltage, exposure to gaseous analytes can affect the conductivity of the conduction channel.[6, 26]

Depending gas analyte-type and the carrier of the channel material (holes/electrons), the charge carrier concentration of the semiconducting channel material and, thus, the channel current, can be altered upon sample exposure. In the case of an n-channel FET (electrons as charge carriers) oxidizing gas exposure leads to electron withdrawing from the n-sensing layer, reducing the majority carriers of the channel region and, thus, decreasing the current flowing through this. In the case of exposure to a reducing gas (electron donating) or FET with a p-type channel (positive holes as charge carriers) exposed to an oxidizing gas, the current flowing through the channel increases. Measurement of current alternations

permit the detection, as well as the quantification of gas analytes, after appropriate calibration.[26] The gate voltage applied permits control of sensor sensitivity, providing it is set in order to permit the maximum conductance variation[165].

A chemical FET can also possess a gas-selective coating/a series of coatings between the transistor gate and the analyte. Different chemical modification of the gate allows reaction with different chemical species, permitting their differentiation.[48,60] For ion sensitive FETs, charged species at the sensing interface of the gate alternate the polarization of the semiconductor/dielectric interface beneath. Electron conductance through the semiconducting channel is sensitive to gate polarization and the chemical modification of the gate can either attract or repel the semiconductor-charge carriers. Thus, measuring the source-drain current, the polarization of the sensitive interface can be determined.[87] Channel conductivity is also affected by the gas-analyte polarity. Adsorption (molecular gating) of polar molecules on the outer surface of the conducting channel is considered to provoke changes in the electric field. Molecular binding of non-polar molecules potentially alternates the density of charged surface states of the functionalized semiconductor surface, due to analyte induced conformational alternations, or affects the dielectric medium close to the semiconductor surface.[6,166]

Sensing materials and diseases/analytes

FET sensors are commonly developed using nanomaterials as sensing elements, comprising the conductive channel, however, mainly for the detection of simple gases. CNTs, specifically SWCNTs acting as p-semiconductors, have been extensively investigated for the CNTFET gas sensor development, possessing p-transistor characteristics.[7,86] Pristine CNTs have been used for the detection of the oxidizing gases NO[167] and NO_2[167,168,169] and the reducing gas NH_3[167,169], as well as for ethanol and benzene detection[169].

2D material-based FETs have been developed as well, using TMDs or graphene derivatives. WS_2 *n*-type semiconducting multilayer nanoflakes have been used for ethanol and NH_3 detection under light illumination[170], while MoS_2 multilayer-based FETs permit NO[171] or NH_3 and NO_2 detection under illumination[172]. rGO-based FETs permit ethanol[173], NH_3 and NO_2 detection achieving low ppb LOD[174], while NH_3 detection is also reported using NO_2-dopped graphene[175].

NWs are also a common sensing material for FET sensors, including SiNWs and MOS NWs, such as SnO_2, ZnO, In_2O_3[105,165]. Using pristine SiNWs, it is possible to accurately discriminate VOCs with high dielectric constants, such as methanol, ethanol and 2-propanol, using pattern recognition methods.[176] As far as MOS NWs are concerned, mainly *n*-type MOS have been studied. SnO_2 NWs, for instance, have been used for acetone, ethanol and methyl ethyl ketone accurate discrimination, by gate or temperature modulation of the FET sensor, that alternates sensor responses and affects VOC selectivity[177]. *p*-type MOS NWs are also reported to achieve effective VOC detection, such as CuO NWs for NO_2 and ethanol vapor detection[178]. Complementary-MOS based sensors have also been investigated, along with pattern recognition methods, especially for acetone, acetic acid ethanol, propanol, butanol and hexanol discrimination. In this case, selectivity was also achieved, alternating the drain-source and gate potential, without any further modification[179].

FET arrays development, with elements based on different nanomaterials have also been reported. For example, n-type semiconducting In_2O_3, SnO_2 and ZnONWs combined with SWCNT-FET, have successfully discriminated H_2 and N_2 and the VOC ethanol.[180]

Hybrid materials have also been used in FET sensors. 2D graphene/MoS_2 heterostructured flexible and potentially wearable devices, in which graphene replaces the metallic electrodes, have been reported for NO_2 detection[181]. Combinations of CNTs with other materials for sensing performance amelioration are also reported in the literature, such as polypyrrole-SWCNTs for NH_3[182] and Au-decorated SWCNTs for H_2S[88] detection. Molecularly functionalized CNTs have also been used for nonpolar and polar VOCs detection. As representative LC biomarkers, decane and 1,2,4-trimethylbenzene, have been effectively detected. Notably, it has been observed that CNT-functionalization determines the semiconducting character of the material (tricosane-CNTs: *p*-type, pentadecane/dioctyl phthalate-CNTs: *n*-type), thus affecting signal responses.[183] More interestingly, molecularly functionalized SiNWs have been used for cross-reactive FET sensors development, targeting exhaled volatile organic biomarkers of asthma/COPD, gastric and LC, not only in synthetic, but also in real-world breath samples, for patient discrimination (Table 5).[60,184] Chemical functionalization allows for the detection of both polar and non-polar VOCs.

4.1.2.6. Chemiresistors

Working Principle

Chemiresistors comprise promising gas-sensors, characterized by simple configuration and working principle[26], increased reliability and decreased size and weight, while they are able to be automatically packaged in wafer level, permitting massive construction of portable, on-chip sensor arrays[87]. Two pairs of electrodes are connected with an overlying sensing layer, either semiconducting or metallic. IDEs are commonly used for enhanced sensing response.[26] Resistance of the sensing material, the physical quantity measured, changes upon gas exposure, while constant current/potential is applied between the two electrodes[26,87]. Quantitative analysis of the analytes is possible, by measuring the change of resistance/current[26]. Notably, the main difference between chemiresistors and FET sensors is the ability of the latter to provide not only current variations, but also threshold voltage changes upon analyte exposure[165].

Sensing materials and diseases/analytes

Nanomaterial-based sensing films, including MOS, graphene and CNTs are commonly used. MOS-based chemiresistors (*e.g.,* WO_3[91], ZnO[185], SnO_2 or Cu_2O[47]) are used for oxidizing/reducing gases detection[186], both for single analyte detection, such as NO[91], and, more essentially, for sensor-arrays[187] (Table 5). Pristine 2D materials, such as graphene derivatives have also been used for cross-reactive applications[109], *e.g.,* for NO_2 and NH_3[188] or toluene and 1,2-dichlorobenzene[113] detection. CNT-based chemiresistors have been used for NO_2[189] or ethanol[190] selective detection, and, remarkably, for the development of a flexible wearable sensor, to be incorporated in face masks, for the detection of exhaled NH_3, ethanol and formaldehyde[191]. Nylon fibers wrapped with SWCNTs, MWCNTs and ZnO QDs-SWCNTs were used for effective gas discrimination[191].

Furthermore, hybrid materials have been extensively used, particularly for sensor-arrays. MNPs-decorated MOS are a common example[92,94,192,193,194] of chemiresistors detecting toluene, acetone, NO_2 and H_2S as LC, diabetes, asthma and halitosis biomarkers, respectively. The combination of MOS, such as WO_3 hemitubes[93], SnO_2NFs[195] or TiO_2 NFs and nanoribbons[196] with graphene derivatives for H_2S[93,195], acetone[93,195,196], ethanol, NO and CO[196] detection, as well as graphene derivatives with conductive polymers for toluene

detection[197] are reported in the literature. Concerning cross-reactive systems, calixarene-functionalized[198] or MNPs-decorated[199] CNTs have been used to detect aromatic compounds or distinguish NH_3, ethanol, CO and CO_2, respectively. Molecularly functionalized rGO layers, with different amine-ligands have also been used for e-Nose development, for exhaled cancer biomarkers-detection. The molecular ligands, serving as the organic sensing film, alter the adsorption capacity and conductivity of the rGO.[200]

The most common type of hybrid sensing layers, however, are those composed of a conductive inorganic materials, surrounded by an organic functional film, on which the gaseous analytes are adsorbed, alternating the relative distance of NPs and, thus, the conductivity[15]. CNTs, MNPs (e.g., Au, Pt) or carbon black can be used as the conductive part[15] and molecular ligands (MCNPs)[87] or polymers[57] as the organic one. Such sensors offer the prospect of cross-reactive sensor-array development, as the polymeric films[57] or the molecular ligands[29] are selected based on the chemical and physical properties of the VOCs.

> *Sensing Mechanism of organically functionalized conductive nanoparticles layer*

The sensing mechanism of the hybrid NP-organic layer sensing films, is based on two main mechanisms, either for molecular ligand or polymer-based films. Upon organic film-exposure to gaseous analytes, the latter diffuse (absorption) into the organic layer, interacting with the functional groups of the organic film[15].

Those interactions cause swelling of the organic matrix[15], posing a stress to the underlying NPs layer[57], thus increasing the interparticle distance of the conducting NPs[6]. NPs layer-conductivity, however, is exponentially dependent on the interparticle distance, since charge transport between two conducting NPs is explained by the tunneling effect. Specifically, the conductivity, σ, of the sensing film is expressed by the following equation:

$$\sigma = \sigma_o \cdot e^{-\beta \cdot \delta} \cdot e^{-E_a/k_B T} \quad (8)$$

where σ is the electronic conductivity for a given temperature, σ_o is a pre-exponential constant, β is the electron transfer coupling coefficient (or else quantum mechanical tunneling factor), δ is the interparticle distance (or else edge-to-edge core separation), k_B is the Boltzmann constant, T is the temperature and E_α is the activation energy for electron transfer. E_α is given by the following equation:

$$E_a = 0.5e^2 \cdot \frac{r^{-1} - (r + \delta)^{-1}}{4\pi\varepsilon_r\varepsilon_o} \qquad (9)$$

where r is the radius of the NP, e is the electronic charge, ε_o is the permittivity constant and ε_r the dielectric constant of the interparticle medium.[57,87],[115] The resistance, R, of the NPs layer is given by the equation:

$$R_\Omega = \frac{1}{\sigma}\frac{w}{dL} \qquad (10)$$

where w is the electrode gap distance, L is the electrode length and d is the film thickness. [115] According to the above equations, increase/decrease of the interparticle distance, δ, decreases/increases conductivity, σ, (eq.8) and, thus, increases/decreases the resistance measured (eq.10)[6].

The second sensing mechanism of the hybrid NPs-organic layer sensing films correlates with the organic part-permittivity[115]. Sorption of gases with dielectric constant higher than the organic layer increases the permittivity of the organic matrix that surrounds the metallic cores, leading to decrease of the activation energy, E_α, (eq.9). Conductivity is, thus, increased (eq.8) and the resistance measured is lower (eq.10). Respectively, sorption of gaseous analytes with dielectric constant lower than the organic layer increases resistivity. The NPs and organic layers used can be sensibly selected for a specific sensing application.[6]

Molecularly-functionalized conducting nanomaterials have been extensively investigated for the cross-reactive detection of VOCs by Haick et al. Molecularly-capped AuNPs and molecularly-coated random SWCNTs networks have been successfully developed for exhaled VOCs-biomarkers detection using real-world samples, usually in combination with chromatographic analysis of breath samples. Ovarian[61], colon, lung, gastric[29], breast and prostate cancer[29,58], chronic kidney diseases[201], multiple sclerosis[101], Alzheimer's and Parkinson's diseases[15,202] have been effectively diagnosed with such chemiresistors. In the case of multiple sclerosis, for instance, PAH-coated SWCNTs sensor-arrays have, notably, exhibited sensitivity, specificity and accuracy percentages comparable to those of the invasive or expensive techniques used (e.g., MRI, cerebrospinal fluid electrophoresis)[101]. VOCs targeted for the diseases mentioned above are presented on Table 5. In an astonishing application of a MCNPs/SWCNTs-based chemiresistor array (20 sensors), 17 different diseases (Table 5) were successfully discriminated, with 86% accuracy, based on the detection of a pattern of only 13 VOC, whose concentration differed significantly

between healthy controls and/or different diseases.[203] More recently, a MCNPs-based chemiresistor was developed for COVID-19 detection, with remarkable diagnostic accuracy over healthy and non-COVID infected subjects[39]. Despite that targeted VOCs were not referred in this study, the most notable VOCs for COVID-19 are probably methylpent-2-enal, 2,4-octadiene, 1-chloroheptane and nonanal (10-250 ppb)[40].

The size, composition and aggregate size of NPs, the interparticle distance and periodicity, as well as the aggregate thermal stability of such sensors comprise essential, yet easily controlled, parameters[87]. One major drawback of those sensors, however, is humidity sensitivity, a major component of exhaled breath. Thus senor reliability and reproducibility for real-world samples analysis is of major concern. Humidity compensation in the samples is proposed as an effective solution, enhancing the diagnostic ability of the sensor.[58]

Taking into consideration the importance of cross-reactivity for disease diagnosis, a series of representative examples of different types of cross-reactive gas sensors, using conventional materials or nanomaterials, are presented on Table 5. It is noticed that VOCs have been used not only for disease diagnosis in relation to healthy subjects, but also for diseases discrimination (*e.g.,* gastric cancer, LC and asthma/COPD), or even distinguishment of different stages of a disease (*e.g.,* chronic kidney disease stages). Sensitivity, selectivity and discriminant accuracy of the cross-reactive sensors designate their promising application as diagnostic tools. It can be observed that the incorporation of nanomaterials in the sensing element ameliorates the sensing performance (*i.e.,* sensitivity, LOD), while appropriate modification permits the desired cross-selectivity. Sufficient LOD, similar to the usual VOCs concentration in exhaled breath are achieved by all sensor types. As far as MOS-based sensors are concerned, it is apparent that their main drawback towards all the other categories is the increased operation temperature. Chemiresistors are probably the most investigated gas sensor type for cross-reactive systems, incorporating different (nano)materials, being particularly attractive for diagnosis of a wide range of diseases.

Table 5: Cross-reactive sensors for exhaled VOCs detection as biomarkers of several diseases, in real-world or synthetic samples, using conventional materials and/or nanomaterials.

In vivo studies – Real-world samples

Chemiresistor – arrays

Sensing Element	Disease	Targeted VOCs	LOD	No.	Classifier	Results	T	Ref.
Molecularly capped AuNPs – 14 different ligands	Lung cancer	1-Methyl-4-(1-methyl ethyl) benzene, Toluene, 3,3-Dimethyl pentane, 2,3,4-Trimethyl hexane, Dodecane, 1,1'-1-Butenylidene)bis benzene	NA	30 LC, 26 CC, 22 BC, 18 PC, 22 HC	PCA	Good discrimination of cancer types from HC, but not between them.	RT	[29]
	Colorectal cancer	1,1'-(1-Butenylidene)bis benzene, 1,3-Dimethyl benzene, 1-Iodo nonane, [(1,1-Dimethylethyl)thio] acetic acid, 4-(4-Propylcyclohexyl)-4'-cyano[1,1'-biphenyl]-4-yl ester benzoic acid, 2-Amino-5-isopropyl-8-methyl-1-azulene carbonitrile				No VOC overlap in abundance between HC and cancer patients.		
	Breast cancer	3,3-Dimethyl pentane, 2-Amino-5-isopropyl-8-methyl-1-azulene carbonitrile, 5-(2-Methylpropyl)nonane, 2,3,4-Trimethyl decane, 6-Ethyl-3-octyl ester 2-trifluoromethyl benzoic acid						
	Prostate cancer	Toluene , 2-Amino-5-isopropyl-8-methyl-1-azulene carbonitrile, 2,2-Dimethyl decane, p-Xylene						
Molecularly capped AuNPs – 7 different ligands	Prostate cancer	Toluene, 2-Amino-5-isopropyl-8-methyl-1-azulene carbonitrile, 2,2-Dimethyl decane, p-Xylene	NA	9 PC, 10 HC	DFA	100% specificity, 100% sensitivity	RT	[58]
	Breast cancer	3,3-Dimethyl pentane, 2-Amino-5-isopropyl-8-methyl-1-azulene carbonitrile, 5-(2-Methylpropyl)nonane, 2,3,4-Trimethyl decane, 6-Ethyl-3-octyl ester 2-trifluoromethyl benzoic acid		10 BC, 11 HC		100% sensitivity, 95% specificity		
Molecularly capped AuNPs – 3 different ligands	Chronic Kidney Disease	*healthy vs stage 2*: Isoprene, Acetone, Styrene, Toluene, 2-Butatone, 2,2,6-Trimethyl octane, 2,4-Dimethyl heptane; *Stage 2 vs 3*: Isoprene, Acetone, 2,2,6-Trimethyl octane, 2-Butatone, 2,4-Dimethyl heptane; *Stage 3 vs 4*: Acetone, Ethylene Glycol, Acetoin	1-5 ppb	42 CKD, 20 HC	SVM	79% accuracy early-stage CKD vs HC; 85% accuracy CKD stage 4 vs stage 5	RT	[201]

43

Sensor material	Disease	VOCs / Biomarkers	LOD	Samples	Analysis	Results	Temp.	Ref.
Molecularly capped AuNPs – 5 different ligands	Ovarian cancer	Styrene, Nonanal, 2-Ethylhexanol, 3-Heptanone, Decanal, Hexadecane	ppb level	17 OV, 26 HC	DFA	82% accuracy	RT	[61]
Molecularly capped AuNPs – 8 different ligands	COVID-19	NA	NA	49 COVID-19, 33 non-COVID symptomatic, 58 HC	DFA	76% accuracy COVID-19 vs HC 95% accuracy COVID-19 vs non-COVID symptomatic	RT	[39]
PAH-coated random SWCNTs network – 4 different PAHs	Multiple Sclerosis	Hexanal, 5-Methyl-undecane	NA	37 MS, 18 HC	DFA	80.4% accuracy	RT	[101]
Molecularly caped AuNPs / CDs-coated random SWCNTs network – 20 different sensing films	Alzheimer's and Parkinson's disease	24 VOCs	1-5 ppb	15 AD, 30 PD, 12 HC	DFA	85% accuracy AD vs HC 78% accuracy PD vs HC 84% accuracy AD vs PD	RT	[202]
Molecularly caped AuNPs / PAH-coated random SWCNTs network – 20 different sensing films	17 diseases (LC, CC, HNC, OC, BLC, PC, KC, GC, CD, UC, IBS, IPD, MS, PDISM, PH, PET, CKD)	2-Ethylhexanol, 3-Methylhexane, 5-Ethyl-3-methyloctane, Acetone, Ethanol, Ethyl acetate, Ethyl benzene, Isononane, Isoprene, Nonanal, Styrene, Toluene, Undecane	10 ppb	813 any of 17 diseases, 591 HC	DFA, HCA	86% average accuracy	RT	[203]
Pristine WO₃, 0.008 wt % and 0.042 wt % Pt-WO₃ macroporous nanofibers	Halitosis	H₂S and Methyl mercaptan (in presence of Toluene and Acetone)	sub-ppm	4 simulated halitosis breath samples (1ppm), 4 HC	PCA	Successful classification	350 °C	[192]
7 different commercial MOS	Lung cancer	Ethyl benzene, 4-Methyl octane, Undecane, 2,3,4-trimethyl hexane	Down to a few ppb	37 NSCLC, 48 HC	PCA	75% accuracy	300 °C	[187]
Field Effect Transistor (FET) – arrays								
Molecularly modified SiNWs	Gastric cancer	2-Propenenitril, Furfural, 6-Methyl-5-heptene-2-one	Down to a few ppb	30 GC, 77 HC	DFA	> 85% accuracy	RT	[184]
Molecularly modified SiNWs	Gastric cancer	2-Propenenitril, Furfural, 6-Methyl-5-heptene-2-one	Down to a few ppb	149 LC, 40 GC, 56 Asthma/COPD, 129 HC	DFA, ANN	> 80% accuracy	RT	[60]
	Lung cancer	Heptane, Decane, 2-Methyl pentane, 2-Ethyl-1-hexanol, Propanal, Pentanal, Acetone						
	Asthma / COPD	Pentane						
Electrochemical sensor								
Commercial NO, CO sensors, Carbon electrode with linear-selective aldehyde porous poly	Diabetes	NO, CO, Formaldehyde, Acrolein, Propanal, Crotonaldehyde, Butanal, Pentanal, Hexanal, Heptanal, Octanal, Nonanal, Decanal, Acetaldehyde	Low ppb	15 diabetic, 14 HC		Discrimination of LC vs HC, diabetic vs HC	RT	[162]
	Lung cancer			3 LC, 3 smokers, 3 HC		Cross-sensitivity for aldehyde sensor: Moderate for high level of		

Sensor	Application	VOCs	Detection limit	Samples	Method	Results	Temp	Ref
tetrafluoroethylene membrane						ethanol and isopropanol / Weak for H_2S, NO, methanol and 3-heptanone / None for NO_2, propofol, isoprene and acetone		
Optical – Colorimetric sensor arrays								
24 chemically reactive colorants	Lung cancer	NA	Low ppm	92 LC, 137 HC	LPM	Accuracy 81.1% LC vs HC, 82.5-89% one histology vs HC, 86.4% ADK vs SCC	RT	[125]
Optical sensors								
PMTFP-coated optical fiber	Vit.E deficiency	Ethane	pmol/L	20 HC	NA	NA	RT	[119]
	Liver diseases, Schizophrenia, Breast cancer, Rheumatoid Arthritis	Pentane						
	Lung cancer	Heptane, Octane, Decane, Benzene, Toluene, Styrene						
Piezoelectric (SAW) sensor arrays								
GC-column / Polyisobutylene-coated SAW, non-coated SAW sensors	Lung cancer	Styrene, Decane, Isoprene, Benzene, Undecane, 1-Hexene, Hexanal, Propyl benzene, Heptanal, 1,2,4-Trimethyl benzene, Methyl cyclopentane	500 ppb	20 LC, 15 HC, 7 chronic bronchitis	ANN	80% sensitivity and specificity	RT	[6], [147]
Piezoelectric (QCM) sensor arrays								
8 different metalloporphyrins	Asthma	NA	NA	27 asthma, 24 HC	PCA, FNN	87.5% accuracy	RT	[136]
8 different metalloporphyrins	Lung cancer	NA	NA	20 LC, 10 HC	PLS-DA	85% accuracy LC vs HC 62% accuracy ADK vs SCC	RT	[137]
8 different metalloporphyrins	Lung cancer	NA	NA	70 LC, 76 HC	PLS-DA	81% sensitivity, 100% specificity	RT	[204]
In vitro studies – Cell lines / Synthetic samples								
Chemiresistor arrays								
CNT-conductive polymer nanocomposites – 5 different polymers	Lung cancer	isopropanol, tetrahydrofuran, dichloromethane, toluene, n-heptane, cyclohexane, methanol, ethanol, water,	NA	NA	PCA	High sensitivity and selectivity for all the analytes, PC1-PC3 98% of total variance, except the two alkanes	RT	[102]

Material	Application	Analyte	Concentration/LOD	Cell lines	Analysis	Remarks	Temp.	Ref.
Pristine rGO and rGO functionalized with 8 different amine ligands – 9 elements	Cancer	Ethanol, 2-Ethylhexanol, Ethyl benzene, Nonanal	25 ppm	NA	PCA	Successful discrimination of VOCs. The LOD and the effect of humidity have to be decreased	RT	[200]
Pristine Pd, ZnO and polypyrrole NWs	Breast cancer	Heptanal / Acetophenone / 2-Propanol / Isopropyl myristate	8.98 ppm / 798 ppb / 129.5 ppm / 134 ppm	NA	PCA	73.2% PC1 variance. High sensitivity and specificity	RT	[185]
Pristine In_2O_3 and WO_3 NRs, Au, Pt or Pd NPs-decorated In_2O_3 and WO_3 NRs – 8 elements	Diabetes / Asthma / Halitosis	Acetone / NO_2 / H_2S	1.48 ppb / 1.9 ppt / 2.47 ppb	NA	Polar plot	Effective visual discrimination between the gases. Future PCA, DFA and HCA analysis.	150 – 300 °C	[194]
WO_3 NTs	Asthma	NO	50 ppb	NA	NA	NA	350 °C	[92]
Pt NPs – WO_3 NTs, Pd NPs – WO_3 NTs	Lung cancer	Toluene	100 ppb	NA	NA	NA	400 °C	
Pristine, 0.1% wt GO- and 0.1 wt % thin layered graphite WO_3 hemitubes	Diabetes / Halitosis	Acetone / H_2S	1 ppm	NA	NA	NA	350 °C	[93]
Densely packed/ thin-wall assembled/ 5% Pt-decorated/ 10% Pt-decorated/ 20% Pt-decorated SnO_2 fibers	Diabetes / Lung cancer	Acetone / Toluene	120 ppb	NA	NA	NA	300 – 400 °C	[94]

Electrochemical sensor

Material	Application	Analyte	Concentration/LOD	Cell lines	Analysis	Remarks	Temp.	Ref.
MWCNTs / Au-Ag NPs / GCE	Gastric cancer	3-Octanone / Butanone	0.3 ppb / 0.5 ppb	MGC-803 GC and GES-1 gastric mucosa cell lines	NA	Easy cell line - discrimination, high sensitivity, good VOCs selectivity in presence of CO_2, acetone and ethanol	RT	[163]
SiNWs-rGO	Infectious diseases	Cyclohexane, Formaldehyde in presence of Methanol, Ethanol, Acetonitrile, Acetaldehyde and humidity	1 ppm	NA	NA	Novel electrode platform with increased sensitivity, selectivity and repeatability	RT	[164]

Piezoelectric (SAW) sensor assays

Material	Application	Analyte	Concentration/LOD	Cell lines	Analysis	Remarks	Temp.	Ref.
SH-Calix[4]arene, AuNRs, AgNCs, Calix[4]arene-AuNRs, Calix[4]arene-AgNCs	Lung cancer	Chloroform, Toluene, Isoprene, Acetone, n-Hexane, Ethanol	1.52-12.34 ppm for $CHCl_3$	NA	NA	Sensitivity ↑ for all VOCs. Chloroform, toluene: 6-8 times higher sensitivity than individual responses	RT	[53]

Sensor material	Disease	Analytes	LOD / concentration		Analysis method	Notable features	T	Ref
Pristine or AuNPs-functionalized zeolitic-imidazole-framework nanocrystals (ZIF-8, ZIF-67)	Diabetes	Acetone, Ammonia, Ethanol	1.54-2.64 ppm for toluene; 1.1-3.6 ppm for acetone; 0.5-3 ppm for ethanol; 1.6-3.2 ppm for ammonia	NA	PCA	Selectivity↑: modified AuNRs for CHCl₃, modified AgNCs for Toluene; Effective discrimination of diabetes biomarkers	RT	[158]

Piezoelectric (QCM) sensor assays

Sensor material	Disease	Analytes	LOD / concentration		Analysis method	Notable features	T	Ref
TiO₂-MWCNTS on Au layer	Diabetes	Acetone	4.33 ppm	NA	NA	High sensitivity	RT	[142]
Cobalt (II) phthalocyanine-silica on Au layer	Asthma	NO	5.75 ppb					

Optical – Colorimetric arrays

Sensor material	Disease	Analytes	LOD / concentration		Analysis method	Notable features	T	Ref
36 chemically responsive dyes (porphyrins, porphyrin derivatives, sodium fluorescein)	Lung cancer	p-Xylene, Styrene, Isoprene, Hexanal	50 ppb	NA	HCA, PCA, BPNN	100% accuracy of kind and concentration discrimination, promising for real-sample future experiments	RT	[124]
AuNRs-modified metalloporphyrins and pH responsive dyes – 36 spots	Lung cancer	Decane, Undecane, Hexanal, Heptanal, 1,2,4-Trimethylbenzene, Benzene	<1 ppm	NA	PCA, HCA	64.2% accuracy of structurally similar VOCs; 93% photoprotection of metalloporphyrins; Increased repeatability, long-term stability	RT	[129]

AD: Alzheimer's Disease, ADK: Adenocarcinoma, ANN: Artificial Neural Network, BC: Breast cancer, BLC: Bladder cancer, BPNN: Back-Propagation Neural Network, BUN: blood urea nitrogen, CC: Colorectal cancer, CD: Crohn's Disease, CDs: Cyclodextrin derivatives, CKD: Chronic Kidney Disease, COPD: Chronic Obstructive Pulmonary disease, DFA: Discriminant Function Analysis, FNN: Feet-forward Neural Network, GC: Gastric cancer, GCE: Glass Carbon Electrode, HC: Healthy control, HCA: Hierarchical Cluster Analysis, HNC: Head and Neck cancer, IBS: Irritable bowel syndrome, IPD: Idiopathic Parkinson's disease, KC: Kidney cancer, LC: Lung cancer, LOD: Limit of Detection, LPM: Logistic prediction model, MLP: Multi-layer Perceptron, MS: Multiple Sclerosis, MWCNTs: Multi-wall carbon nanotubes, NA: Not Applicable, NCs: Nanocubes, NPs: Nanoparticles, NRs: Nanorods, NSCLC: Non-small Cell Lung Carcinoma, OC: Ovarian cancer, PAH: Polycyclic aromatic hydrocarbons, PC: Prostate cancer, PCA: Principal Component Analysis, PD: Parkinson's Disease, PDISM: Atypical Parkinsonism, PET: Pre-eclampsia toxemia, PH: Pulmonary Hypertension, PLS-DA: Partial Least Square Discriminant Analysis, PMTFP: Poly[methyl(3,3,3-trifluoropropyl)siloxane], RT: Room temperature, SCC: Squamous cell carcinoma, SiNWs: Silicon nanowires, SVM: Support Vector Machine, T: Temperature, TFB: Poly[(9,9-dioctylfluorenyl-2,7-diyl)-co-(4,4'-(N-(4-s-butylphenyl)diphenylamine)], UC: Ulcerative Colitis

4.1.3. Commercially available electronic noses

Various e-Noses technologies, able to "learn" a complex pattern of gases and, then, recognize a sample by comparing them, have been developed. On Table 6, the transducer types used in already marketed e-Noses are presented.

Research concerning application of marketed e-Noses in disease diagnosis via breath analysis is intense. Asthma[205], COPD[206], BC[207] or Pneumonia[208] patient discrimination from healthy subjects using Cyranose 320, as well as discrimination between different diseases, such as asthma/COPD/LC with SripoNose[209], LC/COPD/healthy with Aeonose®[210] and asthma/COPD[211,212], LC/COPD[213] and LC/COPD/LC+COPD/healthy[214] with Cyranose 320 are some representative examples. Disease phenotyping is also possible, discriminating, for example, different asthma phenotypes[215], children with partially controlled and uncontrolled asthma[205] or patients with bronchial/advanced laryngeal SCC[216], using Cyranose 320. However, use in clinical practice is not feasible yet[217,218].

Table 6. Commercially available e-Noses.

Electronic Nose	Technology used	Ref.
Aeonose	Micro hotplate metal-oxide sensors	[217]
BIONOTE e-Nose	QCM sensors using anthocyanin-coated gold electrodes	[217]
Cyranose 320	32 Carbon black-polymer composite chemiresistors	[217], [218]
Tor Vergata e-Nose	QCM covered with Metalloporphyrins	[217]
Common Invent e-Nose	Metal oxide semiconductor sensors	[217]
Owlstone Lonestar e-Nose	Field asymmetric ion mobility spectrometry	[217]
SpiroNose	Cross-reactive metal-oxide semiconductor sensors	[217]
DiagNose	12 Metal oxide semiconductors	[218]
LibraNose	8 QCM gas sensors	[218]

*e-Nose: Electronic Nose, **QCM:** Quartz Crustal Microbalance*

4.2. Polymer-coated MNPs-based chemiresistors

In general, polymer-based gas sensors are able to operate at RT, while the combination with functional nanomaterials further improves sensing ability[57]. Polymers and hybrid NPs-polymer composites have been extensively investigated as sensing films in different sensor types, for detection of VOCs[72,89,100,219], particularly, as potential disease biomarkers[102,118,220]. One type of such hybrid sensing films is composed of chemically unmodified MNPs (Pt[49,52] or Au[115] of mean diameter 4-5 nm[49,52,57]), coated with a polymeric film[57]. The sensing film is formed upon Au IDEs, of overall thickness lower than 30 nm[57],

formed on rigid (*e.g.,* oxidized Si wafer[52,57]) or flexible (*e.g.,* polyimide[49]) substrate as depicted on Figure 10. The sensing mechanism of those hybrid films is described on section *4.1.2.5*.
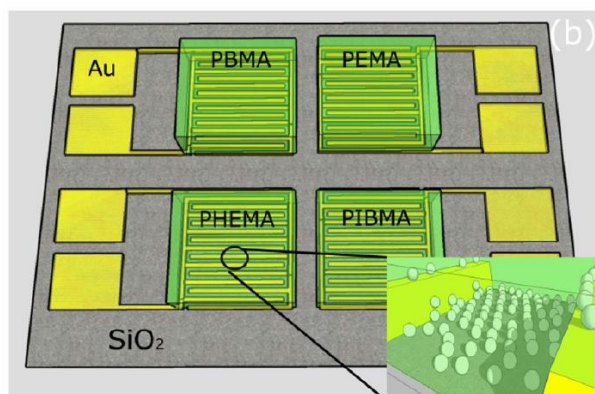
Figure 10. Schematic representation of an array of polymer-coated nanoparticle-based chemiresistors. *Reprinted with permission from Ref [57]. Copyright © 2018 Elsevier Ltd.*

For optimum sensor performance, a series of sensor characteristics have been defined. Device resistance should fall within the range of 600 kΩ-10 MΩ. The ideal IDEs spacing is 10μm, while the NPs-surface coverage should be between 42-46%. NP-surface coverage greater that 46% leads to significantly increased available charge-transport pathways and, consequently, metal-like conductivity, reducing sensing sensitivity. Film thickness, also, affects sensor sensitivity, which is increased by thin polymeric films, possibly due to gas penetration deeper in the matrix.[57] Arrays of this sensor type, possessing polymeric films with affinity for different compounds, along with pattern recognition methods, have been investigated for pesticide detection[57] and are potentially particularly promising for disease diagnosis applications, as semi-selective sensors of exhaled VOCs.

Sensible hybrid film selection, for semi-selectivity to be achieved, is closely dependent on the chemical and physical properties (*e.g.,* polarity, dielectric constant, size and steric effect) of the targeted compounds[6]. The factors affecting swelling and analyte-affinity of the hybrid film are analyzed in detail in the following section.

4.2.1. Factors affecting sensor response and selectivity

Polymer swelling due to gas absorption depends on temperature and sorptive gas pressure[69,64], as well as on the amount of gas absorbed[64]. Polymer selection for the hybrid sensing films should be guided by the factors affecting gas absorption (in given temperature

and gas pressure), which are also expected to affect sensor response and selectivity. As analyzed in section *2.4*, gas diffusion and solubility are closely related with gas absorption into the polymeric film. The factors reported to affect those processes, as well as polymeric film affinity for certain compounds, are briefly presented.

4.2.1.1.   Polymer crystallinity

Both diffusion and gas solubility in polymers are fundamentally correlated with polymeric matrix crystallinity. The increased order of polymer chain packing, characteristic of polymer crystallinity, decreases gas solubility in polymers, since gas solubility is favored by the high free volume of the polymer. It is notable, however, that sorption of different molecules will be affected by the ordered chains of a crystalline polymer to a similar degree.[221] Gas diffusion, on the other hand, is feasible only in amorphous polymers. In the crystalline parts of a polymer, the average length of the paths that the molecules have to travel is significantly increased, inhibiting molecule movement.[66] Thus, polymer crystallinity is of great importance for sensor performance[65,69]. Dong et al. have demonstrated that the addition of crystalline polymer to carbon-black filled amorphous polymeric composites, utilized as swellable gas-sensing film, reduces the maximum responsivity to organic vapors. The group concluded that polymeric sensing film swelling occurs in the amorphous part.[65] Consequently, it could be concluded that crystalline polymers are not deemed as appropriate for the development of swellable gas sensing films.

4.2.1.2.   Polymer Intrinsic Viscosity

It has been reported that the intrinsic viscosity of swellable polymeric sensing films is closely related with sensor response/recovery time. Polymeric matrix viscosity is influenced by the length of the side chains of a polymeric chain, with longer side chains decreasing viscosity values.[69] The ability of the polymeric chains of an amorphous polymer, which form a tangled mass, to untangle and slide towards each other determines the polymeric mass deformability[222] For gas diffusion to occur and the polymeric matrix to respond to the osmotic swelling pressure, relaxation of the polymeric matrix is demanded. The macromolecular chains have to be rearranged, in order to accommodate the absorbed molecules. Apparently, polymer diffusivity and, thus, sensor response time, are favored by low viscosity values.[69]

4.2.1.3. Polymer Glass Transition Temperature (T_g)

Along with viscosity, glass transition temperature (T_g) of the polymeric matrix is reported to affect sensor response/recovery time, as well, no matter gas concentration[69]. It is noted that T_g is a characteristic of amorphous polymers, defined as the temperature at which a viscous, rubbery polymer is transformed to a rigid, glassy solid upon cooling[223]. Polymers with higher T_g are more rigid and diffusion is expected to be lower. Diffusion of small molecules in rigid polymers can also be observed, providing, though, that holes of appropriate size between polymeric chains exist, permitting quite increased diffusion rate.[67] After all, lower T_g values are expected to benefit gas diffusion, enhancing sensor responsivity. Zhang et al. have observed that lower T_g values, as well as viscosity – which vary between different polymers with the same order – lead to lower response time, as well as higher responsivity to organic vapors.[69] Solubility dependence on T_g has also been proposed, by expressing the solubility parameter δ as a function of the difference between ambient temperature and T_g.[66] In general, sorption of a given gas is typically less favored in the glassy form of a polymer, than in the rubbery one[221], since polymeric chains in the rubbery phase possess sufficient thermal energy to move relatively freely[224]. Consequently, the rate and extent of swelling are expected to be higher for a less rigid polymeric matrix. However, there are, also, reports[57,102] of efficient use of polymeric sensing films in $T<T_g$ (glassy phase), despite the theoretical predictions mentioned above.

4.2.1.4. Steric Effects – Molecular Size and Shape

In general, solubility, permeation and diffusion of a compound in a solvent is affected by the molecular size of both the compound and the solvent. Concerning solubility, it is reported that for two solvents with identical solubility parameters (§ 2.4.2.1) and significantly different molar volumes, the solvent of higher molar volume exhibits lower performance. Respectively, solubility is increased for smaller molecules.[67] In the case of polymers, sorption is, also, less favorable for molecules of greater size[221]. Kinetic phenomena, including diffusion and equilibrium attainment, are also favored by smaller molecules. Along with size, shape is also deemed as an important factor for such processes. More linear molecules are characterized by faster diffusion than the bulky ones. Diffusion coefficients for some molecules in rigid polymers may be extremely low, with equilibrium

being unattainable for hundreds of years, at RT.[67] Consequently, polymer/solvent (or polymer/VOCs) miscibility is probably affected by steric and orientation factors.[71]

4.2.1.5. Gas – Polymer Miscibility

It is reasonable that the parameters mentioned above comprise important factors that primarily affect sensor response and performance, so they should be taken into account. However, selectivity and sensitivity of a polymeric sensing film for different organic vapors is expected to depend on VOCs physicochemical characteristics[6], which determine VOC absorption. Thus, VOC nature affects polymer swelling and, consequently, film conductivity.[65] The polarity and the geometric characteristics of the desired VOCs are the most important properties affecting selective vapor absorption.[6] The effects of the geometric characteristics of the absorbed compounds, specifically those of size and shape, were analyzed earlier.

VOC polarity is of great importance, since absorption and swelling are achieved via intermolecular interactions, including Van der Waals interactions, hydrogen bonding, π-π, electrostatic or charge-transfer interactions[87]. The type of interactions developed are determined by the functional groups of the sensing polymer and the targeted compounds. For example, aldehyde detection is favored by the existence of carboxyl and amino groups in the sensing material, mainly due to hydrogen bonding and amino-acid Schiff base formation, without excluding, though, the response towards other gas molecules as well[118]. Apparently, polymer and analyte chemical structures are of great importance.[66,221] In general, polar compounds detection is easier than for non-polar, due to the wide range of potential interactions. For non-polar compounds, where only dispersion forces are developed, steric effects and dielectric changes may also affect the response of the conducting hybrid film.[6] In any case, it is noticed that intermolecular interactions between the sensing polymer and the targeted VOCs are of great importance for gas absorption and impact on sensing film (semi-) selectivity.

HSP concept (§ 2.4.2.1) takes into consideration the intermolecular interactions – dispersion, polar and hydrogen bonding – developed between molecules of the same or different, miscible compounds.[67] Molecular volume incorporation in a new combination of solubility and size parameters has been attempted, for steric effects to be included, without

success though. This is possibly due to the different nature of those parameters (solubility: thermodynamic factor, steric effects: kinetic factor, mainly affecting diffusion rates).[67] HSPs have effectively predicted gas solubility not only in liquids, but also in polymers,[67] as well as for polymer swelling prediction, among others, despite not taking into account penetrant size and shape[67]. For extremely large/bulky molecules, inadequate absorption has been observed, even if the polymer and molecule HPSs indicate this as favorable. Thus, targeting such VOCs with polymer-coated MNPs-based chemiresistors should be avoided.[67]

Interestingly, solubility parameters have been used to interpret polymeric sensing film gas sensitivity, as well. Fu et al. have correlated the maximum resistance response of conductive carbon-nanofibers and/or carbon-black-filled polystyrene hybrid film, with the solubility parameter difference between polystyrene and VOCs studied. Maximum sensor resistance for VOCs with significantly different δ from polystyrene was several orders of magnitude lower than those possessing similar δ.[81] The same relation between maximum responses and δ differences between sensing film and the targeted organic vapors has been observed by Dong et al., for carbon-black filled PEG/PMMA hybrid composites[65].

4.3. Potential application of polymer-coated MNP-based chemiresistors in Asthma, COPD, Lung and Breast Cancer diagnosis, via breath analysis

Taking all the above into consideration, it is proposed that solubility parameters could be used for polymer selection of the hybrid film described earlier (*§ 4.2*). *Δδ* calculation for polymers and targeted VOCs is expected to reflect the different degree of susceptibility of a series of polymeric films for the different targeted VOCs and, thus, sensor (semi)selectivity. For this reason, an extensive literature research was conducted, to compile the VOCs detected by analytical methods, for a series of diseases. Breath samples of patients and healthy subjects are composed of numerous VOCs, the identity of which varies between subjects. VOCs reported as discriminant in more than one studies are considered promising biomarkers[124].

4.3.1. Targeted VOCs

4.3.1.1. Asthma

Asthma is a chronic, not curable[225], inflammatory disease[14], characterized by increased bronchial responsiveness[45,226] and reversible airways obstruction[19]. Asthma, especially allergic, is widespread among children[45,227,228], while wheezing, short breath, short

episodes of chest tightness[14,19] and coughing are the most common symptoms, usually manifesting during the night or after intense physical exercise[19]. Globally, about one third of preschool children with coughing, wheezing or dyspnea develop asthma in their life[229]. Comorbidity may be observed in asthma patients, including eosinophilia, neutrophilia, allergic rhinitis, obstructive sleep apnea, gastroesophageal refluxes and atopy (*i.e.*, asthma, allergic rhinitis and eczema combination). The exact causes of asthma remain unknown, however allergens like dust, pollen or fur, irritant agents, environmental pollution and some drugs, such as aspirin and beta blockers, comprise important risk factors.[19]

Asthma maintenance treatment includes antileukotrienes and ICS and targets the modification of the various underlying inflammation mechanisms[230], responsible for the disease heterogeneity and disease subtypes[45]. Namely, asthma subtypes include eosinophilic, neutrophilic, mixed granulocytic and paucigranulocytic asthma[230], depending on the percentage of inflammatory cells in sputum[225]. Symptoms similarity exists among different inflammation phenotypes[231,225], for which different treatment is needed[225]. For instance, anti-inflammatory treatment with ICS controls eosinophilic inflammation, contrary to the neutrophilic inflammation, triggered by innate immunity[230]. Thus, reliable phenotyping is needed, for the appropriate medication to be administered[45,225].

Another characteristic of asthma are the exacerbation episodes[231,226], *i.e.*, attack crises[19] characterized by respiratory symptoms deterioration[228]. Exacerbations may be provoked by atopy[19] and are in general linked with increased sputum eosinophils[231]. ICS are administered in minimum doses [226] for asthma re-control [19,231,226,228], according to the general symptoms and lung function[231,226], which are not always representative, though[226].

Spirometry, FeNO and sputum analysis are used for asthma diagnosis, phenotyping and monitoring[45]. Spirometry measures either the forced vital capacity (FVC), *i.e.*, the maximum air volume forcefully exhaled, or the forced expiratory volume (FEV), *i.e.*, the air volume exhaled in a second, it is, though, time consuming[19]. Concerning asthma phenotyping, empirical methods may be used[225], *e.g.*, steroid response, trigger-factors exposure (smoke, air pollution, allergens, aspirin, exercise), obesity and fixed airway damage[14]. The gold standard method for inflammation phenotyping[230] as well as asthma control assessment[231], is the induced sputum analysis, which is, though, complex, time-consuming[230] and invasive

[225], irritating for the patient, particularly for those with uncontrolled asthma[231]. Blood cell count and FeNO, a clinically applicable method, with provided standards and guidelines[226] comprise alternative diagnostic methods, however they are confined only to eosinophilic asthma discrimination[225]. Inflammation-related non-volatile biomarkers of exhaled breath condensate have been investigated, however their diagnostic ability is under question[226].

In contrast, exhaled VOCs have attracted research interest, as they potentially hold a great promise, even if clinical translation is not realized yet[45]. Airway inflammation characterizing asthma potentially leads to alternated exhaled VOCs composition[227,228], while, in case of lung function deterioration, enhanced inflammation may occur before deteriorated symptom manifestation. Thus, exhaled VOCs are explored not only for early asthma diagnosis[19,229], but also for asthma stability assessment, exacerbation prediction[226] and inflammation phenotyping, for which reliable, simple and cost-effective methods are needed[230] One of the main advantages of breath analysis for asthma diagnosis, usually presented in (preschool) children[45,229], is the non-invasiveness of the method[19,45,229].

Among the fifteen articles selected, four studies included pediatric population, of ages varying between 2 to 16 years old, aiming to differentiate asthmatic children from healthy controls[227,229,232,233]. In two studies[227,232] asthmatic children suffering also from allergic rhinitis were included and successfully differentiated from healthy controls, with classification rates 96%[227] and 88%[232], using patterns of 9 and 28 VOCs, respectively. Notably, it has been observed that asthma-specific alkanes identified by Caldeira et al. derive from aldehydes found characteristic for healthy controls in the same study[227]. Smolinska et al. attempted to differentiate asthmatic children from healthy subjects, as well as from transient wheezers, using 17 VOCs, with respective classification rates 73.3% and 86.7 %.[229] Among those four studies, tetradecane, decane, dodecane, 2,4-dimethyl heptane, acetone and limonene are reported in two different studies, none of which appertain to the eight VOCs identified by Gahleitner et al.[233].

Four studies among retrieved articles targeted the differentiation of asthmatic adults from healthy controls[14,55,234,235]. Two studies achieved differentiation of asthmatic and healthy subjects using both GC-MS analysis and Cyranose 320[55,234], and identified 5[55] and 11[234] discriminant VOCs, while Ibrahim et al.[235] detected a discriminant pattern of 15 VOCs.

Meyer et al.[14], that identified 16 VOCs discriminant for asthmatic and healthy subjects, demonstrated the existence of clusters with different clinical features (*e.g.,* asthma subtype, treatment, spirometry values) and similar VOCs and clusters with similar clinical characteristics and different VOCs, highlighting the importance of clinical presentation, along with inflammation processes, for asthma subtypes classification. Among those studies, 2,6,11-trimethyl dodecane, 2,4-dimethyl heptane, toluene, isoprene and acetone were identified in two studies, predominantly in higher levels for asthmatic subjects.

Remarkably, more recent studies focus on asthma phenotyping[225,230,231,235] and exacerbation prediction[226,228,231,235,236]. Brinkman et al.[231] identified 3 VOCs significantly correlated with sputum eosinophils, while Schleich et al.[230] identified 4 VOCs discriminating eosinophilic from neutrophilic, eosinophilic from paucigranulocytic and neutrophilic from paucigranulocytic asthma, with accuracy similar to blood eosinophils and FeNO tests. Additionally, Ibrahim et al.[235] identified VOC-patterns differentiating eosinophilic from non-eosinophilic (6 VOCs), neutrophilic from non-neutrophilic (7 VOCs) and controlled from uncontrolled asthma (9 VOCs), apart from asthmatic and healthy subjects. However, among those studies, only nonanal was reported in two studies, while 3,7,7-trimethyl bicyclo[4.1.0]hept-2-ene[235] and 4-methyl bicyclo[2.2.2]octan-1-ol[231], correlated to sputum eosinophils, are characterized as related molecules[231]. The limited number of VOCs and, mainly, the bulky structure do not permit analysis for polymer selection.

Apart from Ibrahim et al., four more studies related to loss-of-control episodes of both children[226,228,236] and adults[231,235] were selected. Similarly to Ibrahim, controlled and uncontrolled asthma differentiation was demonstrated by van Vliet et al. (15 VOCs)[226]. Discrimination of stable periods and exacerbations was achieved by Brinkman et al.[231], using 3 VOCs. Notably, Robroeks et al.[236] identified 6 VOCs predictive for asthma exacerbation in children, comparing baseline breath samples before (baseline samples) and during exacerbation (intrasubject), as well as breath baseline samples of patients with controlled and uncontrolled asthma (intersubject). Five predictive VOCs were identified by a more recent study[228], other than Robroeks'. Among the two studies of adult population, no common VOCs were reported, while, for the studies on pediatric population, only 2-methyl furan, 3-methyl furan and 1,2-dimethyl cyclohexane were reported more than once.

Table 7: Studies aiming at asthma diagnosis, phenotyping and/or exacerbation prediction, using exhaled VOC patterns, identified using analytical methods.

Number or subjects	Age Range	Differentiation	Analytical Technique	Statistical Method / Classifier	Ref.
Diagnosis – Children					
22 allergic asthma, 13 allergic asthma + rhinitis, 15 HC (50 total)	4–13 all	Asthma vs HC	GC-qMS	PLS-DA	[232]
22 allergic asthma, 10 allergic asthma + rhinitis), 27 HC (59 total)	4–16 asthma, 3–6 HC	Asthma vs HC	GC x GC – ToF-MS	PLS-DA	[227]
11 asthma, 12 healthy (23 total)	10–14 asthma, 9–15 HC	Asthma vs HC	GC-MS	PCA	[233]
76 asthma, 121 Trans. wheezers, 6 unclassified, 49 HC (252 total)	2–6 all	Asthma vs Transient wheezers, Asthma vs HC	GC – ToF-MS	RFC, PCA, PLS-DA	[229]
Diagnosis – Adults					
20 asthmatic, 20 healthy (40 total)	18–75 all	Asthma vs HC	GC-MS / Cyranose 320	PCA	[234]
35 asthma, 23 HC (58 total)	32–61 asthma, 37–65 HC	Asthma vs HC	GC-MS	PCA	[235]
10 asthma, 10 HC (20 total)	25–47 asthma, 38–58 HC	Asthma vs HC	GC-MS / Cyranose 320	CDA	[55]
195 asthma, 40 HC (235 total)	35–65 asthma	Asthma vs HC	GC-MS	SPSS, Graphpad Prism	[14]
Phenotyping					
22 eosinophil	21–32 asthma	NA	GC-MS/eNoses*	PCA	[231]
Discovery study: 122 eosinophilic, 50 neutrophilic, 90 paucigranulocytic, 14 mixed-granulocytic (276 total)	35–65 all	Eosinophilic vs Paucigranulocytic Neutrophilic vs Paucigranulocytic, Eosinophilic vs Neutrophilic	GC-ToF-MS, GCxGC-HR-ToF-MS	RFC	[230]
Replication study: 90 eosinophilic, 53 neutrophilic, 90 paucigranulocytic, 12 mixed-granulocytic (245 total)	39–69 all				
18 eosinophil, 22 non-eosinophil (40 total)	47–71 eosinophil 38–68 non-eosinophil	Eosinophil vs Neutrophilic/ Paucigranulocytic	GCxGC-HR-ToF-MS	PCA	[225]
8 eosinophil , 10 non-eosinophil (18 total)	32–62 eosinophil 37–58 non-eosinophil	Eosinophil vs Non eosinophil	GC-MS	PCA	[235]
10 neutrophilic, 8 non-neutrophilic (18 total)	42–64 neutrophilic 29–52 non-neutrophilic	Neutrophilic vs Non neutrophilic			
Exacerbation					
18 uncontrolled, 17 controlled asthma (35 total)	37–62 loss of control 27–59 controlled	Uncontrolled vs controlled asthma	GC-MS	PCA	[235]
16 uncontrolled 23 controlled (39 total)	10–11 all	Uncontrolled vs controlled asthma (intrasubject and intersubject comparison – exacerbation prediction)	GC-ToF-MS	SVM	[236]
53 variable asthma control, 9 persistently uncontrolled, 34 persistently controlled (96 total)	6–17 all	Uncontrolled vs controlled asthma	GC-ToF-MS	RFC	[226]
22 partly controlled, persistent asthma	21–32	Uncontrolled vs controlled asthma periods	GC-MS/eNoses*	PCA	[231]
45 uncontrolled, 49 controlled asthma (96 total)	6–17 all	Uncontrolled vs controlled asthma	GC-ToF-MS	RFC,PCA	[228]

*eNoses: Cyranose C320, Tor Vergata, Common Invent, Owlstone Lonestar

CDA: Canonical Discriminant Analysis, **GC:** gas chromatography, **GC-HR-ToF-MS:** two-dimensional gas chromatography – high-resolution time-of-flight mass spectrometry, **GC-MS:** Gas Chromatography - Mass Spectrometry, **GC-qMS:** gas chromatography – quadrupole mass spectrometry, **GC-ToF-MS:** gas chromatography time-of-flight mass spectrometry, **HC:** healthy controls, **PCA:** Principal Component Analysis, **PLS-DA:** Partial Least Square Discriminant Analysis, **RFC:** Random forest classification, **SVM:** Support Vector Machine

Table 8: VOCs characterized as able to differentiate asthmatic patients from healthy controls.

VOCs	Expression	CAS No	Category	Ref.
Children Diagnosis				
Decanal	–	112-31-2	Aldehyde	[227]
Dodecanal	–	112-54-9	Aldehyde	[227]
Nonanal	–	124-19-6	Aldehyde	[227]
Oct-2-enal	+	2363-89-5	Aldehyde	[233]
Undec-2-enal	+	2463-77-6	Aldehyde	[229]
Decane	+	124-18-5	Alkane	[232]
Decane	+	124-18-5	Alkane	[227]
Dodecane	+	112-40-3	Alkane	[232]
Dodecane	+	112-40-3	Alkane	[227]
Nonane	+	111-84-2	Alkane	[227]
Octane	+	111-65-9	Alkane	[229]
Tetradecane	+	629-59-4	Alkane	[232]
Tetradecane	+	629-59-4	Alkane	[227]
Hexane, 2-Methyl-	+	591-76-4	Alkane, Methylated	[229]
Decane, 2,3,6-Trimethyl-	+	62238-12-4	Alkane, Methylated	[232]
Decane, 3,6-Dimethyl-	+	17312-53-7	Alkane, Methylated	[227]
Dodecane, 2,6,10-trimethyl-	–	3891-98-3	Alkane, Methylated	[229]
Heptane, 2,2,4,6,6-Pentamethyl-	+	13475-82-6	Alkane, Methylated	[227]
Heptane, 2,2,4-trimethyl-	–	14720-74-2	Alkane, Methylated	[229]
Heptane, 2,4-dimethyl	+	2213-23-2	Alkane, Methylated	[229]
Heptane, 2,4-Dimethyl-	–	2213-23-2	Alkane, Methylated	[232]
Hexane, 2,2-Dimethyl-	+	590-73-8	Alkane, Methylated	[232]
Isodecane	+	871-83-0	Alkane, Methylated	[227]
Octane, 2,3,6-trimethyl-	–	62016-33-5	Alkane, Methylated	[229]
Octane, 2,4-Dimethyl	+	4032-94-4	Alkane, Methylated	[232]
Octane, 4-Methyl-	–	2216-34-4	Alkane, Methylated	[232]
Pentane, 2,4-Dimethyl-	+	108-08-7	Alkane, Methylated	[229]
Pentane, 2-Methyl-	+	107-83-5	Alkane, Methylated	[229]
Dodec-1-ene	–	112-41-4	Alkene	[227]
Octadecyne	+	629-89-0	Alkyne	[233]
Benzene, 1-Isopropyl-3-methyl-	+	535-77-3	Aromatic Hydrocarbon	[233]
Benzene, Ethyl-	+	100-41-4	Aromatic Hydrocarbon	[233]
Biphenyl	–	92-52-4	Aromatic Hydrocarbon	[229]
Naphthalene, 1,7-Dimethyl-	+	575-37-1	Aromatic Hydrocarbon	[233]
Naphthalene, 2-ethenyl-	–	939-27-5	Aromatic Hydrocarbon	[229]
Isoprene	+	78-79-5	Diene	[232]
Benzene, 1,4-Dichloro-	+	106-46-7	Halogen Compound	[233]
6-methyl-5-hepten-2-one	–	110-93-0	Ketone	[227]
Acetone	–	67-64-1	Ketone	[232]
Acetone	–	67-64-1	Ketone	[229]
Pent-2-ene, 4-Methyl-	+	4461-48-7	Methylated alkene	[229]
Propane, 1-(Methylsulfanyl)-	+	3877-15-4	Sulfur Compound	[233]
Limonene	–	138-86-3	Terpene	[229]
Limonene	+	138-86-3	Terpene	[233]
Adults Diagnosis				
Dodecan-1-ol, 3,7,11-Trimethyl-	+	6750-34-1	Alcohol	[14]
Isopropanol	+	67-63-0	Alcohol	[234]
Propanol, 1-	+	71-23-8	Alcohol	[55]
Octanal	–	124-13-0	Aldehyde	[14]
Pentadecanal	–	2765-11-9	Aldehyde	[235]
Alkane	+	NA	Alkane	[234]
Dodecane	–	112-40-3	Alkane	[14]
Decane, 2-Methyl-	+	6975-98-0	Alkane, Methylated	[235]
Dodecane, 2,6,10-Trimethyl-	+	3891-98-3	Alkane, Methylated	[235]
Dodecane, 2,6,11-Trimethyl-	+	31295-56-4	Alkane, Methylated	[234]
Dodecane, 2,6,11-Trimethyl-	+	31295-56-4	Alkane, Methylated	[235]
Heptane, 2,3-Dimethyl-	+	3074-71-3	Alkane, Methylated	[234]
Heptane, 2,4-Dimethyl-	+	2213-23-2	Alkane, Methylated	[234]
Heptane, 2,4-dimethyl-	NA	2213-23-2	Alkane, Methylated	[14]
Octane, 4-Methyl-	+	2216-34-4	Alkane, Methylated	[234]
Undecane, 3,7-Dimethyl-	+	17301-29-0	Alkane, Methylated	[234]
1,3-Dioxolane, 2-Benzyl	+	101-49-5	Aromatic Acetal	[14]
Benzyl alcohol	+	100-51-6	Aromatic Alcohol	[235]

Phenol	–	108-95-2	Aromatic Alcohol	[14]
Benzene	+	71-43-2	Aromatic Hydrocarbon	[14]
Toluene	+	108-88-3	Aromatic Hydrocarbon	[234]
Toluene	+	108-88-3	Aromatic Hydrocarbon	[55]
Xylene, o-, 4-Ethyl-	–	934-80-5	Aromatic Hydrocarbon	[235]
Nonane, 5,5-Dibutyl-	–	6008-17-9	Butylated Alkane	[235]
Acetic acid	+	64-19-7	Carboxylic acid	[234]
Hex-5-enoic acid	NA	1577-22-6	Carboxylic acid	[14]
Tetradecanoic acid	–	544-63-8	Carboxylic acid	[14]
Cyclohexanol, 2-Butyl-	–	36159-49-6	Cyclic Alcohol	[235]
Cyclopent-4-ene-1,3-dione, 4-phenyl-	+	51306-96-8	Cycloalkene	[14]
Isoprene	+	78-79-5	Diene	[234]
Isoprene	+	78-79-5	Diene	[55]
Octa-2,7-dien-1-ol, 2-Butyl-	NA	NA	Diene, Alcohol	[14]
Ethyl 2,2-dimethyl-3-oxobutanoate	+	597-04-6	Ester	[235]
Propionyllactic acid thiomethyl ester	–	66292-29-3	Ester	[14]
Acetone	+	67-64-1	Ketone	[234]
Acetone	+	67-64-1	Ketone	[55]
Butanone	+	78-93-3	Ketone	[235]
Benzoate, Ethyl 4-nitro-	–	99-77-4	Nitrogen compound	[235]
Benzonitrile, 3,4-Dihydroxy-	+	17345-61-8	Nitrogen Compound	[235]
Quinoline, decahydro-	–	2051-28-7	Nitrogen compound	[14]
2,6-Di-*tert*-butyl-1,4-benzoquinone	–	719-22-2	Quinone	[235]
Allyl methyl sulphide	+	10152-76-8	Sulfur Compound	[235]
Carbon disulphide	+	75-15-0	Sulfur Compound	[55]
Terpinolene	+	586-62-9	Terpene	[235]

* *"Expression" refers to the concentration of the VOC in patient's breath in comparison to healthy controls; (+) indicates higher concentration in patient's breath, (–) indicates lower concentration in patient's breath.*

Table 9: VOCs characterized as able to differentiate asthma subtypes (eosinophilic, neutrophilic, paucigranulocytic).

S.1	VOCs	Expression	CAS No	Category	S.2	Ref.
E	Acetonitrile	+	75-05-8	Nitrogen compound	NA	[231]
E	Bicyclo[2.2.2]octan-1-ol, 4-methyl-	+	824-13-5	Cyclic Alcohol	NA	[231]
E	6-Octen-1-ol, 3,7-dimethyl-, acetate	NA	150-84-5	Ester	N/P	[225]
E	Acetic acid, phenyl ester	NA	122-79-2	Aromatic Ester	N/P	[225]
E	Butanedioic acid dimethyl ester	NA	106-65-0	Ester	N/P	[225]
E	Cyclopentane, 1,1,3,3-tetramethyl-	NA	50876-33-0	Cycloalkane	N/P	[225]
E	Decane, 2,5,9-trimethyl	NA	62108-22-9	Alkane, methylated	N/P	[225]
E	Diphenyl ether	NA	101-84-8	Aromatic Ether	N/P	[225]
E	Nonanal	NA	124-19-6	Aldehyde	N/P	[225]
E	Nonene, 1-	NA	124-11-8	Alkene	N/P	[225
E	Octane-1,7-diol, 3,7-dimethyl-	NA	107-74-4	Alcohol	N/P	[225]
E	Undeca-5,9-dien-2-one, 6,10-dimethyl-	NA	689-67-8	Ketone, Diene	N/P	[225]
E	1,1-Dimethylpropyl 2-Ethylhexanoate	–	NA	Ester	Non E	[235]
E	(7a-Isopropenyl-4,5-dimethyloctahydroinden-4-yl) methanol	–	NA	Cyclic Alcohol, Alkene	Non E	[235]
E	Bicyclo[4.1.0]hept- 2-ene, 3,7,7-trimethyl-	–	NA	Terpenoid	Non E	[235]
E	Camphene	–	79-92-5	Terpenoid	Non E	[235]
E	Cyclohexanone	–	108-94-1	Cyclic Ketone	Non E	[235]
E	Cyclohexene-4-methylene	–	13407-18-6	Cyclic Alkene, Diene	Non E	[235]
E	Dodecane, 2,6,10-trimethyl-	–	3891-98-3	Alkane, methylated	Non E	[235]
E	Hexane	–	110-54-3	Alkane	P	[230]
E	Hexanone, 2-	–	591-78-6	Ketone	P	[230]
E	Propanol, 1-	–	71-23-8	Alcohol	P	[230]
N	Hexane	+	110-54-3	Alkane	E	[230]
N	Nonanal	+	124-19-6	Aldehyde	E	[230]
N	Nonane, 3,7-Dimethyl-	+	17302-32-8	Alkane, methylated	E	[230]
N	Propanol, 1-	+	71-23-8	Alcohol	E	[230]
N	Cyclohexanol, 3,5-dimethyl-	+	5441-52-1	Cyclic Alcohol	Non N	[235]
N	Cyclopentene, 1,3-dimethyl-2-(1 methylethyl)-	+	NA	Cyclic Alkene	Non N	[235]
N	Naphthalene, 2,7-dimethyl-	+	582-16-1	Aromatic Hydrocarbon	Non N	[235]
N	Naphthalene, Decahydro-8a-ethyl-1,1,4a,6-tetramethyl-	+	NA	Aromatic Hydrocarbon	Non N	[235]
N	Tetradecane, 4-methyl-	+	25117-24-2	Alkane, methylated	Non N	[235]
N	Nonanal	+	124-19-6	Aldehyde	P	[230]

N	Pentadecene	+	13360-61-7	Alkene	P	[230]
N	Tetradecene, 3-	+	41446-68-8/ 41446-67-7	Alkene	P	[230]
N	Undecane	−	1120-21-4	Alkane	P	[230]

"Expression" refers to the concentration of the VOC in patient's breath, with asthmatic S.1 in comparison to S.2; (+) indicates higher concentration in patient's breath with S.1, (−) indicates lower concentration in patient's breath with S.2.

E: Eosinophilic, **N/P:** Neutrophilic/Paucigranulocytic, **N:** Neutrophilic, **NA:** not applicable, **P:** paucigranulocytic, **S.1:** Subtype 1, **S.2:** Subtype 2

Table 10: VOCs related to loss of asthma control.

VOCs	Expression	CAS No	Category	Ref.
Children Exacerbation				
Pentan-1-ol, 2-ethyl-4-methyl-	NA	106-67-2	Alcohol	[236]
Oct-2-en-1-ol	NA	18409-17-1	Alcohol, Alkene	[236]
Hexanal, 2-ethyl-	NA	123-05-7	Aldehyde	[228]
Nonanal	NA	124-19-6	Aldehyde	[228]
Octanal	NA	124-13-0	Aldehyde	[228]
Pentane, 3-methyl-	NA	96-14-0	Alkane, methylated	[236]
Buta-1,3-diene, 2-ethyl-	NA	3404-63-5	Alkene (Diene)	[236]
Hexa-2,4-diene	NA	592-46-1	Alkene (Diene)	[226]
Nonadeca-4,6,9-triene	NA	NA	Alkene (Triene)	[236]
Furan, 2-methyl-	NA	534-22-5	Aromatic Ether	[226]
Furan, 3-methyl-	NA	930-27-8	Aromatic Ether	[226]
Furan, 2-methyl- / 3-methyl-	NA	534-22-5 / 930-27-8	Aromatic Heterocyclic	[228]
Benzene	NA	71-43-2	Aromatic Hydrocarbon	[236]
But-1-ene, 1-phenyl	NA	1005-64-7 / 1560-09-4	Aromatic Hydrocarbon	[236]
m-cymene	NA	535-77-3	Aromatic Hydrocarbon	[226]
Xylene, p-	NA	106-42-3	Aromatic Hydrocarbon	[236]
Branched C14H30	NA	NA	Alkane, Branched	[226]
Butanoic acid	NA	107-92-6	Carboxylic Acid	[226]
Cyclohexane	NA	110-82-7	Cycloalkane	[236]
Cyclohexane, 1,2-dimethyl-	NA	583-57-3	Cycloalkane	[228]
Cyclohexane, 1,2-dimethyl-	NA	583-57-3	Cycloalkane	[226]
Cyclohexane, Propyl-	NA	1678-92-8	Cycloalkane	[226]
Ethylene, Tetrachloro-	NA	127-18-4	Halogen Compound	[226]
Undeca-5,9-dien-2-one, 6, 10-dimethyl-	NA	689-67-8	Ketone	[228]
1,2-methyl-4H-1,3-benzoxathiine	NA	NA	Sulfur Compound	[236]
Dimethyl sulfone	NA	67-71-0	Sulfur Compound	[226]
Sulphur dioxide	NA	7446-09-5	Sulfur Compound	[226]
C10H16 unknown monoterpene	NA	NA	Terpene	[226]
C10H16 unknown monoterpene	NA	NA	Terpene	[226]
Adults exacerbation				
Methanol	−	67-56-1	Alcohol	[231]
Octane, 2,2,4,4-Tetramethyl-	−	62183-79-3	Alkane, methylated	[235]
Pentadecane, 1-methoxy-13-methyl-	−	56196-09-9	Alkane, methylated	[235]
Benzene	−	71-43-2	Aromatic Hydrocarbon	[235]
Naphthalene, 2,6-diisopropyl-	−	24157-81-1	Aromatic Hydrocarbon	[235]
Xylene, o-	+	95-47-6	Aromatic Hydrocarbon	[235]
Heptanoic acid	−	111-14-8	Carboxylic acid	[235]
Bicyclo[2.2.2]octan-1-ol, 4-methyl-	−	824-13-5	Cyclic Alcohol	[231]
2-Butanone, 3-methyl/butanal, 2-methyl-	−	563-80-4 / 96-17-3	Ketone / Aldehyde	[235]
Acetonitrile	−	75-05-8	Nitrogen compound	[231]
Prop-1-ene, (1E)-1-(methylsulphanyl)-	−	10152-77-9	Sulfur Compound	[235]
Dehydrosabinene	+	36262-09-6	Terpenoid	[235]

"Expression" refers to the concentration of the VOC in the breath of patients with uncontrolled asthma in comparison to controlled asthma; (+) indicates higher concentration and (−) indicates lower concentration in case of uncontrolled asthma.

4.3.1.2. Chronic Obstructive Pulmonary Disease (COPD)

COPD comprises a multiphenotypic respiratory syndrome related with chronic, progressive and not fully reversible airflow obstruction[21,237,] and inflammation[21], mainly neutrophilic[206]. Various symptoms have been observed inter-individually[206], the main of which include

dyspnea, cough and sputum excretion[237]. Emphysema, small airways disease, chronic bronchitis and asthma-like characteristics (*e.g.,* hyper-responsiveness) are also related clinical features[206]. Symptom and exacerbation severity is comorbidity dependent[237].

The major challenge is the underdiagnosis or the diagnosis at late-stages[22], possibly attributed to limited use of spirometry, as well as the low awareness of general population and health care professionals[23]. The common symptoms with asthma or even the diseases coexistence, on the other hand, renders difficult their differentiation. The increased smooth muscle and the abnormally bronchi thick walls, the augmented airway neutrophils and sputum production and the irreversible airways limitation, not significantly improved using bronchodilators, comprise characteristic signs of COPD, contrary to asthma.[19]

Chronic tobacco smoke inhalation is considered as the major COPD cause[19,21,237], while biomass smoke has also been connected with COPD, always depending on exposure extend [23]. Free radicals, ROS and nitrogen species of tobacco smoke enhance oxidative stress and pulmonary inflammation, leading to the production and exhalation of alkanes, aldehydes or carboxylic acids, as inflammation biomarkers[237]. The identification of such COPD-specific patterns of exhaled biomarkers hold a great promise for early and precise disease diagnosis[22], with research being yet in early stage concerning sampling methods and VOCs data analysis[18]. Remarkably, apart from COPD diagnosis, research interest focuses, also, on phenotyping, treatment monitoring and detection of "high risk" smokers, using VOCs[21].

Among the twelve studies selected based on inclusion criteria (*§ 3.2*), eight studies aimed only at differentiating COPD patients from healthy subjects[18,22,62,237,238,239,240,241]. As the most important risk factor, smoking habits have been taken into consideration in some cases[18,237,241]. Remarkably, Gaida et al. collected breath samples from residents (healthy and COPD patients) of two different sites and detected 14 VOCs relative to COPD – among which 10 were reported for the first time – in a total of 134 VOCs. Apart from smoking, also sampling-environment related VOCs were identified, demonstrating the effect of habits, as well as environmental factors, on diagnostic results.[18] COPD patients suffering from LC have also been effectively distinguished from healthy subjects, however differentiation between COPD patient with and without LC was not feasible[242]. Recently, Pizzini et al. attempted to differentiate not only COPD patients from healthy subjects (12 VOCs) but also acute

exacerbations COPD from stable COPD and healthy subjects. 4 VOCs, from which 3 attain to ketones, were increased in AECOPD patients' breath[243]. However, no other study related to COPD exacerbations was retrieved. Only two studies attempted to distinguish different phenotypes (neutrophilic, eosinophilic), however no common VOCs were detected.[206,239]

The VOCs used to differentiate COPD patients and healthy controls in the studies of Table 11, were compiled (Table 12). Aldehydes were detected in higher levers in COPD patients' breath in comparison to healthy controls, with hexanal being reported in five studies, while each of the alkanes butane, heptane, octane and nonadecane were reported in two studies. The methylated alkanes 2,4-dimethyl heptane and 2,6-dimethyl heptane comprise isomers found decreased in COPD patients' breath. The aromatic compounds phenol, benzaldehyde, benzene, toluene, xylenes (o-, m-, p-) and indole have also been characterized as discriminative for COPD more than once, found in increased for COPD patients, except indole. Notably, as already mentioned (*§ 2.3.1*), aromatic compounds are considered as exogenous VOCs, rather than metabolic products, deriving mainly from tobacco smoke[240]. Last but not least, acetic acid, cyclohexanone and 2-pentanone differentiated COPD patients and healthy subjects in two and isoprene in three studies.

4.3.1.3. Lung Cancer (LC)

LC is the most widespread kind of cancer worldwide[11,245] and one of the five most common and mortal cancer types[4]. Cigarette smoking, active or passive, is the most common LC cause[245] with about 85% of LC cases being attributed to tobacco smoking[19]. Radiation, radon, asbestos and air pollution comprise causes of the rest 15% of cases[19], along with Cd, As and Be exposure[245] while, in some cases genetic factors are responsible[19].

Primary LCs, called carcinomas, are divided into two large groups, based on the histological type; SCLC and NSCLC[19]. SCLC, with 20-25% percentage of occurrence[245], are dense cells in which blister-like neurosecretory granules filled with endocrine hormones are contained[19], characterized by increased metabolic and proliferation rates that other cancer cells[35]. NSCLC, which accounts for 70-75 % of LC cases, is subdivided into SCC[245] and non-squamous cell carcinomas[19] including adenocarcinomas and LCC[245]. SCC, closely correlated with smoking[19,246], is commonly developed centrally in lungs, with greater frequency to men than women[19]. In contrast, adenocarcinoma, usually appearing in the lung periphery is the

Table 11: Studies aiming at COPD diagnosis, phenotyping and/or exacerbation prediction, using exhaled VOC patterns, identified using analytical methods.

Number or subjects	Age Range	Differentiation	Analytical Technique	Statistical Method / Classifier	Ref.
Diagnosis					
36 NSCLC, 25 COPD, 35 HS, 50 HNS (146 total)	67 LC, 70 COPD, 54 HS, 56 HNS	NSCLC vs HNS, COPD/HS vs HNS	SPME-GC-MS	PCA	[244]
50 COPD, 29 HC (79 total)	63 – 79 COPD, 41 – 59 HC	COPD vs Healthy	GC-MS	SVM	[238]
Validation study: 16 COPD, 16 HC (32 total)	57 – 69 COPD, 45 – 57 HC				
35 COPD, 62 COPD and LC 35 HC (132 total)	NA	COPD/COPD + LC vs Healthy	MCC/IMS	PCA	[242]
39 COPD, 32 HC (71 total)	59 – 73 COPD, 48 – 62 HC	COPD vs Healthy	GC-ToF-MS	PCA	[239]
119 stable COPD, 63 HC (182 total)	59 – 75 COPD, 58 – 77 HC	Stable COPD vs Healthy	GC-MS	J48, JRIP, PART, SMO, FNN, FRNN, RFC, VGNN	[62]
118 stable COPD, 63 HC (181 total)	59 – 75 COPD, 58 – 77 HC	Stable COPD vs Healthy	GC-MS	J48, JRIP, PART, 73,4%	[240]
52 COPD ES, 37 COPD S, 52 HNS, 49 HS (190 total)	*Hannover:* 58 – 68 COPD NS/ES, 54 – 68 COPD S, 25 – 51 HNS/HES, 34 – 60 HS *Marburg:* 58 – 72 COPD NS/ES, 43 – 79 COPD S, 19 – 45 HNS/HES, 26 – 54 HS	COPD vs Healthy (S, NS)	TD-GC-MS	LDA	[18]
21 COPD S, 25 COPD ES, 25 HS, 23 HNS (94 total)	56–68 COPD S, 60–70 COPD ES, 34–58 HS, 23–51 HNS	COPD vs Healthy (NS, ES)	TD-GC-APCI-MS	MATLAB algorithm/ Welch's *t*-test	[241]
8 COPD S, 49 COPD ES, 33 HS, 28 HES, 39 HNS (157 total)	64 – 83 COPD, 40 – 58 HC	COPD vs Healthy (NS, ES)	TD-CG-MS	Kolmogorov-Smirnov test, Student's t-test and Fisher's exact test	[237]
14 AECOPD, 16 COPD, 24 HC (54 total)	64–79 AECOPD, 58–76 COPD, 22–34 HC	COPD/AECOPD vs Healthy, COPD vs Healthy, AECOPD vs Healthy	TD-GC-ToF-MS	ANOVA test, RFC	[243]
23 COPD, 33 HC (56 total)	59–73 COPD, 47–64 HC	COPD vs Healthy	FGC eNose	PCA, CDA	[22]
Phenotyping					
12 GOLD stage I, 16 GOLD stage II (28 total)	52–66 GOLD stage I, 50–66 GOLD stage II	Eosinophil vs Neutrophil	GC-MS / Cyranose 320	SPSS, Graphpad Prism and MATLAB	[206]
39 COPD (eosinophil >1% 11, <1% 13), 32HC	59-73 COPD, 48-62 HC	Eosinophil vs Non-eosinophil	GC-ToF-MS	PCA	[239]

AECOPD: acute exacerbations chronic obstructive pulmonary disease, **APCI:** atmospheric pressure chemical ionization, **CDA:** Canonical Discriminant Analysis, **COPD:** Chronic Obstructive Pulmonary disease, **ES:** ex-smokers, **FGC:** ultrafast gas chromatography **FNN:** fuzzy nearest-neighbor classifier, **FRNN:** a fuzzy-rough set nearest-neighbor approach, **GC-ToF-MS:** gas chromatography time-of-flight mass spectrometry, **GOLD:** Global Initiative for Chronic Obstructive Lung Disease, **HC:** healthy controls, **HES:** healthy ex-smokers, **HNS:** healthy non-smokers, **HS:** healthy smokers, **J48:** version of Quinlan's ID3 decision-tree algorithm, **JRIP:** rule-based 'ripper' classifier which generates rules and uses these to classify 'new' objects, **MCC/IMS:** multi-capillary column/ ion mobility spectrometry, **NS:** non-smokers, **NSCLC:** non-small-cell lung carcinoma, **PART:** rule-based classifier, **PCA:** Principal Component Analysis, **RFC:** Random forest classification, **S:** smokers, **SMO:** sequential minimal optimization approach for support vector machines, **SPME:** Solid-phase Microextraction, **SVM:** Support Vector Machine, **TD:** Thermal Desorption, **VQNN:** noise-tolerant fuzzy-rough set-based classifier

Table 12: VOCs characterized as able to differentiate COPD patients from healthy controls.

VOCs	Expression*	CAS No	Category	Ref.
Octanol, 2-Butyl-	+	3913-02-8	Alcohol	[22]
Propanol, 2-	+	67-63-0	Alcohol	[22]
Acetaldehyde	+	75-07-0	Aldehyde	[22]
Butanal	+	123-72-8	Aldehyde	[22]
Decanal	+	112-31-2	Aldehyde	[239]
Dodecanal	+	112-54-9	Aldehyde	[239]
Hexanal	−	66-25-1	Aldehyde	[238]
Hexanal	+	66-25-1	Aldehyde	[239]
Hexanal	Similar	66-25-1	Aldehyde	[62]
Hexanal	+	66-25-1	Aldehyde	[240]
Hexanal	+	66-25-1	Aldehyde	[237]
Nonanal	+	124-19-6	Aldehyde	[239]
Pentadecanal	+	2765-11-9	Aldehyde	[239]
Propanal	+	123-38-6	Aldehyde	[22]
Undecanal	+	112-44-7	Aldehyde	[239]
Butane, n-	+	106-97-8	Alkane	[62]
Butane, n-	−	106-97-8	Alkane	[243]
Decane, n-	+	124-18-5	Alkane	[244]
Heptane, n-	+	142-82-5	Alkane	[244]
Heptane, n-	+	142-82-5	Alkane	[243]
Hexadecane, n-	−	544-76-3	Alkane	[238]
Nonadecane, n-	−	629-92-5	Alkane	[62]
Nonadecane, n-	+	629-92-5	Alkane	[240]
Octadecane, n-	−	593-45-3	Alkane	[238]
Octane, n-	+	111-65-9	Alkane	[244]
Octane, n-	+	111-65-9	Alkane	[22]
Pentane, n-	+	109-66-0	Alkane	[244]
Tetradecane, n-	−	629-59-4	Alkane	[22]
Tridecane, n-	+	629-50-5	Alkane	[18]
Undecane, n-	−	1120-21-4	Alkane	[238]
Decane, 2,4,6-Trimethyl-	−	62108-27-4	Alkane, methylated	[238]
Heptane, 2,4-dimethyl-	−	2213-23-2	Alkane, methylated	[243]
Heptane, 2,6-Dimethyl-	−	1072-05-5	Alkane, methylated	[238]
Hexane, 2-methyl-	+	591-76-4	Alkane, methylated	[243]
Octane, 2,6-dimethyl-	−	2051-30-1	Alkane, methylated	[243]
Octane, 4-Methyl-	−	2216-34-4	Alkane, methylated	[238]
Pentane, 2-Methyl-	+	107-83-5	Alkane, methylated	[244]
Undecane, 4,7-Dimethyl-	−	17301-32-5	Alkane, methylated	[238]
Cresol, m/p-	−	108-39-4/106-44-5	Aromatic Alcohol	[18]
Phenol	+	108-95-2	Aromatic Alcohol	[62]
Phenol	similar	108-95-2	Aromatic Alcohol	[18]
[E]-Cinnamaldehyde	−	104-55-2	Aromatic aldehyde	[22]
Benzaldehyde	Similar	100-52-7	Aromatic Aldehyde	[62]
Benzaldehyde	+	100-52-7	Aromatic Aldehyde	[240]
Phthalic anhydride	+	85-44-9	Aromatic Anhydride	[62]
Furan,2-pentyl	−	3777-69-3	Aromatic Ether	[239]
Benzene	+	71-43-2	Aromatic Hydrocarbon	[240]
Benzene	+	71-43-2	Aromatic Hydrocarbon	[18]
Benzene, 1-Ethyl-3-methyl-	+	620-14-4	Aromatic Hydrocarbon	[18]
Benzene, Ethyl-	+	100-41-4	Aromatic Hydrocarbon	[244]
Benzene, Trimethyl-	+	NA	Aromatic Hydrocarbon	[244]
Styrene	+	100-42-5	Aromatic Hydrocarbon	[244]
Toluene	Similar	108-88-3	Aromatic Hydrocarbon	[62]
Toluene	+	108-88-3	Aromatic Hydrocarbon	[240]
Toluene	+	108-88-3	Aromatic Hydrocarbon	[18]
Xylene, m/p-	+	108-38-3/106-42-3	Aromatic Hydrocarbon	[18]
Xylene, o-	+	95-47-6	Aromatic Hydrocarbon	[18]
Xylenes	+	108-38-3/ 106-42-3/ 95-47-6	Aromatic Hydrocarbon	[244]
Benzonitrile	−	100-47-0	Aromatic, Nitrogen compound	[238]
Indole	−	120-72-9	Aromatic, Nitrogen compound	[18]
Indole	−	120-72-9	Aromatic, Nitrogen Compound	[22]
Pyrazine, Vinyl-	−	4177-16-6	Aromatic, Nitrogen Compound	[22]
Pyridine, 2-Acetyl-	−	1122-62-9	Aromatic, Nitrogen Compound	[22]
Acetic acid	Similar	64-19-7	Carboxylic Acid	[62]

Acetic Acid	similar	64-19-7	Carboxylic Acid	[18]
Butanoic acid, 2-Methyl-	–	116-53-0	Carboxylic Acid	[22]
Pentanoic acid	–	109-52-4	Carboxylic acid	[239]
Menthol	+	1490-04-6	Cyclic Alcohol	[239]
Cyclohexanone	+	108-94-1	Cyclic Ketone	[242]
Cyclohexanone	+	108-94-1	Cyclic Ketone	[243]
Cyclopentanone, 3-methyl-	+	1757-42-2	Cyclic Ketone	[22]
Cyclohexane	+	110-82-7	Cycloalkane	[243]
Isoprene	–	78-79-5	Diene	[238]
Isoprene	Similar	78-79-5	Diene	[62]
Isoprene	+	78-79-5	Diene	[240]
Carbon dioxide	Similar	124-38-9	Dioxide	[62]
Oxirane, dodecyl-	+	3234-28-4	Epoxide	[239]
Acetate, Vinyl	+	108-05-4	Ester	[18]
Ethyl 2,2-dimethyl-3-oxobutanoate	–	597-04-6	Ester	[239]
Isobutyrate, Methyl	+	547-63-7	Ester	[22]
Linalyl Acetate	–	115-95-7	Ester	[18]
C16 hydrocarbon	–	NA	Hydrocarbon	[238]
Butanone	+	78-93-3	Ketone	[18]
Hept-5-en-2-one, 6-methyl-	–	110-93-0	Ketone	[243]
Heptanone, 4-	+	123-19-3	Ketone	[243]
Hexanone, 3-	+	589-38-8	Ketone	[22]
Pentanone, 2-	+	107-87-9	Ketone	[241]
Pentanone, 2-	+	107-87-9	Ketone	[243]
Delta-dodecalactone	–	713-95-1	Lactone	[22]
Dimethyl disulfide	–	75-18-3	Sulfide	[243]
Methyl propyl sulfide	+	3877-15-4	Sulfide	[243]
Sulphur dioxide	+	7446-09-5	Sulfur Compound	[62]
Pinene, α-	+	80-56-8	Terpene	[22]
Terpineol	–	98-55-5	Terpenoid	[238]
Hepta-1,3,5-triene, 1,6-Dimethyl-	+	928-67-6	Triene	[18]
Octa-1,3,6-triene, 3,7-Dimethyl-	–	3338-55-4/13877-91-3	Triene	[238]

"Expression" refers to the concentration of the VOC in patient's breath in comparison to healthy controls; (+) indicates higher concentration in patient's breath, (–) indicates lower concentration in patient's breath.

most widespread NSCLC type, with an occurrence percentage of 40%[19], while smoking association is minor[246]. LCC is a malignant neoplasm deriving from transformed epithelial cells in lungs. It is composed by large tumor cells and can be differentiated from the other NSCLC types using light microscopy[19].

Commonly, no symptoms are expressed in early stages[25]. On the other hand, disease manifestation is limited to non-specific symptoms[25], including cough, short breath, chest pain and weight loss[19]. LC diagnosis at early stages is particularly important, as chances for effective treatment are greater, in comparison to advanced-stages[25]. Thus, improved screening is essential for LC mortality reduction[4,12,245]. For LC diagnosis and screening chest radiography, low-dose spiral CT[11,19,25], sputum cytology, fluorescence bronchoscopy[11,25] or positron emission tomography[11] are used, while confirmation by the invasive, expensive and time consuming biopsy is essential[19]. Among those techniques, it is indicated that low-dose CT comprises the only method reducing high-risk patients' mortality[25].

For this reason, research interest has turned towards biomarkers and, specifically exhaled VOCs[19,35] identification, produced by induced oxidative stress and oxidase enzymes[247]. Common proposed cancer biomarkers include branched and oxygenated hydrocarbons[35]. Identification of VOCs derived from LC nodules the same is of particular importance but yet not achieved[19]. In contrast, some potential VOCs-biomarkers (*e.g.,* aromatic or unsaturated compounds, cyclic hydrocarbons) are purely exogenous, correlated with smoking, disinfectants, medications, plastics or fuel combustion[35]. Despite the great number of relevant studies, low concordance between them, concerning the determination of (patterns of) VOCs, has delayed the development of a non-invasive breath test[19].

Among the twenty three studies selected according to the inclusion criteria (*§ 3.2*), almost all attempt to differentiate LC patients – including both SCLC and NSCLC histologies, of different LC stages – from healthy controls, taking into account the smoking habits [35,33,245,248, 249,250,251,252,253]. In some cases, only NSCLC patients were included[11,254], while the differentiation of LC patients from patients with BPN has also been extensively reported[25,31,247,255,256]. Smoking-related VOCs present in the breath of smokers should be taken into account, as important confounding factors[19]. Aromatic compounds, for instance, have been found to be increased in the breath of healthy smokers, in contrast to the levels of oxygenated species (aldehydes, ketones and alcohols) found increased in LC patients[257]. Interestingly, age, considered as important risk factor, has also been selected as a variable in statistical analysis, along with specific VOCs, for LC detection[253].

Apart from LC diagnosis, histology characterization is, also, an important target of the research field. It is reported that 1-butanol and 3-hydroxy-2-butanone[11], as well as 4-hydroxyhexenal[247] can differentiate SCC from adenocarcinoma patients, while SCLC and NSCLC can be potentially distinguished from 4-hydroxynonenal and $C_5H_{10}O$, increased in the former case[247]. The differentiation of LC stages (I, II, III or IV) has been attempted, as well. Recently, Chen et al. detected a pattern of 19 VOCs to distinguish early (I,II) and advanced LC stages (III,IV) [25], while Fu et al. demonstrated that exhaled 2-butanone concentration is significantly different between stages I and II-IV, distinguishing them[247]. Carbonyl compounds, in general, have attracted research interest, not only for LC stages discrimination[247], but also to differentiate early-stage LC patients from healthy controls[256] and BPD patients[255,256]. Aldehydes seem promising LC biomarkers produced by tissue

damage[254], thus it has been attempted to determine their concentration to differentiate healthy subjects from NSCLC[35] or both SCLC and NSCLC patients[254]. LC discrimination from other diseases is also reported. In an attempt to discriminate NSCLC, COPD patients and healthy subjects, considering smoking habits, 4 VOCs were found in different levels for NSCLC and COPD patients.[244] In another study, LC patients were effectively distinguished from PNMD (COPD, pulmonary tuberculosis and asthma) patients using 10 VOCs[258].

The VOCs used to differentiate LC patients and healthy controls in the studies of on Table 13, were compiled (Table 14). In general, aliphatic hydrocarbons and aldehydes are reported in the literature as the most abundant in the breath of LC patients, followed by aromatic hydrocarbons and ketones, as well as alcohols in lower levels[19]. On Table 14, it is observed that alcohols, aldehydes, ketones, hydroxylated aldehydes and ketones, alkanes, aromatic, nitrogen as well as non-aromatic compounds are included in the commonly identified discriminant VOCs of LC towards healthy subjects. Specifically, 39 VOCs, including methanol, ethanol, 1-butanol, 1-propanol, 2-propanol, propanal, butanal, pentanal, hexanal, heptanal, octanal, nonanal, acetone, 2-butanone, 2-pentnone, 3-hydroxy-2-butanone, 2-hydroxyacetaldehyde, 4-hydroxyhexenal, hexane, octane, nonane, dodecane, isoprene, furan, 2,5-dimethyl furan, benzene, ethyl benzene, n-propyl benzene, 1,2,3-trimethyl benzene, 1-methyl-3-propyl benzene, toluene, xylenes, cyclohexanone, cyclohexane, methyl cyclohexane, propyl cyclohexane and acetonitrile have been identified in more than one studies, predominantly in higher levels in LC patients' breath. In some cases, for some VOCs, either lower or similar concentrations between LC patients and healthy controls are observed, however, in any case, those studies are fewer.

4.3.1.4. Breast Cancer (BC)

BC, one of the top five most frequent and mortal cancer types[4], comprises the most common cancer among female population, following skin cancer[3,32] and the main cause of women deaths[13]. Genetic and epigenetic alternations in breast cells, due to a combination of genetic and environmental factors, can induce BC. Such alternations, *e.g.,* inactivation of DNA repair genes or DNA methylation of certain genes, may occur in pre-malignant lesions, during carcinogenesis[260]. BC is subdivided into milk ducts and lobular cancer[32].

Table 13: Studies aiming at LC diagnosis, using exhaled VOC patterns, identified using analytical methods.

Number of subjects	Age Range	Differentiation	Analytical Technique	Statistical method / Classifier	Ref.
36 NSCLC, 25 COPD, 35 HS, 50 HNS (146 total)	67 LC, 70 COPD, 54 HS, 56 HNS	NSCLC vs HNS, COPD/HS vs HNS	SPME-GC-MS	PCA	[244]
17 LC, 170 HC (187 total)	51-74 LC, 26-74 HC	SCLC/NSCLC vs HS/HNS/HES	PTR-MS	Fisher's QDA	[248]
193 LC, 211 HC (404 total)	55-77 LC, 62-73 HC	SCLC/NSCLC vs HS/HES	TD-GC-MS	Fuzzy logic model-random classifier	[249]
65 LC, 31 HC (96 total)	37-84 LC, 21-65 HC	SCLC/NSCLC vs HS/HNS/HES	GC-MS	Kruskal-Wallis test	[250]
12 LC, 12 HS, 12 HNS (36 total)	51-81 LC, 26-56 HS, 22-39 HNS/occasionally S	SCLC/NSCLC ES vs HS/HNS/occasionally S	SPME-GC-MS	Kruskal–Wallis test/ SPSS	[35]
40 NSCLC, 38 HC (78 total)	58-78 NSCLC, 34-65 HC	NSCLC vs HNS/HES	SPME–GC-MS	ANOVA, Tukey's test / SPSS	[254]
43 NSCLC, 41 HC (84 total)	50-66 NSCLC, 41-54 HC	NSCLC NS/ES vs HNS	SPME-GC-MS	Wilcoxon rank sum test / SPSS	[11]
137 LC, 143 HC (280 total)	38-86 LC, 20-58 HC	SCLC/adenocarcinoma/Planoepitheliale/other NSCLC/other vs HNS	SPME-GC-MS	DA, CHAID	[33]
29 LC, 44 HC (73 total)	NA	SCLC/NSCLC vs HS/HNS	GC-ToF-MS	FA, PCA	[245]
97 LC, 88 HC, 32 BPN (217 total)	NA	HSCLC/NSCLC vs HS/HNS/BPN	Silicon Microreactor, FT-ICR-MS	Wilcoxon test / Minitab	[247]
107 LC, 88 HC, 40 BPN (235 total)	56-76 LC, 36-65 BPN, 28-57 HC	SCLC/NSCLC vs HS/HNS/BPN	Silicon Microreactor, FT-ICR-MS	Wilcoxon test / Minitab	[255]
50 LC, 39 HC (89 total)	58-78 LC, 24-40 HC	SCLC/NSCLC vs HC	IMS	Wilcoxon-Mann-Whitney test	[251]
13 LC, 25 HC (38 total)	50-70 LC, 22-57 HC	LC S/ LC NS vs HS/HNS	SPME-GCxGC	PLS-DA, Mann–Whitney Test	[12]
79 LC, 54 PNMD, 38 HC (171 total)	55-72 LC, 50-69 PNMD, 45-60 HC	SCLC/NSCLC vs HC/PNMD	SPME-GCMS	PCA	[258]
85 LC, 34 BPN, 85 HCs (204 total)	56-76 LC, 36-67 BPN, 28-56 HC	SCLC/NSCLC vs HS/HNS/BPN	Silicon Microreactor, FT-ICR-MS	Kruskal- Wallis test, PLS, SVM, RF, LDA, QDA	[256]
37 LC, 23 HC (60 total)	52-81 LC, 51-78 HC	LC vs HS/HNS/HES	SPME-GC-MS	LDA	[257]
116 LC , 37 HC (153 total)	36-96 LC, 24-64 HC	SCLC/NSCLC vs HC	GC	Mann-Whitney U-test, Kruskal Wallis test, Jonckheere-Terpstra trend test, Wilcoxon's rank test / SPSS, Graph prism	[252]
107 LC, 29 healthy (136 total)	NA	LC vs HS/HNS/HES	GC-MS	SVM	[259]
57 LC, 72 HC (129 total)	37-70 LC, 30-58 HC	SCLC/NSCLS vs HS/HNS	zNOSE4200 (GC-SAW)	Mann-Whitney U test / SPSS	[253]
58 LC, 24 BPD, 125 HC (207 total) 108 LC, 87 BPD, 82 HC (277 total)	49-72 LC, 43-70 BPD, 41-61 HC	LC vs HS/HNS/HES, LC vs BPD	TD-GC-MS SPME-GCMS	SPSS	[31]
51 LC, 53 HC (104 total)	63-79 LC, 56-78 HC	LC vs HS/HNS/HES	SPME-GCMS	Kruskal–Wallis test, Mann-Whitney test / SPSS	[34]
75 LC, 75 HC (150 total)	30-74 LC, 18-71 HC	LC vs HS	GC-FID/GC-MS	Kolmogorov–Smirnov test / StatSoft STATISTICA, Multilayer perceptron neural networks	[2]
160 LC, 70 BPN, 122 HC (352 total)	51-71 LC, 45-68 BPN, 42-57 HC	SCLC/NSCLC vs HS/HNS/HES, SCLC/NSCLC vs BNP	TD-GC-MS	t-test/ SPSS, Graph Prism, MatLab, ANN	[25]

ANN: artificial neural network, **BPD:** Benign Pulmonary Disease, **BPN:** benign pulmonary nodules, **CHAID:** chi-squared automatic interaction detector, **DA:** Discriminant Analysis, **ES:** ex-smokers, **FA:** Factor Analysis, **FT-ICR-MS:** Fourier transform-ion cyclotron resonance – mass spectrometry, **GC-MS:** Gas Chromatography - Mass Spectrometry, **HC:** healthy controls, **HES:** healthy ex-smokers, **HNS:** healthy non-smokers, **HS:** healthy smokers, **IMS:** Ion mobility spectrometry, **LDA:** linear discriminant analysis, **NS:** non-smokers, **NSCLC:** non-small-cell lung cancer, **PCA:** principal component analysis, **PNMD:** pulmonary non-malignant disease, **PTR-MS:** proton transfer reaction mass spectrometry, **QDA:** quadratic discriminant analysis, **RFC:** Random forest classification, **S:** smokers, **SCLC:** small-cell lung cancer, **SPME:** Solid-phase Microextraction, **SVM:** Support Vector Machine, **TD:** Thermal Desorption

Table 14: VOCs characterized as able to differentiate LC patients from healthy controls.

VOCs	Expression*	CAS No	Category	Ref.
Butan-1-ol, 3-Methyl-	+	123-51-3	Alcohol	[251]
Butan-2-ol, 2,3-dimethyl-	+	594-60-5	Alcohol	[250]
Butanol, 1-	+	71-36-3	Alcohol	[11]
Butanol, 1-	+	71-36-3	Alcohol	[257]
Butanol, 1-	NA	71-36-3	Alcohol	[34]
Ethanol	+	64-17-5	Alcohol	[33]
Ethanol	+	64-17-5	Alcohol	[253]
Methanol	+	67-56-1	Alcohol	[12]
Methanol	NA	67-56-1	Alcohol	[259]
Propanol, 1-	+	71-23-8	Alcohol	[12]
Propanol, 1-	+	71-23-8	Alcohol	[249]
Propanol, 1-	+	71-23-8	Alcohol	[250]
Propanol, 1-	+	71-23-8	Alcohol	[33]
Propanol, 1-	+	71-23-8	Alcohol	[245]
Propanol, 1-	NA	71-23-8	Alcohol	[259]
Propanol, 1-	−	71-23-8	Alcohol	[34]
Propanol, 2-	+	67-63-0	Alcohol	[248]
Propanol, 2-	+	67-63-0	Alcohol	[245]
Propanol, 2-	+	67-63-0	Alcohol	[34]
But-3-yn-2-ol	+	2028-63-9	Alcohol + Alkyne	[250]
Butanal	+	123-72-8	Aldehyde	[254]
Butanal	+	123-72-8	Aldehyde	[245]
Butanal	+	123-72-8	Aldehyde	[2]
Formaldehyde	+	50-00-0	Aldehyde	[248]
Heptanal	+	111-71-7	Aldehyde	[254]
Heptanal	+	111-71-7	Aldehyde	[251]
Hexadecanal	+	629-80-1	Aldehyde	[258]
Hexanal	+	66-25-1	Aldehyde	[35]
Hexanal	+	66-25-1	Aldehyde	[254]
Hexanal	LC only	66-25-1	Aldehyde	[33]
Hexanal	+	66-25-1	Aldehyde	[251]
Hexanal	Similar	66-25-1	Aldehyde	[34]
Hexanal	+	66-25-1	Aldehyde	[25]
Hexanal	NA	66-25-1	Aldehyde	[31]
Nonanal	+	124-19-6	Aldehyde	[35]
Nonanal	+	124-19-6	Aldehyde	[254]
Nonanal	Similar	124-19-6	Aldehyde	[34]
Nonanal	+	124-19-6	Aldehyde	[257]
Octanal	+	124-13-0	Aldehyde	[35]
Octanal	+	124-13-0	Aldehyde	[254]
Octanal	Similar	124-13-0	Aldehyde	[34]
Pentanal	+	110-62-3	Aldehyde	[35]
Pentanal	+	110-62-3	Aldehyde	[254]
Pentanal	LC only	110-62-3	Aldehyde	[33]
Pentanal	−	110-62-3	Aldehyde	[2]
Pentanal	+	110-62-3	Aldehyde	[250]
Propanal	+	123-38-6	Aldehyde	[254]
Propanal	+	123-38-6	Aldehyde	[33]
Propanal	+	123-38-6	Aldehyde	[245]
Propenal, 2-	+	107-02-8	Aldehyde	[245]
Acetaldehyde, 2-hydroxy-	+	141-46-8	Aldehyde, Hydroxylated	[255]
Acetaldehyde, 2-hydroxy-	+	141-46-8	Aldehyde, Hydroxylated	[247]
Acetaldehyde, 2-hydroxy-	+	141-46-8	Aldehyde, Hydroxylated	[256]
Hexenal, 4-hydroxy-	+	17427-08-6	Aldehyde, Hydroxylated	[247]
Hexenal, 4-hydroxy-	+	17427-08-6	Aldehyde, Hydroxylated	[255]
Hexenal, 4-hydroxy-	+	17427-08-6	Aldehyde, Hydroxylated	[256]
Non-2-enal, 4-hydroxy-	+	75899-68-2	Aldehyde, Hydroxylated	[256]
Butane	+	106-97-8	Alkane	[33]
Decane	+	124-18-5	Alkane	[244]
Dodecane	+	112-40-3	Alkane	[253]
Dodecane	NA	112-40-3	Alkane	[31]
Dodecane, n-	+	112-40-3	Alkane	[251]
Heneicosane	NA	629-94-7	Alkane	[31]
Heptane	+	142-82-5	Alkane	[25]

Heptane, 3-ethyl-3-methyl	+	14676-29-0	Alkane	[25]
Hexane	+	110-54-3	Alkane	[253]
Hexane	+	110-54-3	Alkane	[34]
Hexane	+	110-54-3	Alkane	[2]
Hexane, n-	+	110-54-3	Alkane	[257]
Methane	+	74-82-8	Alkane	[253]
Nonadecane	NA	629-92-5	Alkane	[31]
Nonane	LC only	111-84-2	Alkane	[33]
Nonane	+	111-84-2	Alkane	[25]
Nonane, 5-(2-methyl-)propyl-	+	62185-53-9	Alkane	[258]
Octane	+	111-65-9	Alkane	[244]
Octane	−	111-65-9	Alkane	[34]
Pentadecane, 8-hexyl-	+	13475-75-7	Alkane	[258]
Pentadecane, n-	NA	629-62-9	Alkane	[31]
Pentane	+	109-66-0	Alkane	[244]
Tetracosane, n-	NA	646-31-1	Alkane	[31]
Undecane, n-	+	1120-21-4	Alkane	[250]
Butane, 2-methyl-	+	78-78-4	Alkane Methylated	[250]
Decane, 4-methyl-	+	2847-72-5	Alkane Methylated	[249]
Heptane, Pentamethyl-	+	30586-18-6	Alkane Methylated	[244]
Pentane, 2-Methyl-	+	107-83-5	Alkane Methylated	[244]
Undecane, 3,7-dimethyl-	+	17301-29-0	Alkane Methylated	[250]
Dodecane, 2,6,11-trimethyl-	+	31295-56-4	Alkane Methylated	[258]
Heptadecane, 8-methyl-	NA	13287-23-5	Alkane Methylated	[31]
Heptane, 2,2,4,6,6-pentamethyl-	+	13475-82-6	Alkane Methylated	[253]
Methane, dimethyl-	+	74-98-6	Alkane Methylated	[253]
Pentadecane, 2,6,10,14-tetramethyl-	NA	1921-70-6	Alkane Methylated	[31]
Pentane, 3-methyl-	−	96-14-0	Alkane Methylated	[257]
But-2-ene, 2-methyl-	+	513-35-9	Alkene	[250]
Hexa-2,4-diene, 2,5-dimethyl-	+	764-13-6	Alkene (Diene)	[249]
Isoprene	+	78-79-5	Alkene (Diene)	[33]
Isoprene	NA	78-79-5	Alkene (Diene)	[259]
Isoprene	Similar	78-79-5	Alkene (Diene)	[34]
Isopropylamine	+	75-31-0	Amine	[251]
Phenol	NA	108-95-2	Aromatic Alcohol	[31]
Phenol, 2,6-di-tert-butyl-, 4-methyl-	+	128-37-0	Aromatic Alcohol	[258]
Benzaldehyde	+	100-52-7	Aromatic Aldehyde	[250]
Benzene, cyclobutyl-	+	4392-30-7	Aromatic Cycloalkane	[250]
Benzene-1,2-dicarboxylic acid, diethyl ester	+	84-66-2	Aromatic Ester	[249]
Benzoic acid, 4-ethoxy-, ethyl ester	+	23676-09-7	Aromatic Ester+Ether	[249]
Benzene, 1-phenoxy-	+	101-84-8	Aromatic Ether	[249]
Furan	+	110-00-9	Aromatic Ether	[33]
Furan	+	110-00-9	Aromatic Ether	[245]
Furan, 2,5-Dimethyl	+	625-86-5	Aromatic Ether	[25]
Furan, 2,5-Dimethyl-	+	625-86-5	Aromatic Ether	[249]
1H-Indene, 2,3-dihydro-1,1,3-trimethyl-3-phenyl-	+	3910-35-8	Aromatic Hydrocarbon	[249]
Benzene	+	71-43-2	Aromatic Hydrocarbon	[244]
Benzene	+	71-43-2	Aromatic Hydrocarbon	[245]
Benzene	−	71-43-2	Aromatic Hydrocarbon	[34]
Benzene	+	71-43-2	Aromatic hydrocarbon	[2]
Benzene	+	71-43-2	Aromatic Hydrocarbon	[25]
Benzene, 1,2,3-trimethyl-	NA	526-73-8	Aromatic Hydrocarbon	[31]
Benzene, 1,2,3-trimethyl-	+	526-73-8	Aromatic Hydrocarbon	[25]
Benzene, 1-methyl-3-propyl-	NA	1074-43-7	Aromatic Hydrocarbon	[31]
Benzene, 1-methyl-3-propyl-	+	1074-43-7	Aromatic Hydrocarbon	[25]
Benzene, 4-ethyl-1, 2-dimethyl	+	934-80-5	Aromatic Hydrocarbon	[25]
Benzene, Ethyl-	+	100-41-4	Aromatic Hydrocarbon	[244]
Benzene, Ethyl-	+	100-41-4	Aromatic Hydrocarbon	[33]
Benzene, Ethyl-	+	100-41-4	Aromatic Hydrocarbon	[245]
Benzene, Ethyl-	+	100-41-4	Aromatic Hydrocarbon	[251]
Benzene, ethyl-	+	100-41-4	Aromatic Hydrocarbon	[34]
Benzene, ethyl-	+	100-41-4	Aromatic Hydrocarbon	[25]
Benzene, n-propyl-	NA	103-65-1	Aromatic Hydrocarbon	[31]
Benzene, n-propyl-	+	103-65-1	Aromatic Hydrocarbon	[25]
Benzene, Trimethyl-	+	NA	Aromatic Hydrocarbon	[244]
Biphenyl, 2,2'-diethyl-	+	13049-35-9	Aromatic Hydrocarbon	[249]

Indan	NA	496-11-7	Aromatic Hydrocarbon	[31]
Naphthalene, 1,2,6-trimethyl-	–	3031-05-8	Aromatic Hydrocarbon	[253]
Styrene	+	100-42-5	Aromatic Hydrocarbon	[34]
Toluene	+	108-88-3	Aromatic Hydrocarbon	[244]
Toluene	+	108-88-3	Aromatic Hydrocarbon	[34]
Toluene	+	108-88-3	Aromatic Hydrocarbon	[2]
Toluene, 3-ethyl-	NA	620-14-4	Aromatic Hydrocarbon	[31]
Xylene (o-,m-,p-)	+	95-47-6/108-38-3/106-42-3	Aromatic Hydrocarbon	[252]
Xylene, o-	+	95-47-6	Aromatic Hydrocarbon	[33]
Xylene, o-	NA	95-47-6	Aromatic Hydrocarbon	[31]
Xylene, o-	+	95-47-6	Aromatic Hydrocarbon	[25]
Xylene, p-, 2-ethyl-	+	1758-88-9	Aromatic Hydrocarbon	[25]
Xylenes (o-,m-,p-)	+	95-47-6/108-38-3/106-42-3	Aromatic Hydrocarbon	[244]
Acetophenone	+	98-86-2	Aromatic Ketone	[250]
10,11-Dihydro-5H-dibenz-(B,F)-azepine	+	494-19-9	Aromatic, Nitrogen Compound	[249]
1-Isoprpyl-4-methylbicyclo [3.1.0] hexane-3-ol	+	513-23-5	Cyclic Alcohol	[253]
Aconityl anhydride	NA	6318-55–4	Cyclic Anhydride	[31]
Cyclohexanone	+	108-94-1	Cyclic Ketone	[251]
Cyclohexanone	+	108-94-1	Cyclic Ketone	[34]
Cyclohexane	–	110-82-7	Cycloalkane	[257]
Cyclohexane	+	110-82-7	Cycloalkane	[252]
Cyclohexane	–	110-82-7	Cycloalkane	[34]
Cyclohexane, methyl-	NA	108-87-2	Cycloalkane	[31]
Cyclohexane, methyl-	+	108-87-2	Cycloalkane	[25]
Cyclohexane, prolyl-	NA	1678-92-8	Cycloalkane	[31]
Cyclohexane, prolyl-	+	1678-92-8	Cycloalkane	[25]
Cyclopentene	+	142-29-0	Cycloalkene	[250]
trans-Caryophyllene	+	87-44-5	Cycloalkene	[249]
Cyclopenta-1,3-diene, 1-methyl-	+	26519-91-5	Cycloalkene (Diene)	[250]
Cyclododeca-1,5,9-triene, 1,5,9-trimethyl-	+	21064-19-7	Cycloalkene (Triene)	[249]
2,4,4-trimethylpentan-1,3-diol-diisobutyrate	+	74381-40-1	Ester	[249]
Acetate, Ethyl-	+	141-78-6	Ester	[245]
Acetate, Propyl-	+	109-60-4	Ester	[25]
Butyl acetate	+	123-86-4	Ester	[250]
DL-sec-Butyl acetate	+	105-46-4	Ester	[25]
Ethyl butyrate	–	105-54-4	Ester	[34]
Pentan-1,3-dioldiisobutyrate, 2,2,4-trimethyl	+	6846-50-0	Ester	[249]
Acetate, 2-metylbutyl / Hexanol, 2-	+	624-41-9 / 626-93-7	Ester/Alcohol	[251]
Acetone	+	67-64-1	Ketone	[33]
Acetone	+	67-64-1	Ketone	[245]
Acetone	+	67-64-1	Ketone	[12]
Acetone	Similar	67-64-1	Ketone	[34]
Acetone	+	67-64-1	Ketone	[2]
Butanedione, 2,3-	+	431-03-8	Ketone	[250]
Butanone, 2-	+	78-93-3	Ketone	[250]
Butanone, 2-	+	78-93-3	Ketone	[245]
Butanone, 2-	+	78-93-3	Ketone	[247]
Butanone, 2-	+	78-93-3	Ketone	[255]
Butanone, 2-	+	78-93-3	Ketone	[256]
Butanone, 2-	+	78-93-3	Ketone	[257]
Butanone, 2-	–	78-93-3	Ketone	[34]
Butanone, 2-	+	78-93-3	Ketone	[2]
Hepta-2,6-dien-4-one, 2,5,5-trimethyl-	–	546-49-6	Ketone	[253]
Pentan-2-one, 4-methyl-	NA	108-10-1	Ketone	[31]
Pentan-3-one, 2,4-dimethyl-	+	565-80-0	Ketone	[249]
Pentanone, 2-	+	107-87-9	Ketone	[33]
Pentanone, 2-	–	107-87-9	Ketone	[257]
Pentanone, 2- / Pentanal	+	107-87-9 / 110-62-3	Ketone	[256]
Pentanone,, 2-	+	107-87-9	Ketone	[245]
Butan-2-one, 3-hydroxy-	+	513-86-0	Ketone Hydroxylated	[250]
Butan-2-one, 3-hydroxy-	+	513-86-0	Ketone Hydroxylated	[11]
Butan-2-one, 3-Hydroxy-	+	513-86-0	Ketone Hydroxylated	[247]
Butan-2-one, 3-Hydroxy-	+	513-86-0	Ketone Hydroxylated	[255]
Butan-2-one, 4-hydroxy-	+	590-90-9	Ketone Hydroxylated	[256]
Acetonitrile	NA	75-05-8	Nitrogen Compound	[259]
Acetonitrile	+	75-05-8	Nitrogen Compound	[2]

Benzylimidazoline, 2-	NA	59-98-3	Nitrogen compound	[31]
Ethylenimine	+	151-56-4	Nitrogen Compound	[250]
Hydrogen isocyanide	NA	6914-07-4	Nitrogen Compound	[259]
Isoquinoline, 1,2,3,4-tetrahydro-	+	91-21-4	Nitrogen compound	[250]
Urea, tetramethyl-	+	632-22-4	Nitrogen Compound	[250]
Benzothiazole	+	95-16-9	Nitrogen – Sulfur Compound	[25]
2,6-Diisopropyl-1,4-benzoquinone	+	1988-11-0	Quinone	[249]
Hexamethylcyclotrisiloxane	+	541-05-9	Siloxane	[25]
Dimethyl Sulfide	+	75-18-3	Sulfur Compound	[33]
Methyl propyl sulfide	+	3877-15-4	Sulfur Compound	[250]

* *"Expression" refers to the concentration of the VOC in patient's breath in comparison to healthy controls; (+) indicates higher concentration in patient's breath, (–) indicates lower concentration in patient's breath.*

Lymph node metastasis, along with large tumor size, comprise signs of unfavorable prognosis[13], that can be avoided by early diagnosis and appropriate treatment, decreasing mortality[3,13,32].

The gold standard method for BC diagnosis, reducing BC mortality, is mammography[13,261]. However, radiation exposure and patient discomfort, decrease compliance[3,261]. MRI and ultrasonography are also used[32]. Ultrasonography surpasses mammography sensitivity, detecting lesions in dense breasts, however detection of microcalcifications, a typical characteristic of DCIS, is not always feasible. This, along with the dependance on technician expertise, are important limitations.[13] Early BC detection is limited, mainly due to lack of early symptoms[32], thus new tools with increased sensitivity are needed[3]. Breath analysis may serve as a painless, safe and accurate diagnostic tool for BC, as breast stromal fibroblast activation potentially enhances oxidative stress and increases CYP450 activity.[262]

Among the seven studies selected according to the inclusion criteria (*§ 3.2*), 3 studies [3,29,263] attempted to differentiate BC patients from healthy women, using 27[3] VOCs and two different groups of 5[29,263] VOCs. In the rest of studies, the differentiation of BC patients from patients with abnormal mammograms and negative biopsies[264], benign tumors[260,265], non-malignant breast diseases[13] or early-stage BC (DCIS)[260], was also a target. Remarkably, Wang et al.[13] differentiated BC patients from healthy controls, cyclomastopathy and mammary gland fibroma, using 21, 6 and 8 VOCs, respectively, while 2,5,6-trimethyloctane, 1,4-dimethoxy-2,3-butanediol and cyclohexanone differentiated BC patients from all the other categories. In another study, Barash et al.[260] identified 21 VOCs significantly different between healthy women and patients suffering from BBT, DCIS and BC and a potentially cancer-related set of 14 VOCs significantly different between malignant and non-malignant

Table 15: Studies aiming at BC diagnosis, using exhaled VOC patterns, identified using analytical methods.

Number of subjects	Age Range	Differentiation	Analytical Technique	Statistical method / Classifier	Ref.
51 abnormal mammograms + BC, 147 abnormal mammograms + negative biopsy, 42 HC (240 total)	≥18 all	BC vs HC	TD-GC-MS	Fuzzy logic model	[264]
56 BC, 204 HC (260 total)	48-62 BC, 44-66 HC	BC vs HC	GC-MS	WDA	[3]
22 BC, 22 HC (44 total)	20-75 all	BC vs HC	SPME-GC-MS, GNP sensor	PCA	[29]
10 BC, 10 HC (20 total)	41-73 BC, 51-70 HC	BC vs HC	GC-MS	Kolmogorov-Smirnov test, Mann-Whitney U test, t-test,	[263]
22 BC, 17 BBT, 24 HC (63 total)	≥18 all	BC NS vs HNS	GC-MS	Kruskal–Wallis test / SPSS, FDA, leave-one-out discriminant analysis	[265]
39 BC, 25 CMP, 21 MGF, 45 HC (130 total)	43-64 BC, 33-50 CMP, 28-44 MGF, 34-56 HC	BS vs HC/CMP/MGF	SPME-GC-MS	PCA, PLS-DA	[13]
169 BC, 25 DCIS, 52 BBT, 30 control (276 total)	21-69 BC, 32-70 DCIS, 24-62 benign, 26-74 HC	BS vs HC/BBT	GC-MS, GNP/SWCNT sensor	Wilcoxon/Kruskal- Wallis test, DFA	[260]

BBT: breast benign tumor, **BC:** breast cancer, **CMP:** cyclomastopathy; **DCIS:** ductal carcinoma *in situ*, **DFA:** Discriminant Factor Analysis, **FDA:** Fisher discriminant analysis, **GC-MS:** Gas chromatography-Mass Spectrometry, **GNP:** gold nanoparticles, **HC:** healthy controls, **MGF:** mammary gland fibroma. **PCA:** Principal component analysis, **PLS-DA:** partial least squares discriminant analysis, **SPME:** Solid-phase Microextraction, **SWCNTs:** single wall carbon nanotubes, **TD:** Thermal Desorption, WDA: weighted digital analysis

patients. Li et al.[265], on the other hand, defined 4 aldehydes discriminant for non-smoker BC patients and healthy controls, however no significant differences were observed between patients with BC and benign tumors.

The VOCs used to differentiate BC patients and healthy controls in the studies of Table 15, were compiled (Table 16). The most common category of VOCs among the studies are (alkylated) alkanes. Only tetradecane, though, is reported in two different studies, in different relative expression levels. Lower levels of some VOCs, including the methylated alkane 3-methyl hexane, the alkane decane, the terpene caryophyllene and the aromatic naphthalene, in BC patients are deemed as a potent consequence of CYP450 alternated function[263]. Among aldehydes, heptanal was found in increased levels in breath samples of BC patients, in two different studies. The same was observed for the methylated alkanes 2,3-dimethyl pentane and 3,3-dimethyl pentane, which comprise isomers of the same compound, while tetradecane and butyl acetate were also observed in two studies.

Table 16: VOCs characterized as able to differentiate BC patients from healthy controls and/or benign diseases.

VOCs	Expression*	CAS No	Category	Ref.
Butane-2,3-diol, 1,4-dimethoxy-	+	33507-82-3	Alcohol	[13]
Ethanol	+	64-17-5	Alcohol	[260]
Hexan-1-ol, 2-ethyl-	+	104-76-7	Alcohol	[260]
Hexan-3-ol, 5-methyl-	−	623-55-2	Alcohol	[13]
Octan-1-ol, 2-butyl-	+	3913-02-8	Alcohol	[3]
Octan-1-ol, 2-hexyl-	+	19780-79-1	Alcohol	[3]
Propanol, 2-	+	67-63-0	Alcohol	[264]
Heptanal	+	111-71-7	Aldehyde	[264]
Heptanal	+	111-71-7	Aldehyde	[265]
Hexanal	+	66-25-1	Aldehyde	[265]
Nonanal	+	124-19-6	Aldehyde	[265]
Octanal	+	124-13-0	Aldehyde	[265]
Dodecane	+	112-40-3	Alkane	[3]
Heptane	+	142-82-5	Alkane	[260]
Hexadecane	−	544-76-3	Alkane	[13]
Nonane, 5-butyl-	−	17312-63-9	Alkane	[13]
Pentadecane	+	629-62-9	Alkane	[3]
Tetradecane	+	629-59-4	Alkane	[3]
Tetradecane	−	629-59-4	Alkane	[13]
Tridecane	+	629-50-5	Alkane	[3]
Undecane	+	1120-21-4	Alkane	[3]
5-(2-methylpropyl)-nonane)	−	62185-53-9	Alkane Branched	[29]
Decane, 2,2-dimethyl-	−	17312-44-6	Alkane Methylated	[13]
Decane, 2,3,4-trimethyl	−	62238-15-7	Alkane Methylated	[29]
Dodecane, 2,7,10-trimethyl-	+	74645-98-0	Alkane Methylated	[3]
Dodecane, 2,7,11-trimethyl-	+	31295-56-4	Alkane Methylated	[3]
Heptane, 2,3,4-trimethyl	−	52896-95-4	Alkane Methylated	[13]
Hexane, 3-methyl-	−	589-34-4	Alkane Methylated	[263]
Octane, 2,5,6-trimethyl	+	62016-14-2	Alkane Methylated	[13]
Pentane, 2,3-dimethyl	+	565-59-3	Alkane Methylated	[260]
Pentane, 3,3-dimethyl	+	562-49-2	Alkane Methylated	[29]
Octane, 2,3,6-trimethyl-	−	62016-33-5	Alkane, Methylated	[13]
Decene	−	872-05-9	Alkene	[263]
Ethylene, trichloro-	+	79-01-6	Halogen Compound, Alkene	[263]
Dimethylacetamide	+	127-19-5	Amide	[13]
1,4-Diethylhexyl 3-(trifluoromethyl) benzoate	−	NA	Aromatic Ester	[29]
1-Methyl-1-phenylethyl acetate	−	3425-72-7	Aromatic Ester	[13]
Benzene, 1,2,3,5-tetramethyl-	+	527-53-7	Aromatic Hydrocarbon	[3]
Benzene, 1,2,4,5-tetramethyl-	+	95-93-2	Aromatic Hydrocarbon	[3]
Xylene, m-	+	108-38-3	Aromatic Hydrocarbon	[260]
Benzene, 1-ethyl-3,5-dimethyl-	+	934-74-7	Aromatic Hydrocarbon	[3]
Benzocyclobutene	−	694-87-1	Aromatic Hydrocarbon	[13]
Naphthalene	−	91-20-3	Aromatic Hydrocarbon	[263]
Toluene	+	108-88-3	Aromatic Hydrocarbon	[260]
Acetophenone	+	98-86-2	Aromatic Ketone	[264]
1-azulenecarbonitrile, 2-amino-5-isopropyl-8-methyl-	−	NA	Aromatic Nitrogen compound	[29]
2,3-dihydro-1-phenyl-4(1H)-quinazolinone	+	35242-43-4	Aromatic Nitrogen compound	[264]
Dimethyl carbonate	+	616-38-6	Carbonate	[260]
Ethylene carbonate	−	96-49-1	Carbonate	[13]
Methylacrylic acid	−	79-41-4	Carboxylic acid	[13]
Butanoic acid, 4-Hydroxy-	−	591-81-1	Carboxylic acid, Alcohol	[13]
Propionic acid, 2-acetyl amino-	−	1115-69-1	Carboxylic Acid, Amide	[13]
Aromadendrene	+	25246-27-9	Cyclic Alkene	[3]
Cyclopropane, ehtylidene	+	18631-83-9	Cyclic Alkene	[3]
Longifolene-(V4)	+	NA	Cyclic Alkene	[3]
1,3,5,7-tetroxane	−	293-30-1	Cyclic Ether	[13]
Cyclohexanone	+	108-94-1	Cyclic Ketone	[13]
Cyclohexane, 1,4-dimethyl-	+	589-90-2	Cycloalkane	[260]
Cyclopentane	+	287-92-3	Cycloalkane	[260]
Cyclohexene, 1-methyl-5-(1-methylethenyl)-	+	1461-27-4	Cycloalkene	[3]
Isoprene	+	78-79-5	Diene	[3]
Pentadiene, 1,4-	+	591-93-5	Diene	[3]
trans-2,3-Epoxybutane	+	21490-63-1	Epoxide	[13]

Acetic acid, 2,6,6-trimethyl-3-methylene-7-(3-oxobutylidene)oxepan-2-yl ester	+	NA	Ester	[3]
Butyl acetate	+	123-86-4	Ester	[260]
Butyl acetate	–	123-86-4	Ester	[13]
Isopropyl myristate	+	110-27-0	Ester	[264]
Prop-2-enoic acid, butyl ester	+	141-32-2	Ester	[260]
Trifluoroacetic acid, *n*-octadecyl ester	+	79392-43-1	Halogen Compound, Ester	[3]
Acetone	+	67-64-1	Ketone	[260]
Hept-5-en-2-one, 6-methyl-	+	110-93-0	Ketone	[260]
Hexane, 2,5-dimethyl-2,5-dihydroperoxy-	–	3025-88-5	Peroxide	[13]
2,5-di-tert-Butyl-1,4-benzoquinone	+	2460-77-7	Quinone	[3]
2,6-di-tert-Butyl-1,4-benzoquinone	+	719-22-2	Quinone	[3]
Benzoic acid, 4-methyl-2-trimethylsilyloxy-, trimethylsilyl ester	+	NA	Silicon Compound	[3]
Cyclotetrasiloxane, octamethyl-	+	556-67-2	Silicon Compound	[3]
3-Ethoxy-1,1,1,5,5,5-hexamethyl-3 (trimethylsiloxy)trisiloxane	+	18030-67-6	Silicone Compound	[3]
Caryophyllene	–	87-44-5	Terpene	[263]
Limonene, D-	+	5989-27-5	Terpene	[3]
Longifolene, (+)	+	475-20-7	Terpene	[3]
Pinene, α-	+	80-56-8	Terpene	[260]

* "Expression" refers to the concentration of the VOC in patient's breath in comparison to healthy controls; (+) indicates higher concentration in patient's breath, (–) indicates lower concentration in patient's breath.

4.3.2. Polymer selection

δ values were not available in the literature for all VOC or polymers selected, thus, they were calculated for all the compounds and polymers, for comparable values to be obtained, as δ calculation with group contribution methods leads to somehow different results (§ *2.4.2*). T_g and VOCs/polymer density values, for molar volume calculation, were retrieved from references [66], [67] and [266] and/or the respective safety data sheets. Especially for benzene, calculated (15.69) and literature (18.5) δ values, as well as δ of similar aromatic compounds (toluene, xylenes) differed significantly, thus literature values were used for $\Delta\delta$ calculation. Also, literature value was used for δ_{water}[66]. Notably, polymer selection was based on $\Delta\delta$, however VOC-polymer structural similarity or functional groups able to form VOC-polymer hydrogen bonds were also taken into account, especially if two different polymers exhibited similar $\Delta\delta$ for VOCs. The selected polymers are amorphous, while for some T_g is greater than RT.

A. *Asthmatic children*

The calculated δ values of the VOCs selected for asthmatic children and the potentially responsive polymers are presented on Table 17. *cis*-PIP is expected to be more sensitive for the alkanes and limonene (dispersion forces) and not acetone, as indicated by $\Delta\delta$. The small PVP- acetone $\Delta\delta$ indicates that acetone absorption is favored (polar interactions), in contrast to the rest of VOCs. Water absorption to polymers seems to be by far less favored

than VOCs. For the levels of limonene and 2,4-dimethyl heptane in asthmatic children breath, there is no clear tendency between the studies retrieved, while the three alkanes are increased. In contrast, acetone concentration is reported to be lower for asthmatic children, thus potential differentiation of acetone and the rest of VOCs using those two polymers could enhance the possibility for effective diagnosis.

Table 17. Solubility parameters of selected VOCs and polymers and solubility parameter difference for each pair.

VOC/polymer	δb $(MJ/m^3)^{1/2}$	δp $(MJ/m^3)^{1/2}$	δh $(MJ/m^3)^{1/2}$	δt $(MJ/m^3)^{1/2}$	$\Delta\delta$ $(MJ/m^3)^{1/2}$	
					cis-PIP	PVP
Limonene	16.44	0	0	16.44	**0.01**	15.48
Heptane, 2,4-dimethyl	14.46	0	0	14.46	**1.97**	15.89
Tetradecane	15.69	0	0	15.69	**0.74**	15.61
Decane	15.46	0	0	15.46	**0.98**	15.65
Dodecane	15.57	0	0	15.57	**0.87**	15.63
Acetone	15.39	10.49	5.22	19.34	11.76	**5.30**
Water	12.30	31.30	34.20	47.96	46.55	32.19
cis-PIP	16.43	0	0	16.43	-	-
PVP	18.67	12.49	8.87	24.15	-	-

cis-**PIP**: cis-polyisoprene, *Tg*: -67℃, **PVP:** polyvilyl pyrrolidone, *Mw:* 40K, *Tg:* 175℃

B. *Asthmatic adults*

The calculated δ of the VOCs selected for asthmatic adults and the potentially responsive polymers are presented on Table 18. It should be noted that instead of the not commercially available 2,6,11-trimethyl dodecane, the isomer 2,6,10-trimethyl dodecane with the same δ, found also increased in asthmatic adults, was used. The small PVP-acetone $\Delta\delta$ indicates the increased polymer affinity for acetone (polar interactions), in contrast to the rest VOCs, exhibiting high $\Delta\delta$. In contrast, *cis*-PIP is expected to absorb the non-polar VOCs to a greater extend (dispersion forces) and not the polar acetone, as indicated by $\Delta\delta$. PS, with, probably, increased affinity for the aromatic toluene (dispersion forces and π-π interactions) in comparison to the alkanes and isoprene, could also be used, to enhance response to the aromatic toluene. PS affinity for acetone is expected to be far lower, as $\Delta\delta$

Table 18. Solubility parameters of selected VOCs and polymers and solubility parameter difference for each pair.

VOC/polymer	δb $(MJ/m^3)^{1/2}$	δp $(MJ/m^3)^{1/2}$	δh $(MJ/m^3)^{1/2}$	δt $(MJ/m^3)^{1/2}$	$\Delta\delta$ $(MJ/m^3)^{1/2}$		
					cis-PIP	PVP	PS
Dodecane, 2,6,10-trimethyl	15.93	0	0	15.93	**0.500**	15.56	**2.30**
Heptane, 2,4-dimethyl	14.46	0	0	14.46	**1.97**	15.89	**3.65**
Toluene	17.41	1.04	0	17.44	**1.42**	14.54	**0.54**
Isoprene	14.85	0	0	14.85	**1.58**	15.79	**3.29**
Acetone	15.39	10.49	5.22	19.34	11.76	**5.30**	11.03
Water	12.30	31.30	34.20	47.96	46.55	32.19	45.97
cis-PIP	16.43	0.00	0.00	16.43	-	-	-
PVP	18.67	12.49	8.87	24.15	-	-	-
PS	17.95	1.11	0.00	17.95	-	-	-

cis-**PIP**: cis-polyisoprene, *Tg*: -67℃, **PS**: polystyrene, *Mw:* 35K, *Tg:* 123-128℃, **PVP:** polyvilyl pyrrolidone, *Mw:* 40K, *Tg:* 175℃

is higher. VOCs concentrations were increased in asthmatic adults breath, thus greater response for those VOCs in contrast to healthy subjects could potentially lead to asthma diagnosis. As previously observed, polymer affinity for water is far less favored.

C. COPD

Table 19. Solubility parameters of selected VOCs and polymers and solubility parameter difference for each pair**.**

VOC/polymer	δb (MJ/m³)¹/²	δp (MJ/m³)¹/²	δh (MJ/m³)¹/²	δt (MJ/m³)¹/²	Δδ (MJ/m³)¹/²					
					P4HS	PVB	PVP	PS	cis-PIP	PLA
n-heptane	14.95	0.00	0.00	14.95	15.00	8.55	15.77	**3.19**	**1.48**	12.24
n-octane	15.14	0.00	0.00	15.14	14.96	8.51	15.72	**3.02**	**1.29**	12.29
n-nonadecane	15.71	0.00	0.00	15.71	14.88	8.40	15.60	**2.49**	**0.72**	12.43
Heptane, 2,4-dimethyl	14.46	0.00	0.00	14.46	15.09	8.69	15.89	**3.65**	**1.97**	12.15
Heptane, 2,6-dimethyl	14.46	0.00	0.00	14.46	15.09	8.69	15.89	**3.65**	**1.97**	12.15
Toluene	17.41	1.04	0.00	17.44	14.44	7.77	14.54	**0.54**	**1.42**	12.48
Benzene	17.6	1.00	0.00	18.5	14.44	7.80	14.65	**0.36**	**1.53**	11.78
o-Xylene	17.49	0.91	0.00	17.51	14.47	7.84	14.63	**0.50**	**1.40**	34.55
m-Xylene	17.17	0.90	0.00	17.20	14.48	7.83	14.68	**0.80**	**1.16**	12.58
p-Xylene	17.11	0.89	0.00	17.14	14.49	7.83	14.68	**0.86**	**1.12**	12.46
Phenol	18.68	5.83	15.09	24.71	**1.80**	8.42	9.11	15.83	16.34	8.29
Benzaldehyde	18.73	7.96	6.66	21.41	7.91	**3.82**	**5.04**	9.59	10.63	7.24
Acetic acid	16.63	7.35	13.23	22.48	**2.71**	6.91	7.04	14.69	15.14	**5.50**
Cyclohexanone	17.62	7.41	4.39	19.61	9.82	**3.88**	6.85	7.69	8.70	7.63
2-Pentanone	15.69	7.23	4.33	17.81	10.03	**4.00**	7.56	7.83	8.47	6.47
Hexanal	16.38	6.65	6.12	18.71	8.07	**2.37**	6.85	8.40	9.04	**5.51**
Water	12.30	31.30	34.20	47.96	33.70	38.51	32.19	45.97	46.55	34.55
P4HS	17.67	4.94	13.90	23.01	-	-	-	-	-	-
PVB	17.07	4.53	6.93	18.98	-	-	-	-	-	-
PVP	18.67	12.49	8.87	24.15	-	-	-	-	-	-
PS	17.95	1.11	0.00	17.95	-	-	-	-	-	-
cis-PIP	16.43	0.00	0.00	16.43	-	-	-	-	-	-

cis-**PIP**: cis-polyisoprene**,** *Tg*: -67℃, **P4HS**: poly(4-hydroxy styrene), *Mw*: 25K/11K, *Tg*: 130-185℃, **PLA**: polylactic acid, *Mw*: 60K, T_g: 50-57℃, **PS**: polystyrene, *Mw*: 35K, *Tg*: 123-128℃, **PVB**: polyvinyl butyral, *Mw*: 170-250K, *Tg*: 72-78℃, **PVP:** polyvilyl pyrrolidone, *Mw:* 40K, *Tg:* 175℃

The calculated δ values of the VOCs selected for COPD patients and the potentially responsive polymers are presented on Table 19. Among the VOCs characterized more than once as COPD-biomarkers, n-butane (gas in RT) and indole (solid in RT) were excluded. The small Δδ for P4HS and the VOCs phenol (hydrogen bonding and π-π stucking) and acetic acid (hydrogen bonding) indicate higher polymer affinity for those VOCs. PLA seems to, also, have high affinity for acetic acid, along with hexanal, thus PLA and P4HS combination may enable phenol identification is some cases. PVB and PVP are indicated as sensitive to benzaldehyde, with the former having, also, affinity for cyclohexanone, 2-pentanone and hexanal. Signal due to benzaldehyde presence could be discriminated, combining those two polymers. PVB affinity for the other VOCs seems to be lower, however it is observed that Δδ are not too high. Notably, phenol and benzaldehyde comprise the only class of

VOCs (polar aromatic) not overlapping with the commonly reported VOC classes of the other three diseases, thus their differentiation may be of particular importance. Concerning the alkanes and the non-polar aromatic VOCs, PS and cis-PIP exhibit low $\Delta\delta$ values, indicating increased affinity. Taking into account the quite lower $\Delta\delta$ values of PS for the non-polar aromatic VOCs (0.36-0.86 (MJ/m^3)$^{1/2}$), in combination with their structural similarity and the development of π-π interactions, it could be expected that higher responses would be obtained for those VOCs. Polymer affinity for water seems to be far less favored.

Among those VOCs, the concentrations of methylated heptanes in COPD patients were diminished, in contrast to those of heptane and octane, while, for nonadecane, no clear tendency is observed among the studies. The differentiation of the methylated from normal alkanes, though, is quite challenging as indicated by $\Delta\delta$ with PS and cis-PIP. Also, acetic acid concentration was found both increased and decreased in relation to healthy subjects. The rest VOCs are reported to be exhaled in higher levels for COPD patients, thus their detection could lead to COPD diagnosis, based mainly on concentration differences.

D. *Lung cancer*

Table 20. Solubility parameters of selected VOCs and polymers and solubility parameter difference for each pair.

VOC/polymer	δb (MJ/m³)¹/²	δp (MJ/m³)¹/²	δh (MJ/m³)¹/²	δt (MJ/m³)¹/²	Δδ (MJ/m³)¹/²			
					PMMA	PHEMA	PS	cis-PIP
Ethanol	15.43	8.57	18.52	25.59	9.94	**3.89**	20.12	20.43
1-Propanol	15.63	6.68	16.35	23.58	7.42	**1.03**	17.42	17.68
Hexanal	16.38	6.65	6.12	18.71	**3.13**	9.38	8.40	9.04
Pentanal	16.01	7.53	6.51	18.85	**3.23**	9.73	9.35	9.96
2-Butanone	15.65	8.61	4.73	18.47	**5.33**	10.99	9.16	9.85
3-Hydroxy-2-butanone	16.20	10.47	15.84	24.96	**5.10**	**4.35**	18.48	18.99
Cyclohexanone	17.62	7.41	4.39	19.61	**5.03**	11.32	7.69	8.70
Cyclohexane	16.18	0.00	0.00	16.18	10.78	16.65	**2.08**	**0.25**
Hexane	14.70	0.00	0.00	14.70	10.98	16.66	**3.43**	**1.73**
Dodecane	15.57	0.00	0.00	15.57	10.84	16.64	**2.62**	**0.86**
Isoprene	14.85	0.00	0.00	14.85	10.95	16.65	**3.29**	**1.58**
Ethyl benzene	17.31	0.90	0.00	17.34	10.32	16.42	**0.67**	**1.26**
o-Xylene	17.49	0.91	0.00	17.51	10.32	16.44	**0.50**	**1.40**
Furan	15.23	5.59	6.47	17.47	**3.08**	9.00	8.33	8.64
Water	12.30	31.30	34.20	47.96	36.10	31.51	45.97	46.54
PMMA	16.24	3.62	7.19	18.13	-	-	-	-
PHEMA	15.55	6.19	15.45	22.78	-	-	-	-
PS	17.95	1.11	0.00	17.95	-	-	-	-
cis-PIP	16.43	0.00	0.00	16.43	-	-	-	-

cis-PIP: cis-polyisoprene**, *Tg*: -67℃, **PHEMA:** poly(2-hydroxyethyl methacrylate, *Mv*: 20K, *Tg:* 84.88℃, **PMMA:** poly(methyl methacrylate), *Mw:* 120K, *Tg:* 105℃ **PS:** polystyrene, *Mw:* 35K, *Tg:* 123-128℃

The calculated δ values of the VOCs selected for LC patients and the potentially responsive polymers are presented on Table 20. Among the VOCs repeatedly characterized as LC-biomarkers, 2-hydroxy acetaldehyde (solid in RT) and the commercially unavailable 4-hydroxy hexenal were excluded. Among the 7 repeatedly reported aldehydes, which possess similar δ, hexanal and pentanal were reported in more studies. Concerning the 5 alcohols, 1-propanol was by far the most commonly reported and was selected along with ethanol which possesses higher δ values. Ethyl benzene and o-xylene comprise the most commonly reported aromatic VOCs, while furan was also selected due to structural differences (no benzene ring). Hexane and dodecane were identified in more studies than the rest alkanes, while among cyclohexane and alkylated cyclohexanes the former was reported in more studies. Butanone was the most common ketone, with lower δ than acetone, while cyclohexanone was also selected, due to structural differences.

The small $\Delta\delta$ for PMMA and hexanal, pentanal, 2-butanone, 3-hydroxy-2-butanone, cyclohexanone and furan indicate high polymer affinity. Specifically, 3-hydroxy-2-butanone affinity is expected to be enhanced by hydrogen bonding formation. Despite their higher $\Delta\delta$, alcohols may also be able to form hydrogen bonds with PMMA carbonyl groups. PHEMA, on the other hand, is expected to have higher affinity for the alcohols ethanol and 1-propanol, as well as 3-hydroxy-2-butanone, all of which can form hydrogen bonds with the carbonyl and hydroxyl groups of PHEMA. Hydrogen bonding between ketones/aldehydes (higher $\Delta\delta$) with PHEMA hydroxyl groups may also be formed. As previously observed, for alkanes, isoprene and aromatic benzene derivatives, PS and *cis*-PIP are supposed to exhibit increased affinity, especially PS for benzene derivatives, as explained earlier (COPD diagnosis). In any case, polymer affinity for water is probably low.

The concentration of VOCs selected, except cyclohexanone, were increased for of LC patients, thus greater response for those VOCs in contrast to healthy subjects could potentially lead to LC diagnosis. Cyclohexanone discrimination from ketones, aldehydes and furan, though, seems to be challenging. Poly(cyclohexyl methacrylate) was also tested, (values not shown) leading, though, to similar $\Delta\delta$ and, thus, semi-selectivity, with PMMA.

E. *Breast cancer*

The calculated δ values of the VOCs selected for BC patients and the polymers potentially responsive to their presence are presented on Table 21. The small $\Delta\delta$ between PMMA and heptanal and butyl acetate, in contrast to alkanes, indicates increased polymer affinity. On the other hand, *cis*-PIP is expected to be more sensitive to the three alkanes, thus discrimination of those VOCs is potentially feasible. Polymer affinity for water is expected to be far lower. The concentrations of those VOCs are clearly found increased in BC patients, compared with healthy subjects, except tetradecane and butyl acetate for which no clear tendency is observed. The detection of those VOCs in increased levels in BC patients' exhaled breath could potentially lead to BC diagnosis, however more classes of VOCs may lead to more precise diagnosis and avoid overlapping with other diseases.

Table 21. Solubility parameters of selected VOCs and polymers and solubility parameter difference for each pair.

VOC/polymer	δb (MJ/m³)^(1/2)	δp (MJ/m³)^(1/2)	δh (MJ/m³)^(1/2)	δt (MJ/m³)^(1/2)	Δδ (MJ/m³)^(1/2) PMMA	Δδ (MJ/m³)^(1/2) cis-PIP
Heptanal	16.67	5.95	5.79	18.63	**3.31**	8.31
Butyl acetate	15.37	3.69	7.26	17.39	**3.14**	8.21
Tetradecane	15.69	0.00	0.00	15.69	10.83	**0.74**
2,3-dimethyl pentane	14.64	0.00	0.00	14.64	10.99	**1.80**
3,3-dimethyl pentane	14.87	0.00	0.00	14.87	10.94	**1.56**
Water	12.30	31.30	34.20	47.96	36.10	46.54
PMMA	16.24	3.62	7.19	18.13	-	-
cis-PIP	16.43	0.00	0.00	16.43	-	-

***cis*-PIP**: cis-polyisoprene, *Tg*: -67°C, **PMMA:** poly(methyl methacrylate), *Mw:* 120K, *Tg:* 105°C

Chapter 5: Conclusions and future perspectives

It has been designated that exhaled breath analysis, using both analytical techniques and sensors, comprises a non-invasive method that holds a great promise for application in early-stage diagnosis of, not only respiratory, but also systemic, diseases. The aim of this diploma thesis was, firstly, to present the main categories of nanomaterials and sensors that have been investigated until now for disease diagnosis applications by exhaled breath analysis. Further on, focusing on chemiresistors possessing hybrid polymer coated-MNPs sensing films, the factors potentially affecting VOC-polymer interaction were studied, and were then taken into account for the proposal of polymers that could possibly detect repeatedly identified VOCs as potential biomarkers of asthma, COPD, lung and breast cancer.

The conclusions concerning the factors to be considered for polymer selection are briefly summarized. Targeted VOCs solubility in the selected polymeric films, as expressed by solubility parameter difference, $\Delta\delta$, is expected to comprise the major (thermodynamic) factor affecting sensor (semi-)selectivity, as it can, also, be observed by the effective application of this factor for polymer selection in similar applications[73,81,83,85]. Structural similarity between the analyte and the polymer, that enables their miscibility should also be taken into account. Analyte diffusivity in polymeric films may also be an important (kinetic) parameter, affecting sensor response. The combination of solubility parameter with a structural parameter, related with the steric factors affecting analyte diffusion in polymers, has been attempted (Prigogine theory), without success though[67]. However, VOC size and shape could be taken into account. Extremely bulky and non-linear molecules are considered to inhibit analyte diffusion (§ *4.2.1.4*) and, thus, sorption, in polymers, rendering δ-based predictions invalid. Consequently, the use of solubility parameters should be limited in the case of non-bulky VOCs of relatively small size, for safe results to be obtained. Concerning polymer characteristics, amorphous polymers, with low intrinsic viscosity and, preferably (but not necessarily), T_g lower than operation temperature (rubbery phase) potentially permit better sensor performance.

More generally, the progressive development of novel nanomaterials offers a great opportunity to develop more effective sensing elements, both for selective and cross-

reactive sensors, especially for point-of-care diagnosis, treatment monitoring or population screening. However, fundamental challenges of the field, which is yet in its infancy, inhibit the application in clinical practice and should, thus, be tackled. Concerning analytical techniques used for exhaled VOCs identification, the bulky, expensive and complex machines limit their application in hospitals, rather than patient's home, for point-of-care use[267]. Apart from this, the validity of results is of major concern. The trace levels of exhaled VOCs affect the analysis accuracy[259]. Simultaneously, the lack of clear breath sampling protocols[259] – *e.g.,* for the part of breath collected[267] (*§ 2.1.3*) – as well as breath storage needed, potentially alternating sample composition[267], comprise important challenges. Sample composition is, also, affected by confounding factors, *i.e.,* age, gender, place of living, habits and nutrition. In the case of sensors, exhalation rate, a hardly controlled parameter, may also play a role, complicating the procedure[267].

For those limitations to be surmounted, relative research should focus on sampling and procedure protocols standardization[218,267] and system amelioration towards technical /physiological/pathophysiological confounders[218], to determine the endogenous VOCs and define valid exhaled (patterns of) biomarkers. Towards this direction, standard correlations between blood and breath VOC concentrations could be established[267]. Further on, the development of portable/wearable, low-cost nanomaterial-based sensors, resistant to humidity[267], that serve the clinical needs (*i.e.,* selectivity for disease-specific VOCs and small recovery time for population screening), along with the optimization of sensor training and validation using different groups of subjects meeting the clinical purposes, comprise critical steps for the development of sensors applicable in clinical diagnosis[218]. Notably, the ability of new sensing systems to discriminate different diseases, to achieve precise early diagnosis of diseases with similar symptoms and underlying mechanisms, should be a major concern[34].

For all those targets to be achieved, interdisciplinary research and co-operation of researchers of different fields, is an essential prerequisite[267]. Hopefully, the overcoming of the existing challenges will permit the clinical translation of breath analysis to become a reality.

References

1. Chen, T., Liu, T., Li, T., Zhao, H., Chen, Q. Exhaled breath analysis in disease detection. *Clin. Chim. Acta* **515**, 61–72 (2021).

2. Gashimova, E. *et al.* Investigation of different approaches for exhaled breath and tumor tissue analyses to identify lung cancer biomarkers. *Heliyon* **6**, e04224 (2020).

3. Phillips, M. *et al.* Volatile biomarkers in the breath of women with breast cancer. *J. Breath Res.* **4**, 026003 (2010).

4. Oakley-Girvan, I., Davis, S. W. Breath based volatile organic compounds in the detection of breast, lung, and colorectal cancers: A systematic review. *Cancer Biomarkers* **21**, 29–39 (2017).

5. Pite, H. Metabolomics in asthma : where do we stand ? *Current opinion in Pulmonary Medicine,* **24**, 94–103 (2018).

6. Vishinkin, R., Haick, H. Nanoscale Sensor Technologies for Disease Detection via Volatolomics. *Small* **11**, 6142–6164 (2015).

7. Broza, Y. Y., Vishinkin, R., Barash, O., Nakhleh, M. K., Haick, H. Synergy between nanomaterials and volatile organic compounds for non-invasive medical evaluation. *Chem. Soc. Rev.,* **47**, 4781-4859 (2018).

8. Tisch, U., Haick, H. Chemical sensors for breath gas analysis: The latest developments at the Breath Analysis Summit 2013. *J. Breath Res.* **8**, 027103 (2014).

9. Hakim, M. *et al.* Volatile organic compounds of lung cancer and possible biochemical pathways. *Chem. Rev.* **112**, 5949–5966 (2012).

10. Corradi, M., Poli, D., Bouza, M. Observation of nonanoic acid and aldehydes in exhaled breath of patients with lung cancer Observation of nonanoic acid and aldehydes in exhaled breath of patients with lung cancer. *J. Breath Res.* **11**, 26004 (2017).

11. Song, G. *et al.* Quantitative breath analysis of volatile organic compounds of lung cancer patients. *Lung Cancer* **67**, 227–231 (2010).

12. Ma, H. *et al.* Analysis of human breath samples of lung cancer patients and healthy controls with solid-phase microextraction (SPME) and flow-modulated comprehensive two-dimensional gas chromatography (GC × GC). *Anal. Methods* **6**, 6841–6849 (2014).

13. Wang, C. *et al.* Volatile organic metabolites identify patients with breast cancer, cyclomastopathy, and mammary gland fibroma. *Sci. Rep.* **4**, 1–6 (2014).

14. Meyer, N. *et al.* Defining adult asthma endotypes by clinical features and patterns of volatile organic compounds in exhaled air. *Respir. Res.* **15**, 1–9 (2014).

15. Broza, Y. Y., Haick, H. Nanomaterial-based sensors for detection of disease by volatile organic compounds. *Nanomedicine* **8**, 785–806 (2013).

16. Wilson, A. D. Advances in electronic-nose technologies for the detection of volatile biomarker metabolites in the human breath. *Metabolites* **5**, 140–163 (2015).

17. Pereira, J. *et al.* Breath analysis as a potential and non-invasive frontier in disease diagnosis: An overview. *Metabolites* **5**, 3–55 (2015).

18. Gaida, A. *et al.* A dual center study to compare breath volatile organic compounds from smokers and non-smokers with and without COPD. *J. Breath Res.* **10**, 026006 (2016).

19. Ratiu, I. A., Ligor, T., Bocos-Bintintan, V., Mayhew, C. A., Buszewski, B. Volatile Organic Compounds in Exhaled Breath as Fingerprints of Lung Cancer, Asthma and COPD. *J. Clin. Med.* **10**, 32 (2020).

20. Amal, H., Haick, H. (2019) *Point of care breath analysis systems*. In: *Advanced Nanomaterials for Inexpensive Gas Microsensors: Synthesis, Integration and Applications*, Valeto, E. L., Elsevier Inc., pp 315-328

21. Basanta, M. *et al.* Non-invasive metabolomic analysis of breath using differential mobility spectrometry in patients with chronic obstructive pulmonary disease and healthy smokers. *Analyst* **135**, 315–320 (2010).

22. Rodríguez-Aguilar, M. *et al.* Ultrafast gas chromatography coupled to electronic nose to identify volatile biomarkers in exhaled breath from chronic obstructive pulmonary disease patients: A pilot study. *Biomed. Chromatogr.* **33**, e4684 (2019).

23. Lõpez-Campos, J. L., Tan, W., Soriano, J. B. Global burden of COPD. *Respirology* **21**, 14–23 (2016).

24. Vasilescu, A., Hrinczenko, B., Swain, G. M., Peteu, S. F. Exhaled breath biomarker sensing. *Biosens. Bioelectron.* **182**, 113193 (2021).

25. Chen, X. *et al.* Calculated indices of volatile organic compounds (VOCs) in exhalation for lung cancer screening and early detection. *Lung Cancer* **154**, 197–205 (2021).

26. Bag, A., Lee, N. E. Recent Advancements in Development of Wearable Gas Sensors. *Adv. Mater. Technol.* **6**, 1–37 (2021).

27. Bos, L. D., Sterk, P. J., Fowler, S. J. Breathomics in the setting of asthma and chronic obstructive pulmonary disease. *J. Allergy Clin. Immunol.* **138**, 970–976 (2016).

28. Fens, N., van der Schee, M. P., Brinkman, P., Sterk, P. J. Exhaled breath analysis by electronic nose in airways disease. Established issues and key questions. *Clin. Exp. Allergy* **43**, 705–715 (2013).

29. Peng, G. *et al.* Detection of lung, breast, colorectal, and prostate cancers from exhaled breath using a single array of nanosensors. *Br. J. Cancer* **103**, 542–551 (2010).

30. Sánchez, C., Santos, J. P., Lozano, J. Use of electronic noses for diagnosis of digestive and respiratory diseases through the breath. *Biosensors* **9**, 1–20 (2019).

31. Wang, M. *et al.* Confounding effect of benign pulmonary diseases in selecting volatile organic compounds as markers of lung cancer. *J. Breath Res.* **12**, 046013 (2018).

32. Buljubasic, F., Buchbauer, G. The scent of human diseases: A review on specific volatile organic compounds as diagnostic biomarkers. *Flavour Fragr. J.* **30**, 5–25 (2015).

33. Ulanowska, A., Kowalkowski, T., Trawińska, E., Buszewski, B. The application of statistical methods using VOCs to identify patients with lung cancer. *J. Breath Res.* **5**, 046008 (2011).

34. Koureas, M. *et al.* Target analysis of volatile organic compounds in exhaled breath for lung cancer discrimination from other pulmonary diseases and healthy persons. *Metabolites* **10**, 1–18 (2020).

35. Fuchs, P., Loeseken, C., Schubert, J. K., Miekisch, W. Breath gas aldehydes as biomarkers of lung cancer. *Int. J. Cancer* **126**, 2663–2670 (2010).

36. Boots, A. W. *et al.* The versatile use of exhaled volatile organic compounds in human health and disease. *J. Breath Res.* **6**, 027108 (2012).

37. Hashoul, D., Haick, H. Sensors for detecting pulmonary diseases from exhaled breath. *Eur. Respir. Rev.* **28**, 190011 (2019).

38. Haick, H., Cohen-Kaminsky, S. Detecting lung infections in breathprints: Empty promise or next generation diagnosis of infections. *Eur. Respir. J.* **45**, 21–24 (2015).

39. Shan, B. *et al.* Multiplexed Nanomaterial-Based Sensor Array for Detection of COVID-19 in Exhaled Breath. *ACS Nano* **14**, 12125–12132 (2020).

40. Giovannini, G., Haick, H., Garoli, D. Detecting COVID-19 from Breath: A Game Changer for a Big Challenge. *ACS Sensors* **6**, 1408–1417 (2021).

41. Grassin-Delyle, S. *et al.* Metabolomics of exhaled breath in critically ill COVID-19 patients: A pilot study. *EBioMedicine* **63**, 103154 (2021).

42. Breathonix - BreFence^TM Go COVID-19 Breath Test System Rapid Breath Test for COVID-19 Detection [Online]. [cited on 30 May 2021]. Available from Internet: Breathonix-BreFence-Go-Breath-Test-System.pdf (secureservercdn.net)

43. Health Sciences Authority - Singapore - HSA Expedites Approval of COVID-19 Diagnostic Tests in Singapore via Provisional Authorisation [Online]. [cited on 30 May 2021]. Available from Internet: HSA Expedites Approval of COVID-19 Diagnostic Tests in Singapore via Provisional Authorisation

44. Provisional Authorisation for COVID-19 Tests - Breathonix Pte Ltd [Online]. [cited on 30 May 2021]. Available from Internet: breathonix_brefence-go-covid-19-breath-test-system_provisional-authorisation-for-covid-19-tests_19052021.pdf (hsa.gov.sg)

45. Neerincx, A. H. *et al.* Breathomics from exhaled volatile organic compounds in pediatric asthma. *Pediatr. Pulmonol.* **52**, 1616–1627 (2017).

46. Monedeiro, F. *et al.* Needle trap device-gc-ms for characterization of lung diseases based on breath voc profiles. *Molecules* **26**, 1–19 (2021).

47. Zhou, X. *et al.* Nanomaterial-based gas sensors used for breath diagnosis. *J. Mater.*

Chem. B **8**, 3231–3248 (2020).

48. Fraden, J. (2010) Chemical sensors. In: Handbook of Modern Sensors: Physics, Designs, and Applications 4th *ed.* Springer, New York, pp 569-606.

49. Skotadis, E., Mousadakos, D., Katsabrokou, K., Stathopoulos, S., Tsoukalas, D. Flexible polyimide chemical sensors using platinum nanoparticles. *Sensors Actuators, B Chem.* **189**, 106–112 (2013).

50. Coyle, S., Curto, V. F., Benito-Lopez, F., Florea, L., Diamond, D. (2014) Wearable Bio and Chemical Sensors. In: Sazonov, E., Neuman, M. R., Wearable Sensors: Fundamentals, Implementation and Applications. Elsevier Inc., United States, pp 65–83.

51. Skotadis, E., Tang, J., Tsouti, V., Tsoukalas, D. Chemiresistive sensor fabricated by the sequential ink-jet printing deposition of a gold nanoparticle and polymer layer. *Microelectron. Eng.* **87**, 2258–2263 (2010).

52. Skotadis, E., Tanner, J. L., Stathopoulos, S., Tsouti, V., Tsoukalas, D. Chemical sensing based on double layer PHEMA polymer and platinum nanoparticle films. *Sensors Actuators, B Chem.* **175**, 85–91 (2012).

53. Kus, F. *et al.* Surface acoustic wave (SAW) sensor for volatile organic compounds (VOCs) detection with calix[4]arene functionalized Gold nanorods (AuNRs) and silver nanocubes (AgNCs). *Sensors Actuators, B Chem.* **330**, 129402 (2021).

54. Tisch, U., Haick, H. Nanomaterials for cross-reactive sensor arrays. *MRS Bull.* **35**, 797–803 (2010).

55. Van Der Schee, M. P. *et al.* Effect of transportation and storage using sorbent tubes of exhaled breath samples on diagnostic accuracy of electronic nose analysis. *J. Breath Res.* **7**, 016002 (2013).

56. Behera, B., Joshi, R., Anil Vishnu, G. K., Bhalerao, S., Pandya, H. J. Electronic nose: A non-invasive technology for breath analysis of diabetes and lung cancer patients. *J. Breath Res.* **13**, 24001 (2019).

57. Madianos, L. *et al.* Nanoparticle based gas-sensing array for pesticide detection. *J. Environ. Chem. Eng.* **6**, 6641–6646 (2018).

58. Konvalina, G., Haick, H. Effect of humidity on nanoparticle-based chemiresistors: A comparison between synthetic and real-world samples. *ACS Appl. Mater. Interfaces* **4**, 317–325 (2012).

59. Madianos, L. *et al.* Nanoparticle based gas-sensing array for pesticide detection. *J. Environ. Chem. Eng.* **6**, 6641–6646 (2018), Supplementary Data

60. Shehada, N. *et al.* Silicon Nanowire Sensors Enable Diagnosis of Patients via Exhaled Breath. *ACS Nano* **10**, 7047–7057 (2016).

61. Kahn, N., Lavie, O., Paz, M., Segev, Y., Haick, H. Dynamic Nanoparticle-Based Flexible Sensors: Diagnosis of Ovarian Carcinoma from Exhaled Breath. *Nano Lett.* **15**, 7023–7028 (2015).

62. Phillips, C. O. *et al.* Machine learning methods on exhaled volatile organic compounds for distinguishing COPD patients from healthy controls. *J. Breath Res.* **6**, 036003 (2012).

63. Hattori, Y., Kaneko, K., Ohba, T. (2013) Adsorption Properties. In: Reedijk, J., Poeppelmeier, K. Comprehensive Inorganic Chemistry II, 2nd *ed.,* From Elements to Applications, Elsevier Ltd., **5,** pp 25-44

64. Keller, J., Staudt, R. (2005) Gas adsorption equilibria - Experimental methods and adsorption isotherms, Siegen, Germany, Springer Science & Business Media, Inc., pp 2

65. Dong, X. M. *et al.* Conducting property of carbon black filled polyethylene glycol/poly(methyl methacrylate) composites as gas-sensing materials. *J. Appl. Polym. Sci.* **107**, 2322-2328 (2008).

66. Van Krevelen, D. W., Te Nijenhuis, K. (2009) Properties of Polymers 4th *ed.* The Netherlands, Elsevier B.V.

67. Hansen, C.M. (2007) Hansen Solubility Parameters - A user's Handbook 2nd *ed.* Boca Raton, Taylor & Francis Group, LLC

68. Baker, R. W., Low, B. T. Gas separation membrane materials: A perspective. *Macromolecules* **47**, 6999–7013 (2014).

69. Dong, X. M., Luo, Y., Xie, L. N., Fu, R. W., Zhang, M. Q. Conductive carbon black-filled polymethacrylate composites as gas sensing materials: Effect of glass transition temperature. *Thin Solid Films* **516**, 7886–7890 (2008).

70. Thgeodorou, D.N. (1996) Molecular simulations of sorption and diffusion in amorphous polymers. In: Neogi, P. Diffusion in polymers, Rolla, Missouri, Marcel Dekker, Inc. pp 69

71. Panayiotou, C. Redefining solubility parameters: The partial solvation parameters. *Phys. Chem. Chem. Phys.* **14**, 3882–3908 (2012).

72. Park, J., Groves, W. A., Zellers, E. T. Vapor recognition with small arrays of polymer-coated microsensors. A comprehensive analysis. *Anal. Chem.* **71**, 3877–3886 (1999).

73. Arshak, K., Moore, E., Cavanagh, L., Cunniffe, C., Clifford, S. Examining the use of oxide particles to enhance the sensitivity of polymer\carbon black nanocomposite gas sensors. *Prog. Solid State Chem.* **33**, 199–205 (2005).

74. Mollet, H., Grubenrnann (2001) Formulation Technology, Weinheim, Germanh, Wiley-VCH

75. Panayiotou, C., Mastrogeorgopoulos, S., Aslanidou, D., Avgidou, M., Hatzimanikatis, V. Redefining solubility parameters: Bulk and surface properties from unified molecular descriptors. *J. Chem. Thermodyn.* **111**, 207–220 (2017).

76. Mengshan, L., Wei, W., Bingsheng, C., Yan, W., Xingyuan, H. Solubility prediction of gases in polymers based on an artificial neural network: A review. *RSC Adv.* **7**, 35274–35282 (2017).

77. Jomekian, A., Bazooyar, B., Poormohammadian, S. J., Darvishi, P. A modified non-equilibrium lattice fluid model based on corrected fractional free volume of polymers for gas solubility prediction. *Korean J. Chem. Eng.* **36**, 2047–2059 (2019).

78. Barnett, J. W. *et al.* Designing exceptional gas-separation polymer membranes using machine learning. *Sci. Adv.* **6**, 1–8 (2020).

79. Zhu, R., Lei, Z. COSMO-based models for predicting the gas solubility in polymers. *Green Energy Environ.* **6**, 311–313 (2021).

80. Tchoupo, G. N., Guiseppi-Elie, A. On pattern recognition dependency of desorption heat, activation energy, and temperature of polymer-based VOC sensors for the electronic NOSE. *Sensors Actuators, B Chem.* **110**, 81–88 (2005).

81. Zhang, B. *et al.* Studies of the vapor-induced sensitivity of hybrid composites fabricated by filling polystyrene with carbon black and carbon nanofibers. *Compos. Part A Appl. Sci. Manuf.* **37**, 1884–1889 (2006).

82. Kitak, T. *et al.* Determination of solubility parameters of ibuprofen and ibuprofen lysinate. *Molecules* **20**, 21549–21568 (2015).

83. Martínez-Hurtado, J. L., Davidson, C. A. B., Blyth, J., Lowe, C. R. Holographic detection of hydrocarbon gases and other volatile organic compounds. *Langmuir* **26**, 15694–15699 (2010).

84. Gao, J., Wu, S., Rogers, M. A. Harnessing Hansen solubility parameters to predict organogel formation. *J. Mater. Chem.* **22**, 12651–12658 (2012).

85. Narses, S., Sadaka, F., Brachais, C. H., Couvercelle, J. P. Polymer stain resistance: Prediction versus experiment. *J. Appl. Polym. Sci.* **129**, 2891–2904 (2013).

86. Zhang, T., Mubeen, S., Myung, N. V., Deshusses, M. A. Recent progress in carbon nanotube-based gas sensors. *Nanotechnology* **19**, 332001 (2008).

87. Haick, H. Chemical sensors based on molecularly modified metallic nanoparticles. *J. Phys. D. Appl. Phys.* **40**, 7173–7186 (2007).

88. Mubeen, S. *et al.* Gas sensing mechanism of gold nanoparticles decorated single-walled carbon nanotubes. *Electroanalysis* **23**, 2687–2692 (2011).

89. Viespe, C., Miu, D. Characteristics of Surface Acoustic Wave Sensors with Nanoparticles Embedded in Polymer Sensitive Layers for VOC Detection. *Sensors*, **18**, 2401 (2018).

90. Yoon, J. W., Lee, J. H. Toward breath analysis on a chip for disease diagnosis using semiconductor-based chemiresistors: Recent progress and future perspectives. *Lab Chip* **17**, 3537–3557 (2017).

91. Moon, H. G. *et al.* Extremely sensitive and selective NO probe based on villi-like WO_3 nanostructures for application to exhaled breath analyzers. *ACS Appl. Mater. Interfaces* **5**, 10591–10596 (2013).

92. Koo, W. T., Choi, S. J., Kim, N. H., Jang, J. S., Kim, I. D. Catalyst-decorated hollow WO3 nanotubes using layer-by-layer self-assembly on polymeric nanofiber templates and

their application in exhaled breath sensor. *Sensors Actuators, B Chem.* **223**, 301–310 (2016).

93. Choi, S. J. *et al.* Fast responding exhaled-breath sensors using WO_3 hemitubes functionalized by graphene-based electronic sensitizers for diagnosis of diseases. *ACS Appl. Mater. Interfaces* **6**, 9061–9070 (2014).

94. Shin, J. *et al.* Thin-wall assembled SnO_2 fibers functionalized by catalytic Pt nanoparticles and their superior exhaled-breath-sensing properties for the diagnosis of diabetes. *Adv. Funct. Mater.* **23**, 2357–2367 (2013).

95. Masuda, Y., Itoh, T., Shin, W., Kato, K. SnO_2 nanosheet/nanoparticle detector for the sensing of 1-nonanal gas produced by lung cancer. *Sci. Rep.* **5**, 1–7 (2015).

96. Giebelhaus, I. *et al.* One-dimensional $CuO-SnO_2$ p-n heterojunctions for enhanced detection of H_2S. *J. Mater. Chem. A* **1**, 11261–11268 (2013).

97. Güntner, A. T., Koren, V., Chikkadi, K., Righettoni, M., Pratsinis, S. E. E-Nose Sensing of Low-ppb Formaldehyde in Gas Mixtures at High Relative Humidity for Breath Screening of Lung Cancer, *ACS Sensors* **1**, 528–535 (2016).

98. Choi, S. J. *et al.* Selective diagnosis of diabetes using Pt-functionalized WO_3 hemitube networks as a sensing layer of acetone in exhaled breath. *Anal. Chem.* **85**, 1792–1796 (2013).

99. Moon, H. G. *et al.* Chemiresistive Electronic Nose toward Detection of Biomarkers in Exhaled Breath. *ACS Appl. Mater. Interfaces* **8**, 20969–20976 (2016).

100. Wei, C., Dai, L., Roy, A., Tolle, T. B. Multifunctional chemical vapor sensors of aligned carbon nanotube and polymer composites. *J. Am. Chem. Soc.* **128**, 1412–1413 (2006).

101. Ionescu, R. *et al.* Detection of multiple sclerosis from exhaled breath using bilayers of polycyclic aromatic hydrocarbons and single-wall carbon nanotubes. *ACS Chem. Neurosci.* **2**, 687–693 (2011).

102. Castro, M. *et al.* Chemical Novel e-nose for the discrimination of volatile organic biomarkers with an array of carbon nanotubes (CNT) conductive polymer nanocomposites (CPC) sensors. *Sensors Actuators B. Chem.* **159**, 213–219 (2011).

103. Bachhav, S. G., Patil, D. R. Study of Polypyrrole-Coated MWCNT Nanocomposites for Ammonia Sensing at Room Temperature. *J. Mater. Sci. Chem. Eng.* **3**, 30–44 (2015).

104. Abdulla, S., Mathew, T. L., Pullithadathil, B. Highly sensitive, room temperature gas sensor based on polyaniline-multiwalled carbon nanotubes (PANI/MWCNTs) nanocomposite for trace-level ammonia detection. *Sensors Actuators, B Chem.* **221**, 1523–1534 (2015).

105. Akbari-Saatlu, M. *et al.* Silicon nanowires for gas sensing: A review. *Nanomaterials* **10**, 1–57 (2020).

106. Wang, B., Haick, H. Effect of chain length on the sensing of volatile organic compounds by means of silicon nanowires. *ACS Appl. Mater. Interfaces* **5**, 5748–5756

(2013).

107. Ermanok, R., Assad, O., Zigelboim, K., Wang, B., Haick, H. Discriminative power of chemically sensitive silicon nanowire field effect transistors to volatile organic compounds. *ACS Appl. Mater. Interfaces* **5**, 11172–11183 (2013).

108. Wang, B., Cancilla, J. C., Torrecilla, J. S., Haick, H. Artificial sensing intelligence with silicon nanowires for ultraselective detection in the gas phase. *Nano Lett.* **14**, 933–938 (2014).

109. Choi, S. J., Kim, I. D. Recent Developments in 2D Nanomaterials for Chemiresistive-Type Gas Sensors. *Electronic Materials Letters*, **14**, 221-260 (2018).

110. Jeong, S., Kim, J., Lee, J. Rational Design of Semiconductor-Based Chemiresistors and their Libraries for Next-Generation Artificial Olfaction. *Adv. Mater.* **2002075**, 1–47 (2020).

111. Chen, W. Y., Yen, C. C., Xue, S., Wang, H., Stanciu, L. A. Surface Functionalization of Layered Molybdenum Disulfide for the Selective Detection of Volatile Organic Compounds at Room Temperature. *ACS Appl. Mater. Interfaces* **11**, 34135–34143 (2019).

112. Chu, X. *et al.* Preparation and gas sensing properties of graphene-Zn_2SnO_4 composite materials. *Sensors Actuators, B Chem.* **251**, 120–126 (2017).

113. Salehi-Khojin, A. *et al.* Polycrystalline graphene ribbons as chemiresistors. *Adv. Mater.* **24**, 53–57 (2012).

114. Robinson, J. T., Perkins, F. K., Snow, E. S., Wei, Z., Sheehan, P. E. Reduced graphene oxide molecular sensors. *Nano Lett.* **8**, 3137–3140 (2008).

115. Tang, J. *et al.* PHEMA functionalization of gold nanoparticles for vapor sensing: Chemi-resistance, chemi-capacitance and chemi-impedance. *Sensors Actuators, B Chem.* **170**, 129–136 (2012).

116. Di Natale, C., Paolesse, R., Martinelli, E., Capuano, R. Solid-state gas sensors for breath analysis: A review. *Anal. Chim. Acta* **824**, 1–17 (2014).

117. Liu, C., Wyszynski, B., Yatabe, R., Hayashi, K., Toko, K. Molecularly imprinted sol-gel-based QCM sensor arrays for the detection and recognition of volatile aldehydes. *Sensors (Switzerland)* **17**, 1–15 (2017).

118. Chen, W., Wang, Z., Gu, S., Wang, J. Chemical Detection of hexanal in humid circumstances using hydrophobic molecularly imprinted polymers composite. *Sensors Actuators B. Chem.* **291**, 141–147 (2019).

119. Silva, L. I. B., Freitas, A. C., Rocha-Santos, T. A. P., Pereira, M. E., Duarte, A. C. Breath analysis by optical fiber sensor for the determination of exhaled organic compounds with a view to diagnostics. *Talanta* **83**, 1586–1594 (2011).

120. Okuda, H., Wang, T., Lee, S. W. Selective Methanol Gas Detection Using a U-Bent Optical Fiber Modified with a Silica Nanoparticle Multilayer. *Electron. Commun. Japan* **100**, 43–49 (2017).

121. Manjula, M., Karthikeyan, B., Sastikumar, D. Sensing characteristics of nanocrystalline bismuth oxide clad-modified fiber optic gas sensor. *Opt. Lasers Eng.* **95**, 78–82 (2017).

122. Yu, C. *et al.* Miniature fiber-optic NH_3 gas sensor based on Pt nanoparticle-incorporated graphene oxide. *Sensors Actuators, B Chem.* **244**, 107–113 (2017).

123. Kavinkumar, T., Manivannan, S. Uniform decoration of silver nanoparticle on exfoliated graphene oxide sheets and its ammonia gas detection. *Ceram. Int.* **42**, 1769–1776 (2016).

124. Zhao, S. *et al.* A colorimetric detector for lung cancer related volatile organic compounds based on cross-response mechanism. *Sensors Actuators B. Chem.* **256**, 543–552 (2018).

125. Mazzone, P. J., Wang, X., Xu, Y. Exhaled Breath Analysis with a Colorimetric Sensor Array for the Identification and Characterization of Lung Cancer. *J. Thorac. Oncol.* **7**, 137–142 (2012).

126. Mazzone, P. J. *et al.* Diagnosis of lung cancer by the analysis of exhaled breath with a colorimetric sensor array. *Thorax* **62**, 565–568 (2007).

127. Zhong, X. *et al.* Rapid recognition of volatile organic compounds with colorimetric sensor arrays for lung cancer screening. *Anal. Bioanal. Chem.* **410**, 3671–3681 (2018).

128. Queralto, N. *et al.* Detecting cancer by breath volatile organic compound analysis: A review of array-based sensors. *J. Breath Res.* **8**, 027112 (2014).

129. Huo, D., Xu, Y., Hou, C., Yang, M., Fa, H. A novel optical chemical sensor based AuNR-MTPP and dyes for lung cancer biomarkers in exhaled breath identification. *Sensors Actuators, B Chem.* **199**, 446–456 (2014).

130. Cha, J. H., Kim, D. H., Choi, S. J., Koo, W. T., Kim, I. D. Sub-Parts-per-Million Hydrogen Sulfide Colorimetric Sensor: Lead Acetate Anchored Nanofibers toward Halitosis Diagnosis. *Anal. Chem.* **90**, 8769–8775 (2018).

131. Cheng, C. S., Chen, Y. Q., Lu, C. J. Organic vapour sensing using localized surface plasmon resonance spectrum of metallic nanoparticles self assemble monolayer. *Talanta* **73**, 358–365 (2007).

132. Chen, B., Liu, C., Ge, L., Hayashi, K. Localized surface plasmon resonance gas sensor of Au nano-islands coated with molecularly imprinted polymer: Influence of polymer thickness on sensitivity and selectivity. *Sensors Actuators, B Chem.* **231**, 787–792 (2016).

133. Cui, J., Hu, K., Sun, J. J., Qu, L. L., Li, D. W. SERS nanoprobes for the monitoring of endogenous nitric oxide in living cells. *Biosens. Bioelectron.* **85**, 324–330 (2016).

134. Qiao, X. *et al.* Selective Surface Enhanced Raman Scattering for Quantitative Detection of Lung Cancer Biomarkers in Superparticle@MOF Structure. *Adv. Mater.* **30**, 1–8 (2018).

135. Zhang, Z. *et al.* Ultrasensitive Surface-Enhanced Raman Scattering Sensor of Gaseous Aldehydes as Biomarkers of Lung Cancer on Dendritic Ag Nanocrystals. *Anal. Chem.* **89**, 1416–1420 (2017).

136. Montuschi, P., Santonico, M., Mondino, C. Diagnostic Performance of an Electronic Nose, Fractional Exhaled Nitric Oxide and Lung Function Testing in Asthma. *Chest* **137**, 790–796 (2010).

137. Santonico, M. *et al.* In situ detection of lung cancer volatile fingerprints using bronchoscopic air-sampling. *Lung Cancer* **77**, 46–50 (2012).

138. Wang, X., Zhang, J., Zhu, Z. Ammonia sensing characteristics of ZnO nanowires studied by quartz crystal microbalance. *Appl. Surf. Sci.* **252**, 2404–2411 (2006).

139. Van Quy, N., Minh, V. A., Van Luan, N., Hung, V. N., Van Hieu, N. Gas sensing properties at room temperature of a quartz crystal microbalance coated with ZnO nanorods. *Sensors Actuators, B Chem.* **153**, 188–193 (2011).

140. Ding, B., Kim, J., Miyazaki, Y., Shiratori, S. Electrospun nanofibrous membranes coated quartz crystal microbalance as gas sensor for NH_3 detection. *Sensors Actuators, B Chem.* **101**, 373–380 (2004).

141. Wang, X., Ding, B., Sun, M., Yu, J., Sun, G. Nanofibrous polyethyleneimine membranes as sensitive coatings for quartz crystal microbalance-based formaldehyde sensors. *Sensors Actuators, B Chem.* **144**, 11–17 (2010).

142. Tao, W. *et al.* Multichannel quartz crystal microbalance array: Fabrication, evaluation, application in biomarker detection. *Anal. Biochem.* **494**, 85–92 (2016).

143. Si, P., Mortensen, J., Komolov, A., Denborg, J., Møller, P. J. Polymer coated quartz crystal microbalance sensors for detection of volatile organic compounds in gas mixtures. *Anal. Chim. Acta* **597**, 223–230 (2007).

144. Koshets, I. A., Kazantseva, Z. I., Shirshov, Y. M., Cherenok, S. A., Kalchenko, V. I. Calixarene films as sensitive coatings for QCM-based gas sensors. *Sensors Actuators, B Chem.* **106**, 177–181 (2005).

145. Phillips, M. *et al.* Rapid point-of-care breath test for biomarkers of breast cancer and abnormal mammograms. *PLoS One* **9**, e90226 (2014).

146. Phillips, M. *et al.* Point-of-care breath test for biomarkers of active pulmonary tuberculosis. *Tuberculosis* **92**, 314–320 (2012).

147. Chen, X. *et al.* A study of an electronic nose for detection of lung cancer based on a virtual SAW gas sensors array and imaging recognition method. *Meas. Sci. Technol.* **16**, 1535–1546 (2005).

148. Lukman Hekiem, N. L. *et al.* Advanced vapour sensing materials: Existing and latent to acoustic wave sensors for VOCs detection as the potential exhaled breath biomarkers for lung cancer. *Sensors Actuators, A Phys.* **329**, 112792 (2021).

149. Tang, Y. L. *et al.* Ammonia gas sensors based on ZnO/SiO_2 bi-layer nanofilms on ST-cut quartz surface acoustic wave devices. *Sensors Actuators, B Chem.* **201**, 114–121

(2014).

150. Tang, Y. *et al.* NH$_3$ sensing property and mechanisms of quartz surface acoustic wave sensors deposited with SiO$_2$, TiO$_2$, and SiO$_2$-TiO$_2$ composite films. *Sensors Actuators, B Chem.* **254**, 1165–1173 (2018).

151. Ippolito, S. J. *et al.* Layered WO$_3$/ZnO/36° LiTaO$_3$ SAW gas sensor sensitive towards ethanol vapour and humidity. *Sensors Actuators, B Chem.* **117**, 442–450 (2006).

152. Matatagui, D. *et al.* Acoustic sensors based on amino-functionalized nanoparticles to detect volatile organic solvents. *Sensors (Switzerland)* **17**, 1–9 (2017).

153. Stahl, U. *et al.* Long-term stability of polymer-coated surface transverse wave sensors for the detection of organic solvent vapors. *Sensors (Switzerland)* **17**, 2529 (2017).

154. Singh, P., Yadava, R. Feature Extraction by Wavelet Decomposition of Surface Acoustic Wave Sensor Array Transients. *Def. Sci. J.* **60**, 377–386 (2010).

155. Penza, M., Antolini, F., Vittori-Antisari, M. Carbon nanotubes-based surface acoustic waves oscillating sensor for vapour detection. *Thin Solid Films* **472**, 246–252 (2005).

156. Sayago, I. *et al.* New sensitive layers for surface acoustic wave gas sensors based on polymer and carbon nanotube composites. *Sensors Actuators, B Chem.* **175**, 67–72 (2012).

157. David, M. *et al.* Carbon nanotubes/ceria composite layers deposited on surface acoustic wave devices for gas detection at room temperature. *Thin Solid Films* **520**, 4786–4791 (2012).

158. Bahos, F. A. *et al.* ZIF nanocrystal-based surface acousticwave (SAW) electronic nose to detect diabetes in human breath. *Biosensors* **9**, 1–13 (2019).

159. Maier, D. *et al.* Toward Continuous Monitoring of Breath Biochemistry: A Paper-Based Wearable Sensor for Real-Time Hydrogen Peroxide Measurement in Simulated Breath. *ACS Sensors* **4**, 2945–2951 (2019).

160. Chuang, M. Y., Chen, C. C., Zan, H. W., Meng, H. F., Lu, C. J. Organic Gas Sensor with an Improved Lifetime for Detecting Breath Ammonia in Hemodialysis Patients. *ACS Sensors* **2**, 1788–1795 (2017).

161. Zhang, J. *et al.* Green Solid Electrolyte with Cofunctionalized Nanocellulose/Graphene Oxide Interpenetrating Network for Electrochemical Gas Sensors. *Small Methods* **1**, 1700237 (2017).

162. Obermeier, J. *et al.* Electrochemical sensor system for breath analysis of aldehydes, CO and NO. *J. Breath Res.* **9**, 016008 (2015).

163. Zhang, Y. *et al.* Identification of volatile biomarkers of gastric cancer cells and ultrasensitive electrochemical detection based on sensing interface of Au-Ag alloy coated MWCNTs. *Theranostics* **4**, 154–162 (2014).

164. Gautam, V., Kumar, A., Kumar, R., Jain, V. K., Nagpal, S. Silicon nanowires/reduced graphene oxide nanocomposite based novel sensor platform for detection of

cyclohexane and formaldehyde. *Mater. Sci. Semicond. Process.* **123**, 105571 (2021).

165. Feng, P., Shao, F., Shi, Y., Wan, Q. Gas sensors based on semiconducting nanowire field-effect transistors. *Sensors (Basel)* **14**, 17406–17429 (2014).

166. Paska, Y. *et al.* Molecular gating of silicon nanowire field-effect transistors with nonpolar analytes. *ACS Nano* **6**, 335–345 (2012).

167. Chen, G., Paronyan, T. M., Pigos, E. M., Harutyunyan, A. R. Enhanced gas sensing in pristine carbon nanotubes under continuous ultraviolet light illumination. *Sci. Rep.* **2**, 1–7 (2012).

168. Zhou, C. *et al.* Printed thin-film transistors and NO2 gas sensors based on sorted semiconducting carbon nanotubes by isoindigo-based copolymer. *Carbon N. Y.* **108**, 372–380 (2016).

169. Chang, Y. W., Oh, J. S., Yoo, S. H., Choi, H. H., Yoo, K. H. Electrically refreshable carbon-nanotube-based gas sensors. *Nanotechnology* **18**, 435504 (2007).

170. Huo, N. *et al.* Photoresponsive and Gas Sensing Field-Effect Transistors based on Multilayer WS$_2$ Nanoflakes. *Sci. Rep.* **4**, 1–9 (2014).

171. Li, H. *et al.* Fabrication of single- and multilayer MoS$_2$ film-based field-effect transistors for sensing NO at room temperature. *Small* **8**, 63–67 (2012).

172. Late, D. J. *et al.* Sensing behavior of atomically thin-layered MoS2 transistors. *ACS Nano* **7**, 4879–4891 (2013).

173. Chen, B. *et al.* Fabrication of a graphene field effect transistor array on microchannels for ethanol sensing. *Appl. Surf. Sci.* **258**, 1971–1975 (2012).

174. Cui, S. *et al.* Ultrasensitive chemical sensing through facile tuning defects and functional groups in reduced graphene oxide. *Anal. Chem.* **86**, 7516–7522 (2014).

175. Mortazavi Zanjani, S. M. *et al.* Enhanced sensitivity of graphene ammonia gas sensors using molecular doping. *Appl. Phys. Lett.* **108**, 1–6 (2016).

176. Niskanen, A. O. *et al.* Silicon nanowire arrays as learning chemical vapour classifiers. *Nanotechnology* **22**, 295502 (2011).

177. Dattoli, E. N., Davydov, A. V., Benkstein, K. D. Tin oxide nanowire sensor with integrated temperature and gate control for multi-gas recognition. *Nanoscale* **4**, 1760–1769 (2012).

178. Li, D., Hu, J., Wu, R., Lu, J. G. Conductometric chemical sensor based on individual CuO nanowires. *Nanotechnology* **21**, 485502 (2010).

179. Mahapatra, N. *et al.* Electrostatic Selectivity of Volatile Organic Compounds Using Electrostatically Formed Nanowire Sensor. *ACS Sensors* **3**, 709–715 (2018).

180. Chen, P. C., Ishikawa, F. N., Chang, H. K., Ryu, K., Zhou, C. A nanoelectronic nose: A hybrid nanowire/carbon nanotube sensor array with integrated micromachined hotplates for sensitive gas discrimination. *Nanotechnology* **20**, 125503 (2009).

181. Cho, B. *et al.* Chemical Sensing of 2D Graphene/MoS2 Heterostructure device. *ACS Appl. Mater. Interfaces* **7**, 16775–16780 (2015).

182. Van Hieu, N., Dung, N. Q., Tam, P. D., Trung, T., Chien, N. D. Thin film polypyrrole/SWCNTs nanocomposites-based NH₃ sensor operated at room temperature. *Sensors Actuators, B Chem.* **140**, 500–507 (2009).

183. Peng, G., Tisch, U., Haick, H. Detection of nonpolar molecules by means of carrier scattering in random networks of carbon nanotubes: Toward diagnosis of diseases via breath samples. *Nano Lett.* **9**, 1362–1368 (2009).

184. Shehada, N. *et al.* Ultrasensitive silicon nanowire for real-world gas sensing: Noninvasive diagnosis of cancer from breath volatolome. *Nano Lett.* **15**, 1288–1295 (2015).

185. Xu, Y. *et al.* Detection and identification of breast cancer volatile organic compounds biomarkers using highly-sensitive single nanowire array on a chip. *J. Biomed. Nanotechnol.* **9**, 1164–1172 (2013).

186. Amor, R. E., Nakhleh, M. K., Barash, O., Haick, H. Breath analysis of cancer in the present and the future. *Eur. Respir. Rev.* **28**, 1–10 (2019).

187. Chang, J. *et al.* Chemical Analysis of volatile organic compounds in exhaled breath for lung cancer diagnosis using a sensor system. *Sensors Actuators B. Chem.* **255**, 800–807 (2018).

188. Hwang, S. *et al.* Chemical vapor sensing properties of graphene based on geometrical evaluation. *Curr. Appl. Phys.* **12**, 1017–1022 (2012).

189. Kumar, D. *et al.* Effect of single wall carbon nanotube networks on gas sensor response and detection limit. *Sensors Actuators, B Chem.* **240**, 1134–1140 (2017).

190. Young, S. J., Lin, Z. D. Ethanol gas sensors based on multi-wall carbon nanotubes on oxidized Si substrate. *Microsyst. Technol.* **24**, 55–58 (2018).

191. Gao, Z. *et al.* Fiber gas sensor-integrated smart face mask for room-temperature distinguishing of target gases. *Nano Res.* **11**, 511–519 (2018).

192. Choi, S. J., Ku, K. H., Kim, B. J., Kim, I. D. Novel Templating Route Using Pt Infiltrated Block Copolymer Microparticles for Catalytic Pt Functionalized Macroporous WO3 Nanofibers and Its Application in Breath Pattern Recognition. *ACS Sensors* **1**, 1124–1131 (2016).

193. Hong, D., Hoon, T., Sohn, W., Min, J., Shim, Y. Chemical Au decoration of vertical hematite nanotube arrays for further selective detection of acetone in exhaled breath. *Sensors Actuators B. Chem.* **274**, 587–594 (2018).

194. Kim, G. S., Park, Y., Shin, J., Song, Y. G., Kang, C. Y. Metal oxide nanorods-based sensor array for selective detection of biomarker gases. *Sensors* **21**, 1–9 (2021).

195. Choi, S. J. *et al.* Selective detection of acetone and hydrogen sulfide for the diagnosis of diabetes and halitosis using SnO2 nanofibers functionalized with reduced graphene oxide nanosheets. *ACS Appl. Mater. Interfaces* **6**, 2588–2597 (2014).

196. Carlos, S., Santos, P., Sayago, I. Graphene-Doped Tin Oxide Nanofibers and Nanoribbons as Gas Sensors to Detect Biomarkers of Di ff erent Diseases through the Breath. *Sensors*, **20**, 7223 (2020).

197. Zhang, L., Li, C., Liu, A., Shi, G. Electrosynthesis of graphene oxide/polypyrene composite films and their applications for sensing organic vapors. *J. Mater. Chem.* **22**, 8438–8443 (2012).

198. Sarkar, T., Srinives, S., Rodriquez, A., Mulchandani, A. Single-walled Carbon Nanotube-Calixarene Based Chemiresistor for Volatile Organic Compounds. *Electroanalysis* **30**, 2077–2084 (2018).

199. Abdelhalim, A. *et al.* Highly sensitive and selective carbon nanotube-based gas sensor arrays functionalized with different metallic nanoparticles. *Sensors Actuators, B Chem.* **220**, 1288–1296 (2015).

200. Liu, B. *et al.* Functionalized graphene-based chemiresistive electronic nose for discrimination of disease-related volatile organic compounds. *Biosens. Bioelectron.* **1**, 100016 (2019).

201. Marom, O. *et al.* Gold nanoparticle sensors for detecting chronic kidney disease and disease progression. *Nanomedicine* **7**, 639–650 (2012).

202. Tisch, U. *et al.* Detection of Alzheimer's and Parkinson's disease from exhaled breath using nanomaterial-based sensors. *Nanomedicine* **8**, 43–56 (2013).

203. Nakhleh, M. K. *et al.* Diagnosis and Classification of 17 Diseases from 1404 Subjects via Pattern Analysis of Exhaled Molecules. *ACS Nano* **11**, 112–125 (2017).

204. Gasparri, R. *et al.* Volatile signature for the early diagnosis of lung cancer. *J. Breath Res.* **10**, 016007 (2016).

205. Tenero, L. *et al.* Electronic nose in discrimination of children with uncontrolled asthma. *J. Breath Res.* **14**, 046003 (2020).

206. Fens, N. *et al.* Exhaled air molecular profiling in relation to inflammatory subtype and activity in COPD. *Eur Respir J* **38**, 1301–1309 (2011).

207. De León-Martínez, L. D. *et al.* Identification of profiles of volatile organic compounds in exhaled breath by means of an electronic nose as a proposal for a screening method for breast cancer: A case-control study. *J. Breath Res.* **14**, 046009 (2020).

208. Chen, C. Y., Lin, W. C., Yang, H. Y. Diagnosis of ventilator-associated pneumonia using electronic nose sensor array signals: Solutions to improve the application of machine learning in respiratory research. *Respir. Res.* **21**, 1–12 (2020).

209. De Vries, R. *et al.* Integration of electronic nose technology with spirometry: Validation of a new approach for exhaled breath analysis. *J. Breath Res.* **9**, 046001 (2015).

210. Krauss, E. *et al.* Recognition of breathprints of lung cancer and chronic obstructive pulmonary disease using the Aeonose®electronic nose. *J. Breath Res.* **14**, 046004 (2020).

211. Fens, N. *et al.* Exhaled Breath Profiling Enables Discrimination of Chronic Obstructive Pulmonary Disease and Asthma. *Am. J. Respir. Crit. Care Med.* **180**, 1076–1082 (2009).

212. Fens, N. *et al.* External validation of exhaled breath profiling using an electronic nose in the discrimination of asthma with fixed airways obstruction and chronic obstructive pulmonary disease. *Clin. Exp. Allergy* **41**, 1371–1378 (2011).

213. Dragonieri, S. *et al.* An electronic nose in the discrimination of patients with non-small cell lung cancer and COPD. *Lung Cancer* **64**, 166–170 (2009).

214. Tirzite, M., Bukovskis, M., Strazda, G., Jurka, N., Taivans, I. Detection of lung cancer in exhaled breath with an electronic nose using support vector machine analysis. *J. Breath Res.* **11**, 036009 (2017).

215. Plaza, V. *et al.* Inflammatory asthma phenotype discrimination using an electronic nose breath analyzer. *J. Investig. Allergol. Clin. Immunol.* **25**, 431–437 (2015).

216. Fielding, D. *et al.* Volatile organic compound breath testing detects in-situ squamous cell carcinoma of bronchial and laryngeal regions and shows distinct profiles of each tumour. *J. Breath Res.* **14**, 046013 (2020).

217. Licht, J. C., Grasemann, H. Potential of the electronic nose for the detection of respiratory diseases with and without infection. *Int. J. Mol. Sci.* **21**, 1–16 (2020).

218. Bikov, A., Lázár, Z., Horvath, I. Established methodological issues in electronic nose research: How far are we from using these instruments in clinical settings of breath analysis? *J. Breath Res.* **9**, 034001 (2015).

219. Lu, Y., Partridge, C., Meyyappan, M., Li, J. A carbon nanotube sensor array for sensitive gas discrimination using principal component analysis. *J. Electroanal. Chem.* **593**, 105–110 (2006).

220. Jha, S. K., Hayashi, K. A quick responding quartz crystal microbalance sensor array based on molecular imprinted polyacrylic acids coating for selective identification of aldehydes in body odor. *Talanta* **134**, 105–119 (2015).

221. Freeman, B. D., Pinnau, I. (1999) Polymeric Materials for Gas Separations. In: Polymer Membranes for Gas and Vapor Separation, Washington, American Chemical Society, pp 1–27

222. Rosen, S.L. (1993) Fundamental propertied of polymeric materials 2nd *ed.*, Rolla, Missuri, John Wiley & Sons, Inc., pp 97

223. Tjong, S. C. (2012) Thermal Properties of Polymer Nanocomposites In: Polymer Composites with Carbonaceous Nanofillers, Weinheim, Germany, Wiley-VCH, pp 103-141

224. Drobny, J. G. (2012) Polymeric Materials. In: Polymers for Electricity and Electronics, Hoboken, New Jersey, John Wiley & Sons, Inc., pp 27-133

225. Stefanuto, P. H. *et al.* Multimodal combination of GC × GC-HRTOFMS and SIFT-MS for asthma phenotyping using exhaled breath. *Sci. Rep.* **10**, 1–11 (2020).

226. Van Vliet, D. *et al.* Association between exhaled inflammatory markers and asthma control in children. *J. Breath Res.* **10**, 016014 (2016).

227. Caldeira, M. *et al.* Allergic asthma exhaled breath metabolome : A challenge for comprehensive two-dimensional gas chromatography. *J. Chromatogr. A* **1254**, 87–97 (2012).

228. Van Vliet, D. *et al.* Can exhaled volatile organic compounds predict asthma exacerbations in children? *J. Breath Res.* **11**, 016016 (2017).

229. Smolinska, A., Klaassen, E. M. M., Dallinga, J. W., Kant, K. D. G. Van De, Jobsis, Q. Profiling of Volatile Organic Compounds in Exhaled Breath As a Strategy to Find Early Predictive Signatures of Asthma in Children. *PLoS One* **9**, e95668 (2014).

230. Schleich, F. N. *et al.* Exhaled Volatile Organic Compounds Are Able to Discriminate between Neutrophilic and Eosinophilic Asthma. *Am. J. Respir. Crit. Care Med.* **200**, 444–453 (2019).

231. Brinkman, P. *et al.* Exhaled breath profiles in the monitoring of loss of control and clinical recovery in asthma. *Clin. Exp. Allergy* **47**, 1159–1169 (2017).

232. Caldeira, M. *et al.* Profiling allergic asthma volatile metabolic patterns using a headspace-solid phase microextraction / gas chromatography based methodology. *J. Chromatogr. A* **1218**, 3771–3780 (2011).

233. Gahleitner, F., Guallar-hoyas, C., Beardsmore, C. S., Pandya, H. C. Metabolomics pilot study to identify volatile organic compound markers of childhood asthma in exhaled breath. *Bioanalysis* **5**, 2239–2247 (2013).

234. Dragonieri, S. *et al.* An electronic nose in the discrimination of patients with asthma and controls. *J. Allergy Clin. Immunol.* **120**, 856–862 (2007).

235. Ibrahim, B. *et al.* Non-invasive phenotyping using exhaled volatile organic compounds in asthma. *Thorax* **66**, 804–809 (2011).

236. Robroeks, C. M. *et al.* Exhaled volatile organic compounds predict exacerbations of childhood asthma in a 1-year prospective study. *Eur. Respir. J.* **42**, 98–106 (2013).

237. Jareño-Esteban, J. J. *et al.* Study of 5 Volatile Organic Compounds in Exhaled Breath in Chronic Obstructive Pulmonary Disease. *Arch. Bronconeumol. (English Ed.)* **53**, 251–256 (2017).

238. Van Berkel, J. J. B. N. *et al.* A profile of volatile organic compounds in breath discriminates COPD patients from controls. *Respir. Med.* **104**, 557–563 (2010).

239. Basanta, M. *et al.* Exhaled volatile organic compounds for phenotyping chronic obstructive pulmonary disease : a cross-sectional study. *Respiratory Research* **13**, 1–9 (2012).

240. Phillips, C. *et al.* Short-term intra-subject variation in exhaled volatile organic compounds (VOCs) in COPD patients and healthy controls and its effect on disease classification. *Metabolites* **4**, 300–318 (2014).

241. Allers, M. *et al.* Measurement of exhaled volatile organic compounds from patients

with chronic obstructive pulmonary disease (COPD) using closed gas loop GC-IMS and GC-APCI-MS. *J. Breath Res.* **10**, 026004 (2016).

242. Westhoff, M. *et al.* Differentiation of chronic obstructive pulmonary disease (COPD) including lung cancer from healthy control group by breath analysis using ion mobility spectrometry. *Int. J. Ion Mobil. Spectrom.* **13**, 131–139 (2010).

243. Pizzini, A. *et al.* Analysis of volatile organic compounds in the breath of patients with stable or acute exacerbation of chronic obstructive pulmonary disease. *J. Breath Res.* **12**, 036002 (2018).

244. Poli, D. *et al.* Exhaled volatile organic compounds in patients with non-small cell lung cancer : cross sectional and nested short-term follow-up study. *Respiratory Research* **10**, 1–10 (2005).

245. Buszewski, B. *et al.* Identification of volatile lung cancer markers by gas chromatography-mass spectrometry: Comparison with discrimination by canines. *Anal. Bioanal. Chem.* **404**, 141–146 (2012).

246. Muñoz-Lucas, M. Á. *et al.* Influence of Chronic Obstructive Pulmonary Disease on Volatile Organic Compounds in Patients with Non-Small Cell Lung Cancer. *Arch. Bronconeumol. (English Ed.)* **56**, 801–805 (2020).

247. Fu, X.-A., Li, M., Knipp, R. J., Nantz, M. H., Bousamra, M. Noninvasive detection of lung cancer using exhaled breath. *Cancer Med.* **3**, 174–181 (2014).

248. Wehinger, A. *et al.* Lung cancer detection by proton transfer reaction mass-spectrometric analysis of human breath gas. *International Journal of Mass Spectrometry* **265**, 49–59 (2007).

249. Phillips, M., Altorki, N., Austin, J. H. M., Cameron, R. B., Cataneo, R. N. Prediction of lung cancer using volatile biomarkers in breath 1. *Cancer Biomarkers* **3**, 95–109 (2007).

250. Bajtarevic, A. *et al.* Noninvasive detection of lung cancer by analysis of exhaled breath. *BMC Cancer* **16**, 1–16 (2009).

251. Ha, H. *et al.* Exhaled breath analysis for lung cancer detection using ion mobility spectrometry. *PLoS One* **9**, 1–13 (2014).

252. Oguma, T. *et al.* Clinical contributions of exhaled volatile organic compounds in the diagnosis of lung cancer. *PLoS One* **12**, 1–10 (2017).

253. Cai, X. *et al.* A prediction model with a combination of variables for diagnosis of lung cancer. *Med. Sci. Monit.* **23**, 5620–5629 (2017).

254. Poli, D. *et al.* Determination of aldehydes in exhaled breath of patients with lung cancer by means of on-fiber-derivatisation SPME-GC/MS. *J. Chromatogr. B Anal. Technol. Biomed. Life Sci.* **878**, 2643–2651 (2010).

255. Ii, M. B. *et al.* Quantitative analysis of exhaled carbonyl compounds distinguishes benign from malignant pulmonary disease. *J. Thorac. Cardiovasc. Surg.* **148**, 1074–1081 (2014).

256. Li, M. *et al.* Breath carbonyl compounds as biomarkers of lung cancer. *Lung Cancer* **90**, 92–97 (2015).

257. Schallschmidt, K. *et al.* Comparison of volatile organic compounds from lung cancer patients and healthy controls - Challenges and limitations of an observational study. *J. Breath Res.* **10**, 046007 (2016).

258. Zou, Y. *et al.* Optimization of volatile markers of lung cancer to exclude interferences of non-malignant disease. *Cancer Biomarkers* **14**, 371–379 (2014).

259. Sakumura, Y. *et al.* Diagnosis by volatile organic compounds in exhaled breath from lung cancer patients using support vector machine algorithm. *Sensors (Switzerland)* **17**, 287 (2017).

260. Barash, O. *et al.* Differentiation between genetic mutations of breast cancer by breath volatolomics. *Oncotarget* **6**, 44864–44876 (2015).

261. Patterson, S. G. *et al.* Breath analysis by mass spectrometry: A new tool for breast cancer detection? *Am. Surg.* **77**, 747–751 (2011).

262. Phillips, M. *et al.* Prediction of breast cancer risk with volatile biomarkers in breath. *Breast Cancer Res. Treat.* **170**, 343–350 (2018).

263. Mangler, M. *et al.* Volatile organic compounds (VOCs) in exhaled breath of patients with breast cancer in a clinical setting. *Ginekol. Pol.* **83**, 730–736 (2012).

264. Phillips, M. *et al.* Prediction of breast cancer using volatile biomarkers in the breath. *Breast Cancer Res. Treat.* **99**, 19–21 (2006).

265. Li, J. *et al.* Investigation of potential breath biomarkers for the early diagnosis of breast cancer using gas chromatography-mass spectrometry. *Clin. Chim. Acta* **436**, 59–67 (2014).

266. James, M.E. (1999) Polymer Data Handbook, Cincinnati, Oxford University Press, Inc.

267. Das, S., Pal, M. Review—Non-Invasive Monitoring of Human Health by Exhaled Breath Analysis: A Comprehensive Review. *J. Electrochem. Soc.* **167**, 037562 (2020).